Using the Non-Intrusive Load Monitor for Shipboard Supervisory Control

by

Patrick Lawrence Bennett
B.S., Computer Science
United States Naval Academy, 1996

Submitted to the Department of Mechanical Engineering in Partial Fulfillment of the Requirements for the Degrees of
Naval Engineer
and
Master of Science in Mechanical Engineering
at the
Massachusetts Institute of Technology

June 2007

Signature of Author _____
Department of Mechanical Engineering
May 11, 2007

Certified by _____
Robert W. Cox, Assistant Professor
Department of Electrical and Computer Engineering
University of North Carolina at Charlotte
Thesis Reader

Certified by _____
Steven B. Leeb
Professor of Electrical Engineering and Computer Science & Mechanical Engineering
Departments of Electrical Engineering and Computer Science & Mechanical Engineering
Thesis Supervisor

Accepted by _____
Lallit Anand, Professor of Mechanical Engineering
Chairman, Department Committee on Graduate Students
Department of Mechanical Engineering

(This Page Intentionally Left Blank)

Using the Non-Intrusive Load Monitor for Shipboard Supervisory Control

by

Patrick Lawrence Bennett

Submitted to the Department of Mechanical Engineering in Partial Fulfillment of the Requirements for the Degrees of

Naval Engineer

and

Master of Science in Mechanical Engineering

ABSTRACT

Field studies have demonstrated that it is possible to evaluate the state of many shipboard systems by analyzing the power drawn by electromechanical actuators [1], [2], [3], [4], [5]. One device that can perform such an analysis is the non-intrusive load monitor (NILM). This thesis investigates the use of the NILM as a supervisory control system in the engineering plant of gas-turbine-powered vessel. Field tests demonstrate that the NILM can potentially reduce overall sensor count if used in a supervisory control system.

To demonstrate the NILM's capabilities in supervisory control systems, experiments are being conducted at the U.S. Navy's Land-Based Engineering Site (LBES) in Philadelphia, Pennsylvania. Following a brief description of the LBES facility and the NILM itself, this thesis presents testing procedures and methodology with results obtained during the extensive field studies. This thesis also describes the on-going efforts to further demonstrate and develop the NILM's capabilities in supervisory control systems.

Thesis Supervisor: Steven B. Leeb
Title: Professor of Electrical Engineering and Computer Science & Mechanical Engineering

Thesis Reader: Robert W. Cox
Title: Assistant Professor, Department of Electrical and Computer Engineering
University of North Carolina at Charlotte

Acknowledgements

I would personally like to thank the following organizations and individuals:

- The Office of Naval Research's Control Challenge, ONR/ESRDC Electric Ship Integration Initiative and the Grainger Foundation, for providing necessary funding.
- Dr. Robert W. Cox for his guidance, patience, wisdom, and friendship.
- Andy Cairns, LBES Director, for allowing me to install my "science project" on his engineering plant.
- Charlie Gilligan, LBES Test Manager, for his assistance, enthusiasm, candor, and friendship.
- Lee Skarbek, LBES Test Manager, for his expertise and assistance.
- Thomas J. "Buck" Ryan, LBES Electrician, for his effort and assistance.
- Frank Facciolo, LBES Engineer, for his effort and assistance.
- Jim Paris, for his NILM computer expertise.
- Dr. Steven Leeb, for his dedication, enthusiasm, and inspiration.
- My wife, Tanya, for without her unwavering support and tireless effort at home this work would not have been possible.

Table of Contents

List of Figures

List of Tables

Chapter 1 Introduction

1.1 Motivation for Research

Engineering plants in modern naval vessels consist of complex and costly networks of electrical and mechanical actuators. In many cases, high-level supervisory systems are required to control the interactions between these devices. To reduce the cost and complexity of maintenance operations, new supervisory systems are also designed to assist in condition-based maintenance. For example, high-level controllers for modern marine gas turbines can now record sensor data and, in some cases, they can even perform automated data assessment [7]. Because of the potential cost savings, there is a push to extend the capabilities of such systems [8], [9]. Doing so, however, usually means that more sensors are deployed throughout the engineering plant. In fact, some estimates indicate that each new ZUMWALT (DDG-1000) class destroyer will feature as many as 200,000 sensing devices [10]. Although such a large sensing network may seem advantageous, it can also be both expensive and difficult to maintain. A simple, low-cost alternative with lower sensor density could provide identical information with higher reliability.

1.2 System Complexity and Cost Increase

Joint Vision 2020, which outlines the direction of U.S. Defense strategy, points out the need to "invest in and develop new military capabilities." The Navy's fulfillment of this vision consists partly of investing in the technological advancement of its ships. This has been a longstanding policy, as throughout history, naval vessels have increased in technological capability. However, the pursuit of improved capability and technology often results in ever increasing cost. In fact, some of the Navy's recent shipbuilding programs have experienced skyrocketing research, development, and acquisition costs.

Between 1985 and 2000 the Navy's overall budget declined. With the end of the Cold War came a shift in U.S. budgetary priorities, as less and less money was spent on defense overall. However, with the rise of al-Qaeda and other organizations and the resulting Global War on Terrorism (GWOT), the Navy has embarked on a fleet recapitalization plan to retain worldwide naval superiority. However, with increased capability comes increased cost. An examination of Navy budget trends since Fiscal Year (FY) 2005 (Figure 1-1 below) reveals an increase in all major budgetary categories: Personnel (MilPers), Operations and Maintenance (O&M), and Investment (includes research, development, and procurement).

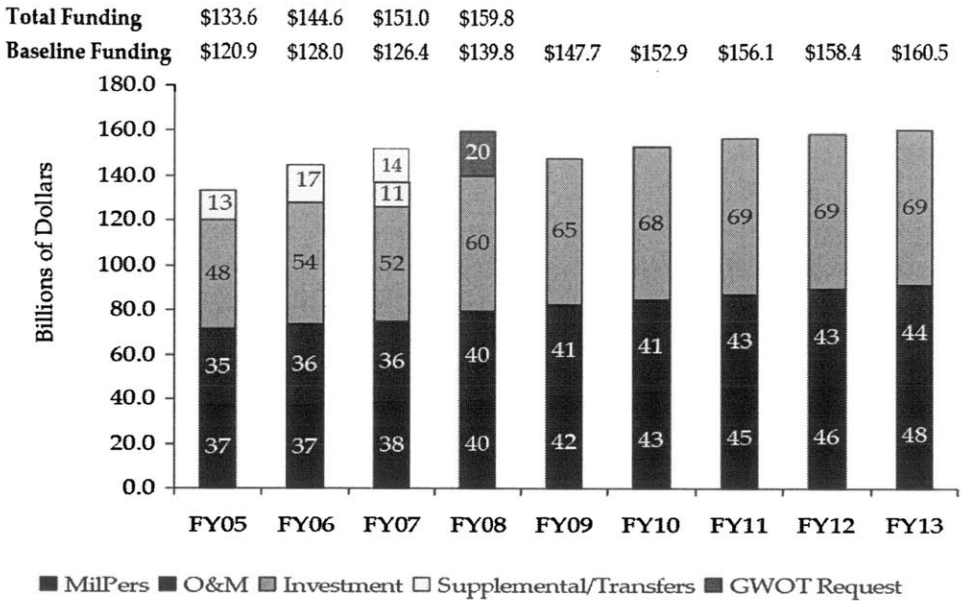

Figure 1-1: Overview of US Navy Budget FY05-13 [31]

As indicated by the Supplemental/Transfers category in the figure, in FY 2005-2007 the initial budget projections were not enough to cover projected costs. For FY 2008 dollars were requested specifically to cover the Navy's cost of the GWOT. Future projections show an increase in budget through FY 2013. The Navy budget cannot continue to spiral out of control, yet fleet recapitalization and operations are paramount if naval superiority is to be retained.

A comparison of the DDG 1000 to DDG 51 costs, shown in Table 1-1 below, provides a solid example of the rising costs of new ship development, procurement, and operation. The DDG 1000 is comprised of many new technologies resulting in a significantly more capable platform [33], [38]. Even when adjusted for inflation, the higher cost associated with increased complexity and capability is apparent. In order to meet the recapitalization strategy goals, fiscal concerns must be addressed and costs must somehow be controlled.

In an effort to control costs to ensure the survival of the recapitalization plan, the Navy has embarked on two initiatives to reduce ship Total Ownership Cost (TOC): reduced manning and condition based maintenance.

Table 1-1: Cost Comparison between DDG 51 and DD(X) (now DDG 1000) [36].

Comparison of the DDG-51 and DD(X) Destroyers

	DDG-51	DD(X)
Procurement Cost for the Lead Ship of the Class (Billions of 2007 dollars)		
Navy's estimate	2.6	3.3
CBO's estimate	2.6	4.7
Displacement (Thousands of long tons)		
Light load	6.6	12.1
Full load	8.3	14.3
Procurement Cost per Thousand Long Tons for the Lead Ship of the Class (Millions of 2007 dollars)		
Navy's estimate	385	275[a]
CBO's estimate	385	385
Annual Operating Costs per Ship (Millions of 2007 dollars)	34	22 to 32
Life-Cycle Costs per Ship (Billions of 2007 dollars)[b]		
Using the Navy's estimate for DD(X) procurement	2.1	2.7 to 2.9
Using CBO's estimate for DD(X) procurement	2.1	3.8 to 4.0

Source: Congressional Budget Office.

a. This number is the same as CBO's estimate for the DDG-51 because it is based on a direct analogy to that ship.

b. Life-cycle costs are shown on a discounted (net-present-value) basis.

1.3 Reduced Manning

In April 2000, the Naval Research Advisory Committee (NRAC) conducted a study on optimized surface ship manning. The study indicated that between 1985 and 2000 the overall Navy budget had decreased by 40% while the Operations and Support (O&S) portion, which includes the personnel budget, had remained relatively constant. In fact, 29% of the projected TOC for the ARLEIGH BURKE (DDG 51) class of destroyers is personnel [26]. Faced with rising recapitalization and personnel costs [31], the Navy must strive to reduce vessel manning. As part of the overall recapitalization strategy the Navy is in the midst of a massive personnel reduction plan. Figure 1-2 depicts not only this plan, but how final end strength has been reduced each fiscal year to help cope with recapitalization costs and now those of the GWOT.

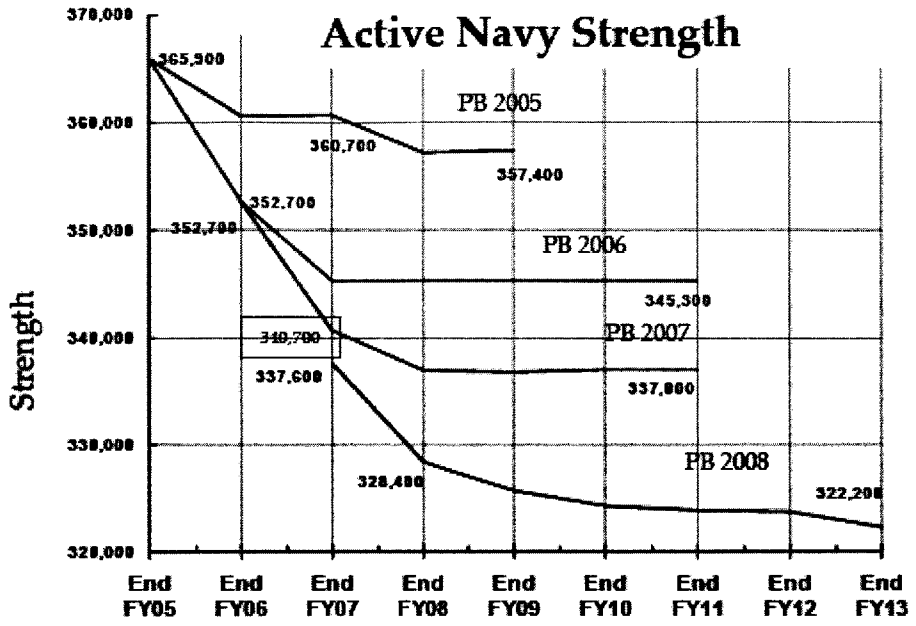

Figure 1-2: President's Budget Navy Personnel Projections

A significant portion of the personnel reduction plan includes reduction of vessel manning which remains a high priority of the Navy's Surface Warfare Division [26]. Current manning of the DDG 51 class destroyer stands at 323 officers and enlisted [34]. In contrast the manning goal for the DDG 1000 class is 142 [38], a significant reduction considering the increased size, capability and complexity of the DDG 1000 over the DDG 51. Another example is the SAN ANTONIO (LPD 17) vessel class. At contract award manning levels were set at 450, but the lead ship was commissioned with just a crew size of 361 [26]. Many factors have promoted achieving these goals including design, work process improvement, maintenance philosophy, and technology advancement. As the personnel drawdown continues, it is imperative that alternatives be developed and implemented to support reduced manning initiatives.

1.4 Condition Based Maintenance

With the reduction in shipboard crew manning comes an increase in automation and a fundamental shift in current Navy maintenance practices. Previously, the Navy used a Preventative Maintenance System (PMS) where maintenance on equipment was conducted at scheduled regular intervals. In many cases the scheduled maintenance included disassembly and inspection whether or not the equipment exhibited signs of malfunction. This is not only manpower intensive but also costly. For example, upon reassembly new expendable parts (i.e. seals) would be installed and the old ones, often still in good working order, discarded.

One of the reduced manning initiatives is termed Condition Based Maintenance (CBM). This philosophy abandons the old, scheduled PMS. Maintenance is conducted when equipment exhibits certain symptoms (i.e. broken). This type of philosophy results in a reduction in maintenance related man-hours. In addition, the Navy is shifting most CBM away from the organizational level. That is, shore maintenance personnel will

conduct any required maintenance on the new modern warship. Less man-hours required for maintenance translates to less manpower requirements overall and ultimately a reduction in vessel manning, as the smaller crew can now be gainfully employed conducting other warfighting tasks.

To assist in the diagnostics of equipment to determine the need and scheduling for CBM, the Navy is currently using the Integrated Condition Assessment System (ICAS). ICAS is an engineering plant monitoring system that collects equipment status (discrete signals, state changes, etc) and automatically transmits that data to a shore facility where it is reviewed for potential problems and abnormal conditions. Any necessary maintenance or repairs are then scheduled for completion according to urgency, budget, and operating schedule. The overall success of ICAS is dependent upon the accurate collection of data and realization of actual cost savings from the transition to the CBM philosophy.

1.5 NILM as Part of Solution

One device that shows promise to greatly simplify the supervisory monitoring and control process thereby reducing the manpower required to operate an engineering plant is the Non-Intrusive Load Monitor (NILM) [6], [11]. The NILM, which measures the current and voltage at one or more central locations in a power-distribution network, can determine both the operating schedule and the operational status of each of the major loads in an engineering plant [4], [12], [13]. In many cases the NILM can also use its electrical data to assess the status of certain mechanical elements such as air filters and components in fluid power systems [1], [2], [3]. Because a NILM-based monitor greatly reduces the number of required sensors, it can decrease costs and increase the efficiency and effectiveness of organizational and intermediate-level maintenance, thereby reducing the overall manning requirements, ultimately leading to reduced TOC of a naval vessel. This thesis will demonstrate how the NILM is a viable alternative that aims to assist the Navy in reducing TOC by providing an inexpensive alternative for engineering plant supervisory control resulting in reduced manning and improved condition based maintenance. The NILM is technologically simple and therefore inexpensive. Previous tests have shown that the NILM is capable of detecting existing mechanical faults and impending failures. The NILM can effectively increase automation thereby reducing the number of personnel required to complete certain operational and maintenance tasks resulting in overall lower TOC.

Chapter 2 NILM Overview

2.1 NILM Theory

Figure 2-1 shows the block diagram of a standard NILM. Note that the NILM measures the aggregate current flowing to a bank of electrical loads. It then disaggregates the operating schedule of individual loads using signal-processing techniques. In an engineering plant, the candidate installation locations include generator output busses and distribution panels.

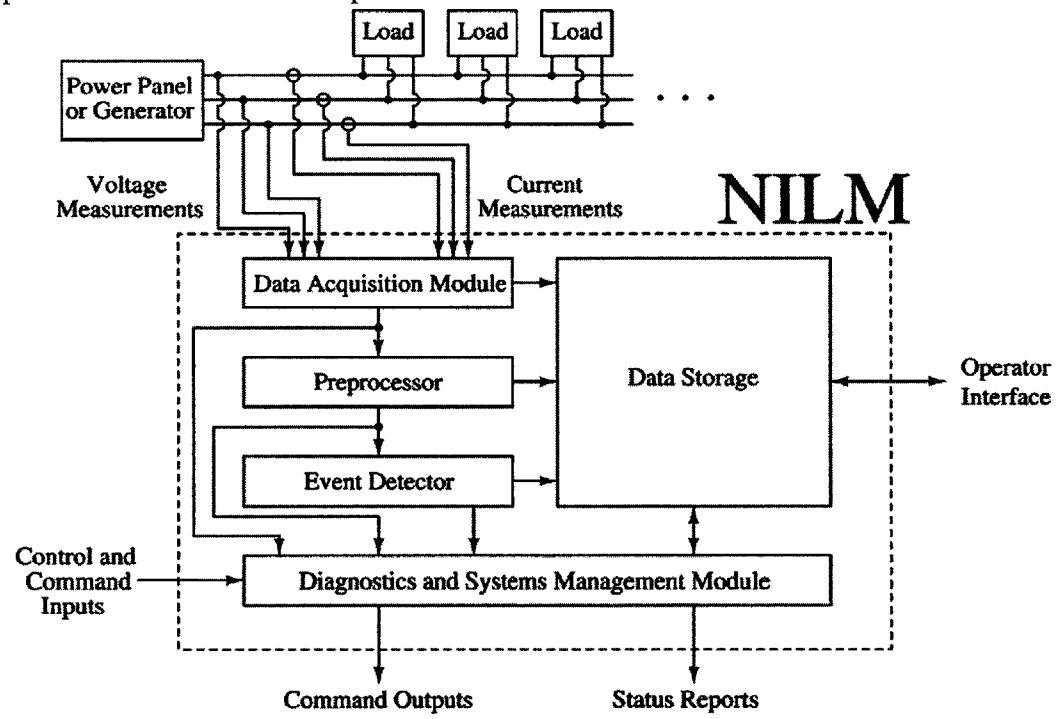

Figure 2-1: Diagram showing the fundamental signal flow path in a NILM [6]

Using measurements of the line voltage and aggregate current, a software-based preprocessor onboard the NILM computes time-varying estimates of the frequency content of the measured line current [13]. Formally, these time-varying estimates, or spectral envelopes, are defined as the quantities [14]:

$$a_m(t) = \frac{2}{T}\int_{t-T}^{T} x(\tau)\sin(m\omega\tau)d\tau$$

$$b_m(t) = \frac{2}{T}\int_{t-T}^{T} x(\tau)\cos(m\omega\tau)d\tau$$

These equations are Fourier-series analysis equations evaluated over a moving window of length T [15]. The coefficients $a_m(t)$ and $b_m(t)$ contain time-local information about the frequency content of $i(t)$. Provided that the basis terms $\sin(m\omega t)$ and $\cos(m\omega t)$ are

synchronized to the line voltage, the spectral envelope coefficients have a useful physical interpretation as real and reactive power and harmonic content [12], [14].

The spectral envelopes computed by the preprocessor are passed to an event detector that identifies the operation of each of the major loads on the monitored electrical service. In a modern NILM, identification is performed using both transient and steady-state information [16]. Field studies have demonstrated that transient details are particularly powerful because the transient electrical behavior of a particular load is strongly influenced by the physical task that is performed [12]. As shown in Figure 2-2, for example, the physical differences between an incandescent lamp and an induction machine result in vastly different transient patterns. Figure 2-3 demonstrates the positive identification of an induction motor driving a small vacuum pump. Further details of the detection and identification process can be found in [16] and [17].

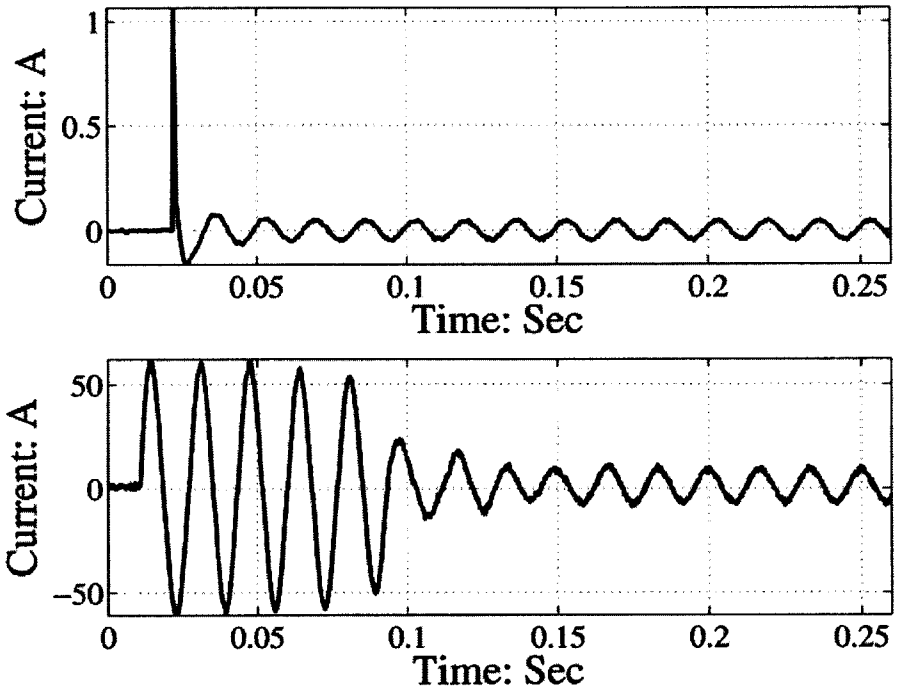

Figure 2-2: Top trace: Current drawn during the start of an incandescent lamp. Bottom trace: Stator current drawn during the start of an unloaded, fractional horsepower induction machine.

The final block in Figure 2-1 is the NILM's diagnostics and systems management module. This software unit assesses load status using any required combination of current data, voltage data, spectral envelopes, and load operating schedules [11]. The successful application of this module has been demonstrated in numerous publications [1], [2], [3], [4], [5], [13], [16], [18], [19], [20]. Shipboard applications are highlighted in [1], [2], [3], [4], and [5].

As shown in Figure 2-1, the modern NILM can interact with human or automated operators in a number of different ways. For instance, the NILM can use its diagnostic information to command certain loads to either commence or cease operations. Additionally, the NILM can provide regular status reports to the Engineering Officer. To assist in future maintenance operations, the NILM stores all of the relevant data streams

(i.e. currents, voltages, operating schedules, etc.) in either a local or remote database [21]. The NILM's vast storage capabilities make it possible for the operator to perform historical data trending. Note that this off-line analysis can be conducted on a remote PC using convenient software packages such as Microsoft Excel [21].

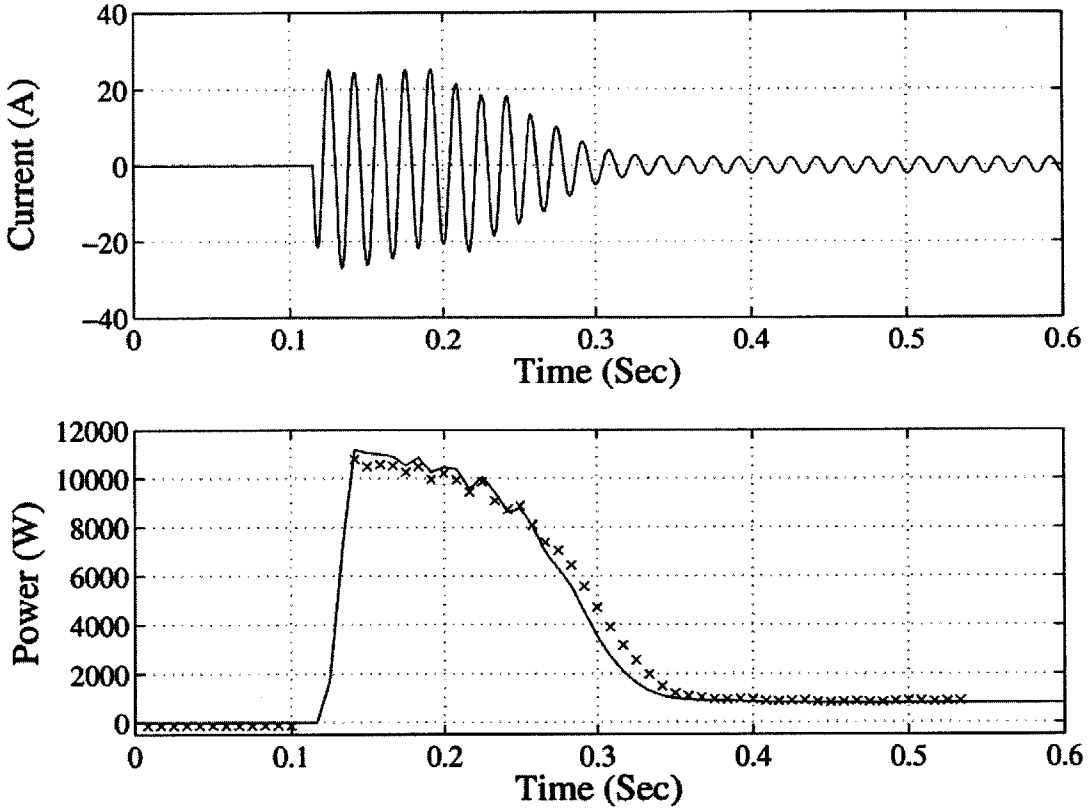

Figure 2-3: Measured current and computed power during the start of 1.7hp vacuum pump motor. Also shown in the power plot is a section of the template that has been successfully matched to the observed transient behavior by the NILM's event detector [6].

2.2 NILM Construction

The NILM is constructed from readily available Commercial-off-the-Shelf (COTS) equipment. COTS materials were chosen for their ease of procurement and assembly. A typical NILM installation consists of a NEMA certified enclosure with voltage transducers and a DC power supply inside, appropriately sized current transducers, and a computer for processing. A list of required parts is in Appendix A . Figure 2-4 is a NILM block diagram and Figure 2-5 shows a typical equipment installation. A complete NILM electrical connection scheme can be found in Appendix B. The following sections describe how to construct a NILM for 3 phase applications utilized in this thesis.

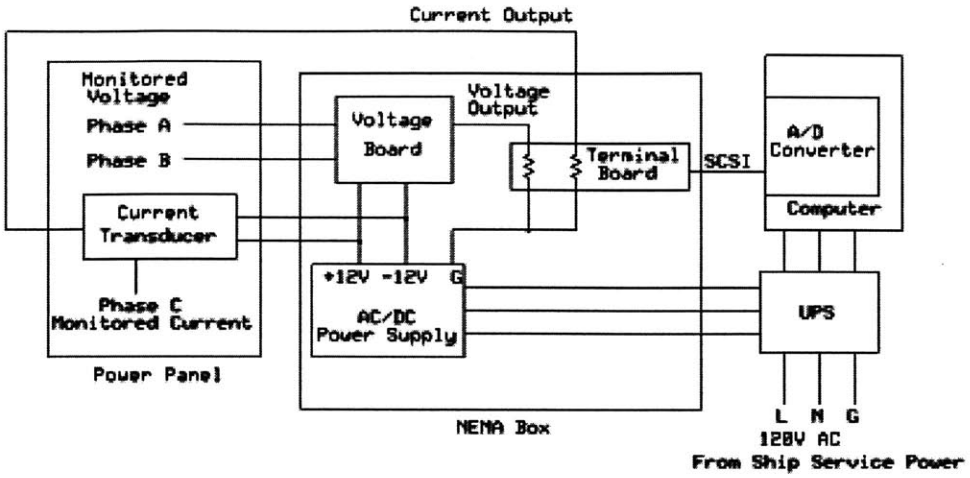

Figure 2-4: Block Diagram of NILM Setup [45]

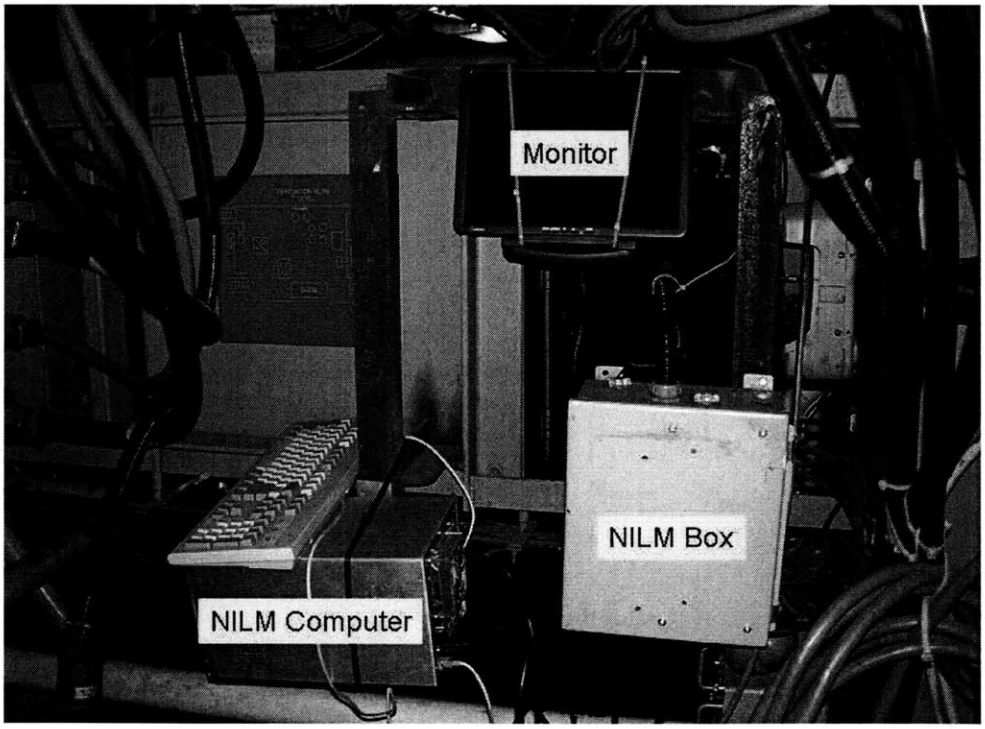

Figure 2-5: Typical NILM Equipment Installation

2.2.1 Transducer Sizing

Before proceeding with NILM construction, the appropriate size of the voltage and current transducers must be determined. For most applications the LV 25-P voltage transducer manufactured by LEM will suffice and is the voltage transducer used in all NILMs described in this thesis. The current transducer (CT) must be sized according to the current rating of the monitored equipment. For electrical panels, a CT with a minimum rating equal to the rating of the panel breaker will suffice. If the installation

will take place on a motor controller the CT rating must account also for the start-up amperage of the motor, usually 10 times the steady state rating. The motor steady state rating is typically the rating reported by the manufacturer. So for example, the CT required for a 20A motor would need to be rated for 200A. A LEM LA 205 would be required. Data sheets for all transducers utilized for this thesis are included in Appendix C.

2.2.2 Resistor Sizing

Once the appropriate transducers are selected, resistor selection can take place. Three types of resistors are required: voltage board resistors, measuring resistors, and ground or reference resistors.

The voltage board requires three 3W resistors wired in parallel for each voltage transducer (see Figure 2-7 below). These resistors are sized as follows: Choose I_p = 3.6mA. Per the LV 25 data sheet (located in Appendix C) Ip can be a maximum of 10 mA. The accuracy of 10 mA is not required for NILM purposes and dissipates too much power through the resistors generating too much heat; 3.6mA suffices for typical applications. For a 120 V application the resistors are sized as follows:

$$I_P = 3.6mA$$

$$VAC = 120V$$

Compute the total resistance required:

$$R_{Tot} = \frac{VAC}{I_P}$$

$$R_{Tot} = 33.33k\Omega$$

Compute the size of the individual resistor (3 required):

$$R_{Individual} = 3 * R_{Tot}$$

$$R_{Individual} = 100k\Omega$$

Thus three 100kΩ resistors are needed for each voltage transducer on the voltage board. Resistors for a 440V application would be sized in a similar manner.

Next the 0.25W measuring resistors (R_m) need to be sized. For the current transducer, the CT data sheet is needed for reference. Take note of the maximum resistor range for the appropriate power supply. Typically NILMs are constructed with 12V power supplies, but 15V are available. In order to not saturate the PCI 1710 analog interface, V_{peak} across R_m must be less than 5V. Therefore:

$$I_{Primary\_RMS} * \sqrt{2} * k * R_M < 5V$$

where k is the conversion ratio from the data sheet and $I_{Primary\_RMS}$ is the monitored equipment maximum current. Remember to allow for start up current if the equipment is a motor. Start with the maximum resistance allowed by the data sheet and work down from there until $V_{peak} < 5V$. For example, for this application a LEM LA-55P CT will be used so $R_m = 100\Omega$, k = 1/1000 and $I_{Primary\_RMS} = 15A$ were chosen:

$$15A * \sqrt{2} * \frac{1}{1000} * 100\Omega = 2.121V$$

So in this case, the 100Ω resistor will suffice. It is possible to use resistor values higher than the maximum recommended if the monitored equipment current will not fluctuate such that transducer becomes saturated. R_m for the voltage transducer is calculated in a similar manner except that $I_{Primary\_RMS}$ is calculated by dividing the measured voltage by R_{Tot} (computed above). In this case 110Ω, k= 2500/1000 (from the LV 25-P voltage transducer data sheet) was used:

$$\frac{120V}{33.333k\Omega} * \sqrt{2} * \frac{2500}{1000} * 110\Omega = 1.4V$$

This results in Vpeak well below 5V and is well within the range specified on the data sheet.

Finally for ground (reference) resistors, use 51Ω. This particular value is an arbitrary value that primarily acts as a fuse to protect the NILM should a large current surge occur. Once all resistors are selected, actual construction can begin.

2.2.3 Voltage Board Construction

The voltage board will be constructed first. Figure 2-6 is a photograph of the board prior to construction. Figure 2-7 is a circuit diagram of the board. It is easier to solder the smallest pieces on first, so solder the capacitors (2 for each transducer used) on first, followed by the resistors and finally the transducers. Once all pieces are soldered on, attach the fuse holder and solder its connecting wire. The fuse can either be inserted now or upon completion of construction. Once the voltage board is complete, conduct continuity checks of the board using a multimeter to ensure all solder joints are satisfactory. Figure 2-8 is a photograph of a completed voltage board for 1 voltage tap.

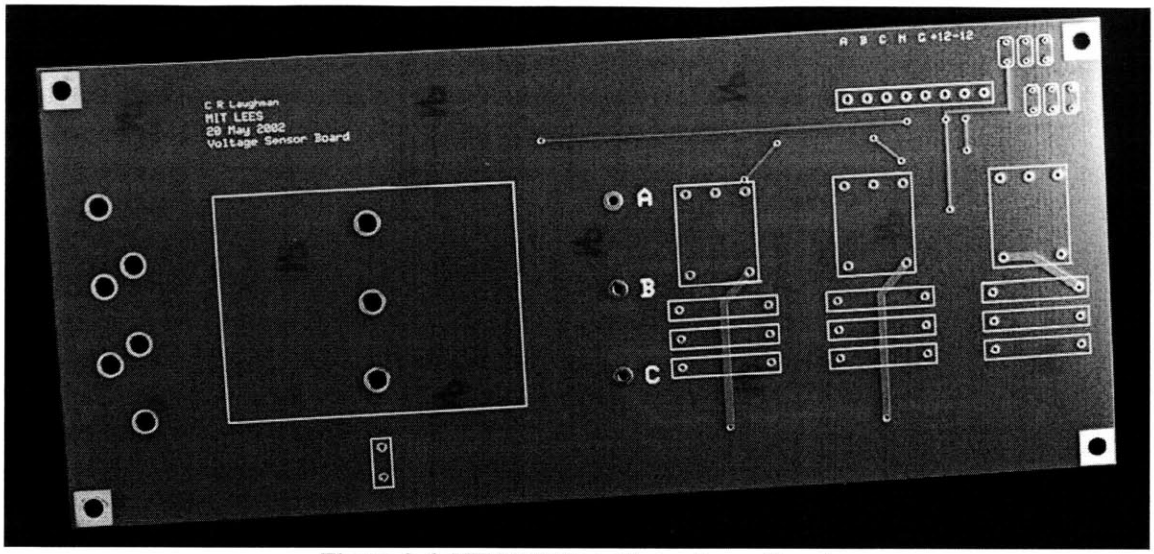

Figure 2-6: NILM Voltage Transducer Board

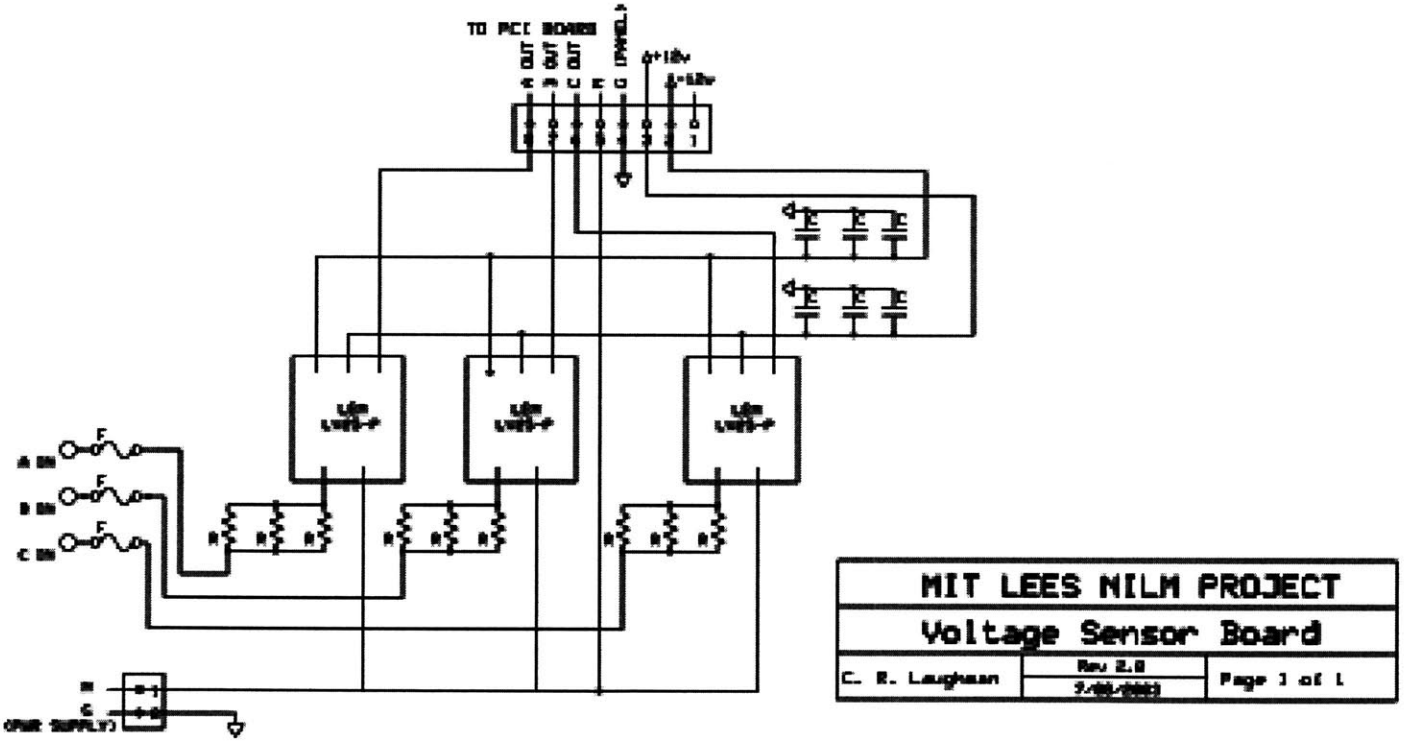

Figure 2-7: Voltage Board Circuit Diagram [45]

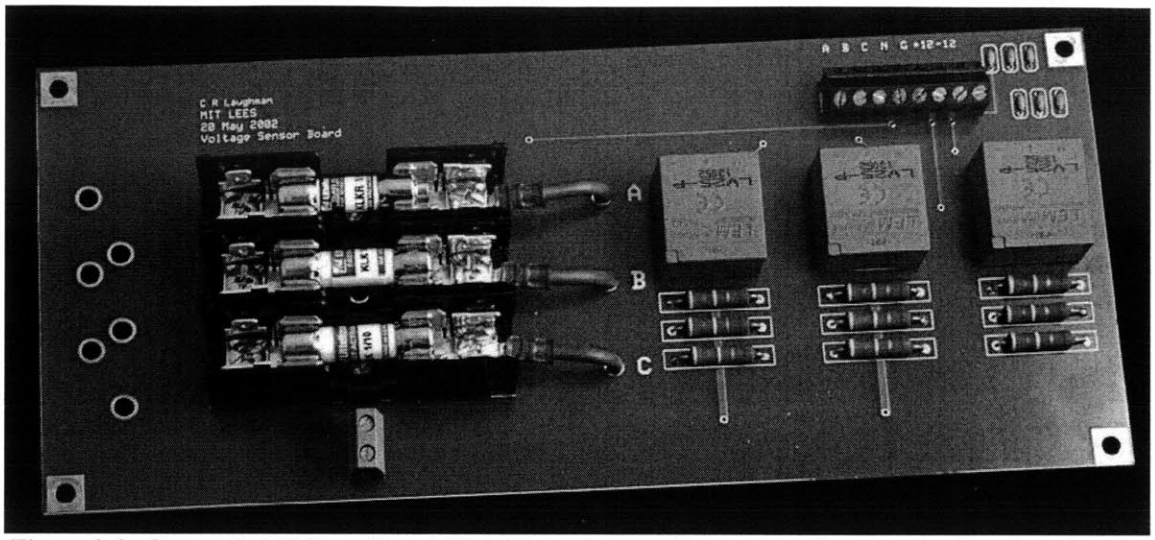

Figure 2-8: Completed Voltage Board. Note that this board is capable of measuring 3 voltage inputs.

2.2.4 Resistor Board Construction

The resistor board was designed specifically for NILM applications in order to provide a secure location for resistor mounting and will be constructed next. Figure 2-9 is a photograph of a resistor board prior to resistor soldering. Following the connection scheme solder the resistors onto the board, followed by the terminal blocks. Looking at the board, the measuring resistors (R_m) go on top, and the reference resistors go on the bottom. Ensure to take note which resistor is in which position for proper hook up later. Again, conduct continuity checks with a multimeter to ensure satisfactory solder joints.

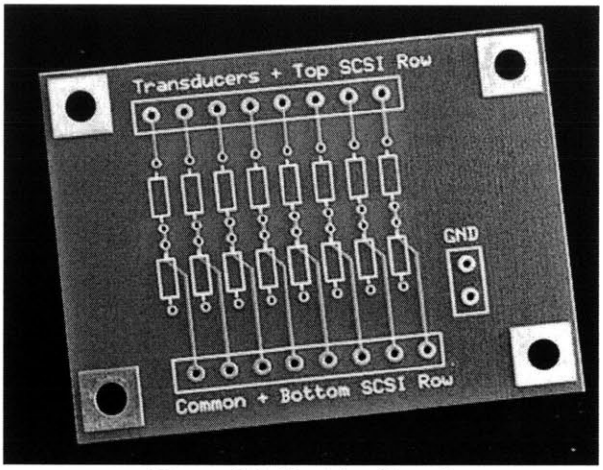

Figure 2-9: Resistor Board

2.2.5 Power Supply Connectors

After the voltage and resistor boards are complete, the MOLEX connectors for the power supply must be prepared. Using the connectors, wires, and MOLEX crimping tool listed in Appendix A, prepare the connectors. The AC input connector requires 2 wires

and the DC output requires 4 wires. Typically only three of the output wires (+12V, -12V, and one COMMON) are used, but it is prudent to add all four wires in case the second COMMON is needed later.

2.2.6 Enclosure Preparations

Once the voltage and resistor boards and power supply MOLEX connectors are complete, preliminary construction is complete and the enclosure and backplane must be prepared. Cable access openings must be cut and holes must be drilled for component mounting. No standard layout for the NILM enclosure exists; layout is at builder discretion. Figure 2-10 is an enclosure prepped for component installation. Figure 2-11 is an enclosure with the power supply and voltage board installed. Four cable access holes must be cut. Three accesses can be holes cut in the top and bottom for the NILM power cable, voltage sensing cable, and current sensing cable. Ensure the holes are large enough to accommodate the ¾ inch Halex clamps. Place the Halex clamps in the holes. The fourth cable access is simply a notch cut in the top for the SCSI cable. The cable access holes and SCSI cable notch can be placed in locations appropriate for the enclosure layout. Place the accesses to minimize cable bending and stress.

Once the cable accesses are complete, drill the required mounting holes for components to be mounted directly to the enclosure. Note that the backplane mounting holes are integral to the enclosure. Typical applications have the power supply and SCSI terminal board mounted directly to the enclosure. The voltage and resistor boards, as well as any required terminal connector blocks are mounted to the backplane. Once the enclosure is has all required mounting holes and accesses cut, drill all required access holes in the backplane. Ensure all holes are the appropriate size to accommodate the standoffs and machine screws to be used in mounting the equipment.

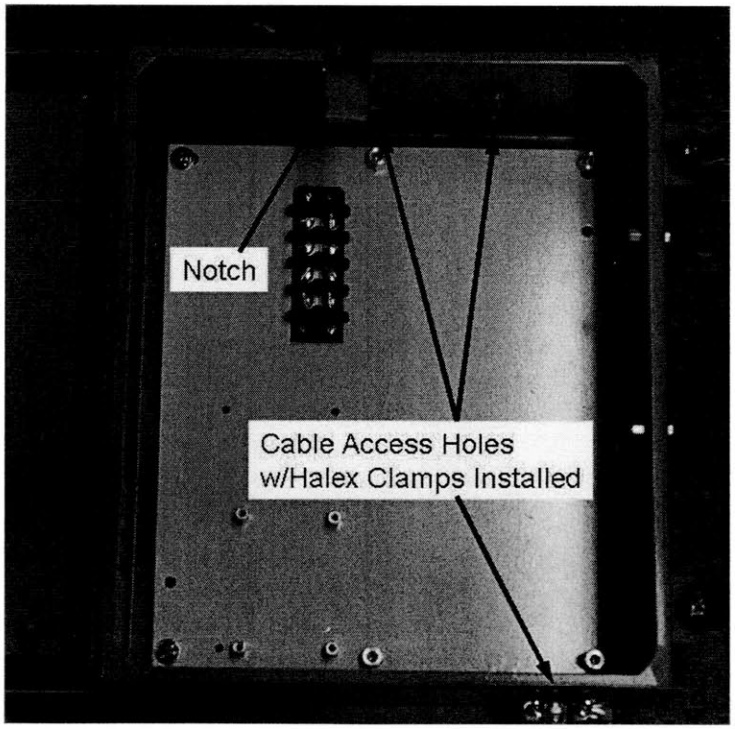

Figure 2-10: NILM Enclosure with Backplane Installed

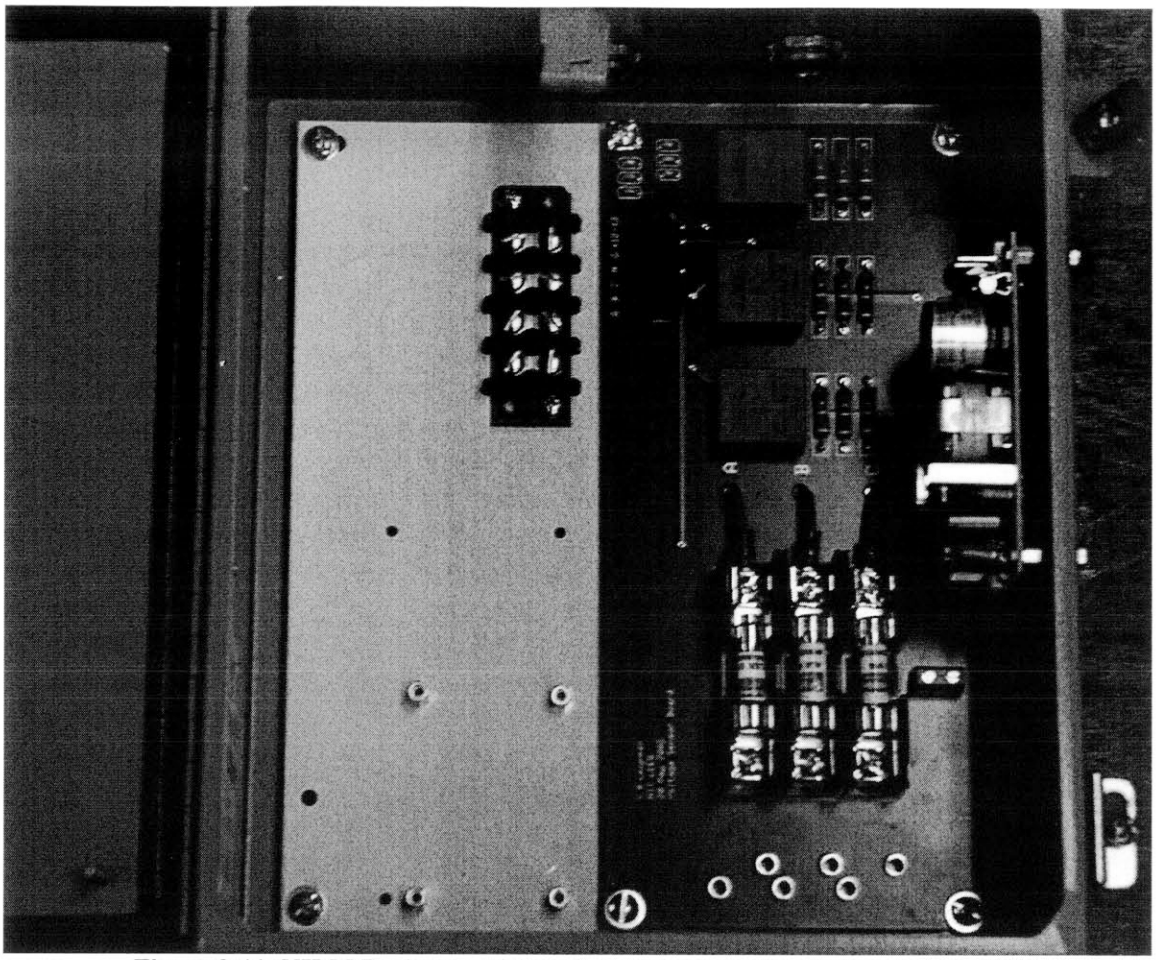

Figure 2-11: NILM Enclosure with Voltage Board and Power Supply Installed

2.2.7 NILM Assembly

Once the enclosure and backplane are ready, attach the voltage and resistor board standoffs with appropriate nuts to the backplane. Install any required terminal connector blocks using appropriately sized machine screws and nuts. Terminal connector blocks may or may not be required depending on the scope of the NILM application, but can make the wiring hook up easier. Once terminal blocks and necessary standoffs are attached, place the backplane in the enclosure and attach it using two 3/8 inch 10-32 machine screws and the two 3/8 inch standoffs to accommodate two voltage board attachment screws. Now install the voltage board using four 3/8 inch 10-32 machine screws. After installing the voltage board, install the resistor board using ¼ inch 6-32 machine screws and standoffs.

With the backplane and associated components installed, required components can be mounted onto the enclosure. Attach the power supply standoffs to the enclosure using the appropriate nuts. Attach the power supply to the standoffs using the same screws as the resistor board. Attach the DIN mounting rail for the SCSI terminal board using two 3/8 inch 10-32 machine screws and appropriate nuts. The DIN rail should be long enough to accommodate the SCSI terminal board. Attach the SCSI terminal board to the mounting rail.

After individual components are installed into the enclosure, install the power supply MOLEX connectors and wire up the NILM according to the electrical connection scheme using 18 AWG braided copper wire. The NILM power supply can be powered via a standard 120V wall outlet using any standard power cord wired to the power supply input wires.

Finally, if using an LA 55-P type CT, solder the specially designed CT circuit board (Figure 2-12) to the CT. Then solder the CT connecting cable to the CT circuit board. Typically the red wire is +12V, the black wire is -12V, and the clear wire is the measuring (M) wire. If using an LA 205 or larger, a MOLEX connector must be prepared using the appropriately sized connectors and the CT connecting cable wired to the MOLEX connector wires using either wire nuts or heat shrink.

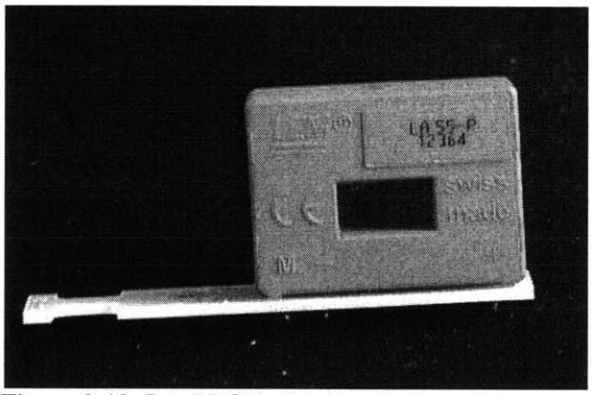

Figure 2-12: LA-55 CT with Circuit Board Attached

2.2.8 NILM Testing

Once the NILM is constructed, it should be tested using a simple shop lamp. The voltage tap should be plugged into the same outlet as the lamp using any standard power cord wired to the voltage tap input in accordance with the NILM connection scheme. Place one lead of the lamp power cord through the CT. Once the voltage tap and CT are connected, connect the NILM to the computer via the SCSI cable. Plug in the lamp and start NILM data collection. Turn the lamp on and off a few times. Stop NILM data collection. Download the data file from the computer and process using the scripts in Appendix D. If the NILM is working properly the power trace should look similar to Figure 2-13.

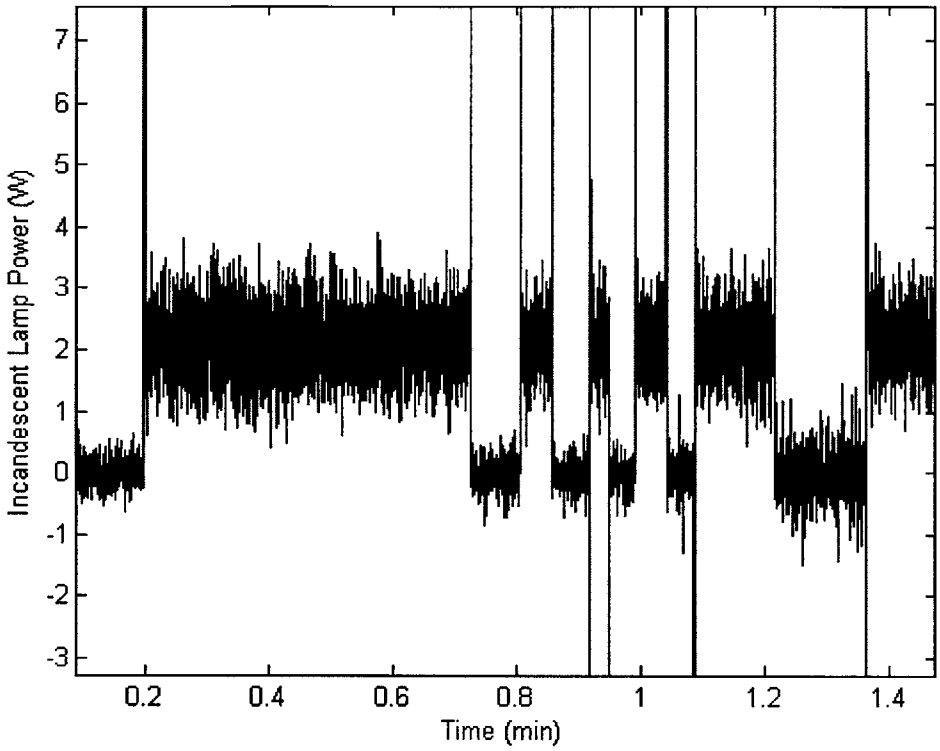

Figure 2-13: NILM power trace for an incandescent lamp taken during a NILM operational test.

Figure 2-13 above is representative of a satisfactorily operating NILM. The operation of the lamp switch and energizing of the bulb can clearly be seen. This particular lamp draws about 2W when energized.

2.2.9 NILM Data Scaling

The NILM software does not complete any kind of power computations. Rather, the NILM records "power counts" which range from -4096 to +4096 and are based on an analog measurement to digital data conversion process. Therefore, it becomes necessary to rescale the NILM power data into appropriate units for analysis. Using MATLAB scripts, the NILM data is converted to current (Amperes) using the top equation below and then converted to power (Watts) using the bottom equation below:

$$I_{RMS} = (NILM\_data) * \left(\frac{1}{64}\right) * \left(\frac{g}{4096}\right) * \left(\frac{1}{R_m * \frac{1}{k}}\right) * \left(\frac{1}{\sqrt{2}}\right)$$

$$P = V_{RMS} * I_{RMS}$$

In the top equation g is the NILM software gain code and k is the CT conversion ratio found on the CT data sheet. There are four possible gain codes written into the NILM software which are listed in Table 2-1 with the default value being 0. The gain code is

selected according to the maximum voltage across R_m. For example, if initial tests indicate this voltage to be 2V, then the appropriate gain code would be 1 for the -2.5V to +2.5V range. The scripts used to scale the recorded NILM data can be found in Appendix D. A complete description of the NILM data collection process and software algorithms can be found in [12]and [21].

Table 2-1: NILM Gain Codes and Signal Ranges

Gain Code	Input Signal Range	g Value
0	-5V to +5V	10
1	-2.5V to +2.5V	5
2	-1.25V to +1.25V	2.5
3	-0.625V to +0.625V	1.25
4	-10V to +10V	20

2.2.10 Final Site Installation

Once the NILM has been tested in the lab, it is then ready for installation in the field. Typically for a 3 phase system the CT is placed on phase A and the voltage tap is hooked to phases B and C. This particular hook up is not required; however for proper NILM operation and computations, it is imperative that the CT be placed on the phase which is not hooked up to the voltage tap. A test plan for a typical NILM installation is located in Appendix E. Figure 2-14 shows a typical voltage and CT hook up inside an electrical panel. Upon completion of the electrical connections, the NILM enclosure and computer must be mounted in close proximity to each other to accommodate the relatively short SCSI cable length. After a suitable location has been chosen and the enclosure and computer have been mounted, connect all power cords to an appropriate power source. In most applications, a standard 120V outlet will suffice. The use of an Uninterrupted Power Supply (UPS) is recommended, but not required. The NILM and associated peripherals are now ready for use.

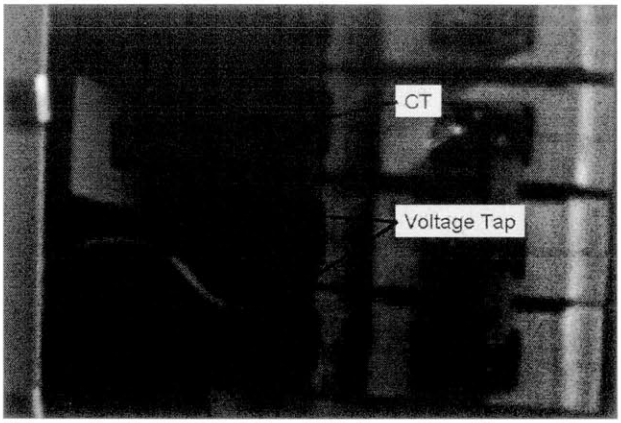

Figure 2-14: NILM CT and Voltage Tap Connections

Chapter 3 NILM Testing at the Land Based Engineering Site (LBES)

3.1 LBES Overview

Several NILMs are installed on equipment at the Navy's Land Based Engineering Site (LBES) located at the Naval Business Center in Philadelphia, PA. The LBES environment provides an excellent opportunity to test and evaluate NILM hardware and software under actual shipboard-like conditions.

The LBES is designed to replicate the Number Two Main Engine Room aboard one of the Navy's ARLEIGH BURKE (DDG-51) class destroyers. The equipment installed in this facility includes two LM2500 gas-turbine propulsion main engines (GTMs); three gas-turbine generators (GTGs); and auxiliary systems providing fuel oil, lube oil, low-pressure air, and cooling water. Additionally, the main engines drive a full-scale propulsion train complete with main reduction gear, shafting, and bearings [6]. A perspective view of this facility is shown in Figure 3-1.

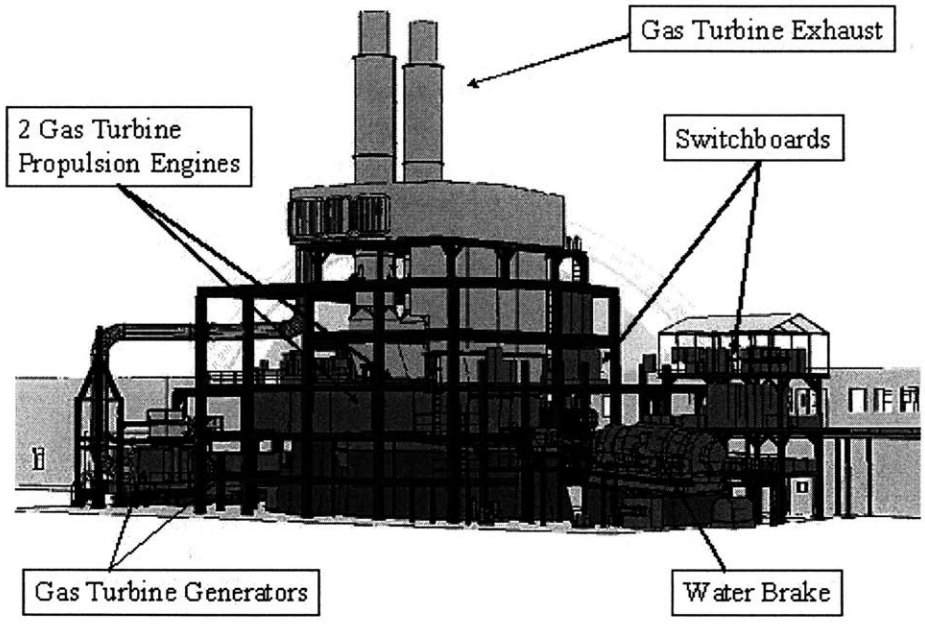

Figure 3-1: US Navy LBES

There are some significant differences between the land-based facility and the machinery spaces on the DDG-51. First, the LBES has a full Zonal Electrical Distribution System (ZEDS), which represents the entire shipboard electric plant of a DDG-51. Thus, the LBES features all three of the Ship's Service Gas Turbine Generators (GTGs). In reality the Number Two Main Engine Room on the DDG-51 houses only one GTG. Additionally, the ZEDS at LBES is physically collocated with the propulsion plant, but it does not supply power to the plant's auxiliary systems. At the LBES the ZEDS

supplies several large load banks, and power for auxiliary systems is provided by the regional utility. A third critical difference is that the LBES does not have a propeller. In order to perform the functions of the DDG Controllable Pitch Propeller (CPP) and simulate the resistance of the ocean on the propulsion train, a large water brake is installed at the end of a shortened shaft [6]. To the equipment in the LBES plant, the propulsion shaft behaves and responds as if a CPP was actually attached. Where appropriate, descriptions of plant operations in this thesis will read as if the LBES was equipped with a CPP.

A more complete description of the LBES, pertinent systems, and equipment can be found in [6], [40], and LBES Trainee Guides located in the LBES NILM information archives in the Laboratory for Electromagnetic and Electronic Systems (LEES) at the Massachusetts Institute of Technology.

3.2 Equipment Listing

To begin testing the NILM's applicability as a shipboard supervisory control system, we have deployed NILM devices throughout the LBES facility for preliminary data collection and assessment. During the course of this work, two complete NILMs were constructed and installed on LBES equipment and modifications were made on three previously installed NILMs. This thesis will summarize the state of each of these installed NILMs.

Five NILM boxes are installed. Some boxes have multiple CTs which are used to monitor multiple systems. The following is a complete listing of the installed NILMs and monitored equipment:

- GTM Controller NILM (installed on Power Panel 1-282-1):
  - Panel aggregate current
  - Universal Engine Controller Plus 2A
  - Universal Engine Controller Plus 2B
  - Shaft Control Unit
- 2A Fuel Oil Service Pump
- 2A Lube Oil Service Pump
- Nr 2 Low Pressure Air Compressor
- AG9140 No Break Power Supply

This chapter will summarize the details of the existing installations and will introduce the functionality of each system.

3.2.1 LBES GTM Controller NILM

The LBES GTM Controller NILM monitors Power Panel 1-282-1 and three LBES controller circuit breakers contained within. This panel provides 120VAC to the Universal Engine Controllers Plus, the Shaft Control Unit, both GTM igniters, and GTM module lighting. Figure 3-2 is a photograph of the power panel with the location of the monitored equipment breakers annotated.

A single NILM box contains all connections for the four CTs and one voltage tap. The GTM Igniters are not monitored by individual CTs, but are included in the aggregate signal monitored by the panel CT. Figure 3-3 shows interior of the panel with the three controller CTs installed on their respective breakers installed on Phase A, and the panel CT also installed on Phase A. The voltage is assumed to be constant throughout the

panel; therefore a single voltage tap is connected to Phases B and C of Universal Engine Controller Plus 2A.

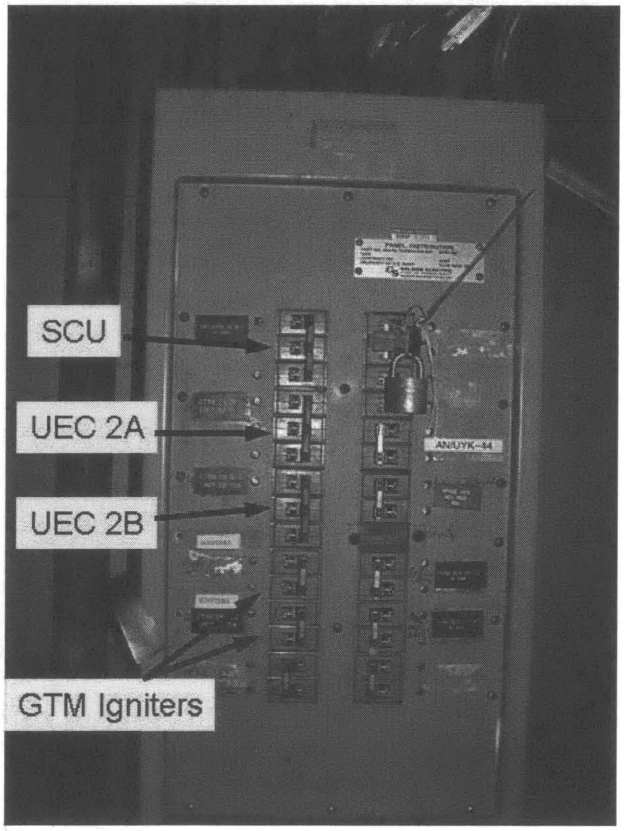

Figure 3-2: Exterior View of Power Panel 1-282-1 with breaker location annotated

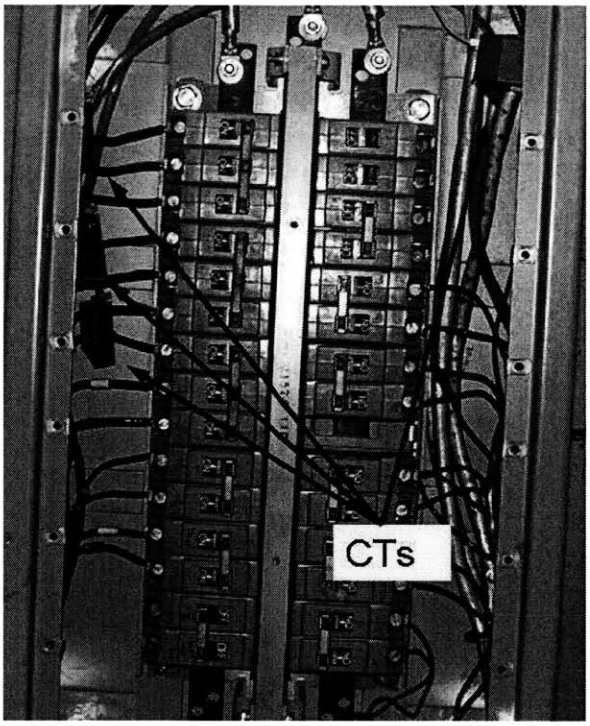

Figure 3-3: Interior view of Power Panel 1-282-1. The location of NILM CTs is annotated. Individual equipment CTs are on the right and the panel CT is on the left.

Table 3-1 below is a summary of the entire NILM setup for Power Panel 1-228-1. A description of the individual monitored subsystems follows in the sections below. The Unix script used to process the controller NILM data files is included in Appendix D.

Table 3-1: Power Distribution Panel 1-282-1 NILM Configuration

NILM Channel	Measurement	Phase	Measurement Resistors (R_M)	Reference Resistors	Transducers	Gain Code
1	Voltage	B and C	110Ω	51Ω	LEM LV-25P	0
2	UEC 2A Current	A	130Ω	51Ω	LEM LA-55P	3
3	UEC 2B Current	A	130Ω	51Ω	LEM LA-55P	3
4	SCU Current	A	130Ω	51Ω	LEM LA-55P	2
5	Panel Current	A	67Ω	51Ω	LEM LA-205P	1

3.2.1.1 Universal Engine Controller Plus

The LBES configuration includes two Universal Engine Controllers (UEC) Plus which serve as the "brains" for the General Electric LM2500 Gas Turbine Main Engines (GTM). Each GTM has its own UEC Plus. The UEC Plus provides control and monitoring of the GTM and performs the following functions [39]:

- Start/sequencer of the gas turbine
- Power Turbine (PT) overspeed protection
- Power Level Actuator (PLA) control

- Digital Fuel Control (DFC)
- Signal conditioning
- Emergency Stop of the gas turbine via remote hardwired contact activation
- Maintenance Computer Interface
- Fault Detection and Isolation
- Software-based calibration and setpoint adjustment
- Status logging
- Local Control capability
- Engine Vibration monitoring
- Power Distribution
- UEC Plus status, alarm, and shutdown processing

The UEC Plus is virtually identical to the UEC described in [6]. The primary difference is the addition of DFC capability, making the UEC plus capable of supporting both the PLA and DFC configurations. For the remainder of this thesis, the term UEC will be used when referencing the UEC Plus.

Additional information about the operation and functions of the UEC can be found in [6], [23], and [39].

3.2.1.2 Shaft Control Unit

The Shaft Control Unit (SCU) interfaces with the propulsion machinery at the LBES to provide local control of the GTMs, shafting, propeller, and propulsion auxiliary equipment. Recall the LBES propulsion shaft does not have a propeller but rather a waterbrake which performs the functions of a Controllable Pitch Propeller (CPP). To the SCU, the propulsion shaft behaves and responds as if a CPP was actually attached. The SCU is normally unmanned with machinery and thrust control residing at the Propulsion and Auxiliary Control Console (PACC)-briefly described in the next paragraph. Controls and indicators are provided to perform the following functions related to the GTM described in this thesis [42]:

- Motor
- On
- Online
- Normal Stop/Cooldown
- GTM Module Fuel Valve Control

Controls and indicators are also provided to perform the following propulsion auxiliary functions described in this thesis [42]:

- Electric Lube Oil Service Pump Speed Control
- Fuel Oil Service Pump Speed Control

Finally, the SCU provides thrust and pitch control for the propulsion shaft [42].

The Propulsion and Auxiliary Control Console (PACC) provides remote, centralized monitoring and control of the propulsion and auxiliary equipment throughout the LBES plant from the LBES Central Control Station (CCS) The console interfaces with the SCU via a fiber optic network. It is important to note that the PACC is designed to interface with two SCUs in two different engine rooms on an actual ship. Only one half on the LBES PACC can actually interface with the LBES SCU. The PACC is the normal

operating station for propulsion machinery and thrust control and is capable of performing the same functions as the SCU listed above [42].

More detailed information about the functions and operation of the SCU and PACC can be found in [6], [41],and [42].

3.2.2 2A Fuel Oil Service Pump

The Fuel Oil Service Pump (FOSP) provides fuel to the GTMs directly and GTGs via a gravity head tank. LBES is equipped with 2 FOSPs, 2A and 2B which are piped to a common header. The FOSP can operate at one of two speeds, slow and fast. FOSP motor and pump details are provided in Table 3-2 and Table 3-3 below.

Table 3-2: Fuel Oil Service Pump Data [40]

Number of Pumps	2
Type	Positive Displacement Rotary Vane
Capacity	36/72 GPM
Discharge Pressure	110 PSI
Suction Lift	10 inches Hg
Pump Speed	260/520 RPM
Type of Drive	Two Speed Helical Reducer
System Pressure	150 PSIG

Table 3-3: Fuel Oil Service Pump Motor Data [40]

Motor Type	Squirrel Cage Induction	
Power Requirements	440 Vac, 3 Phase, 60 Hz, 10 FLA	
Conductor Type/Diameter	LSTSGU-3/0.06 inches	
Motor Horsepower	3.75/7.5 HP	
Motor Speed	900/1800 RPM	
Stator Windings	Low Speed	High Speed
Number of Poles	8	4
Connection	Delta One Circuit	Wye Two Circuit

The NILM connections were made in the 2A FOSP motor controller such that both pump operating speeds can be measured by the NILM. Table 3-4 below summarizes the 2A FOSP NILM configuration. More detailed information about the FOSP can be found in [43] and a diagram of the LBES Fuel Oil Service System is located in [6].

Table 3-4: FOSP NILM Configuration Data

NILM Channel	Measurement	Phase	Measurement Resistors (R_M)	Reference Resistors	Transducers	Gain Code
1	Voltage	A and B	177Ω	61Ω	LEM LV-25P	0
2	2A FOSP Current	C	61Ω	61Ω	LEM LA-55P	0

3.2.3 Nr 2 Low Pressure Air Compressor

The purpose of the Low Pressure Air Compressor (LPAC) is to provide compressed air at approximately 125 psig to the LBES Low Pressure Air System for valve control and pneumatic power for specified plant equipment. LBES is equipped with 2 LPACs, 1 and 2. LPAC details are provided below in Table 3-5 and Table 3-6.

Table 3-5: Low Pressure Air Compressor Data [6]

Nomenclature	Low Pressure Air Compressor
Model	NAXI 100-4A
Manufacturer	Ingersoll-Rand
Inlet Capacity	100 CFM
Discharge Pressure Settings	115/120/125 psig
Brake Horsepower	28.8 HP Maximum
Motor Speed	3600 rpm

Table 3-6: Low Pressure Air Compressor Motor Data [6]

Power Requirements	440V, 3-phase, 60 Hz, 35A Full Load
Horsepower	35 HP
Rotor	Squirrel Cage
Speed Class	Constant
RPM Synchronous	3600 rpm
RPM Full Load	3535 rpm
Torque Class	Design B
Current Class	Design B

In addition to the standard NILM current and voltage connections, which were made in the LPAC controller, an Omega PX209 pressure transducer was installed to measure compressor discharge pressure. Details about the pressure transducer can be found at <http://www.omega.com>. Table 3-7 provides a summary of the LPAC NILM

configuration. A complete description and system diagram of the LBES Low Pressure Air System and details about the Nr 2 LPAC can be found in [6]. Additional details about the operation of the LPAC are located in [44].

Table 3-7: LPAC NILM Configuration Data

NILM Channel	Measurement	Phase	Measurement Resistors (R_M)	Reference Resistors	Transducers	Gain Code
1	Voltage	A and B	180Ω	62Ω	LEM LV-25P	0
2	LPAC Current	C	36Ω	62Ω	LEM LA-305S	0
3	Pressure	None	None	62Ω	Omega PX209	0

3.2.4 2A Lube Oil Service Pump

The Lube Oil Service Pump (LOSP) provides lubricating oil to the Main Reduction Gear (MRG) and propulsion shaft thrust bearing. LBES is equipped with 2 electric LOSPs, 2A and 2B piped to a common header and a mechanical LOSP attached to the MRG also piped to the same common header. The LOSP has two operating speeds slow and fast. LOSP motor and pump details are provided in Table 3-8 and Table 3-9 below.

Table 3-8: Lube Oil Service Pump Data [40]

Number of Pumps	2
Type	Screw
Capacity	225/560 GPM at 100PSIG
Discharge Pressure	100 PSI
Suction Lift	10 inches Hg
Efficiency %	58.0/67.5
BHP	24.3/51.6
RPM	880/1780
Liquid	Lube Oil 2190 TEP

Table 3-9: Lube Oil Service Pump Motor Data [40]

Motor Type	Induction
Power Requirements	440 Vac, 3 Phase, 60 Hz, 61/72FLA
Conductor Type/Diameter	LSFSGU-50/0.26 inches
Motor Horsepower	30/60 HP
Motor Speed	900/1800 SYN
<u>Stator Windings</u>	
Number of Poles	2
Connection	Delta One Circuit

The NILM connections were installed in the pump motor controller such that the NILM can monitor both operating speeds. The LOSP NILM configuration is outlined below in Table 3-10. Additional information about the LOSP and Lube Oil Service System, including a system diagram, can be found in [40].

Table 3-10: LOSP NILM Configuration

NILM Channel	Measurement	Phase	Measurement Resistors (R_M)	Reference Resistors	Transducers	Gain Code
1	Voltage	A and B	110Ω	51Ω	LEM LV-25P	0
2	LOSP 2A Current	C	20Ω	51Ω	LEM LA-305P	0

3.2.5 AG9140RF Gas Turbine Generator

LBES is equipped with three Gas Turbine Generators (GTGs). LBES Nr1 GTG, designated AG9410RF, consists of an Allison 501-K34 gas turbine engine turning a KATO 3000 kW generator. The AG9140 was chosen for NILM installation because it is equipped with the Redundant Independent Mechanical Start System (RIMSS), which is a small gas turbine engine mechanically coupled to the generator reduction gear. During a GTG start, a small DC motor first spins the RIMSS turbine. Eventually, fuel is admitted into the RIMSS gas-producer turbine and it is ignited. When the gas-producer turbine has reached approximately 40,000 rpm, the RIMSS power turbine begins to rotate and rotates the main turbine through the reduction gear [7].

The AG9140RF GTG is equipped with a Full Authority Digital Control (FADC) Local Operating Panel (LOCOP). The FADC LOCOP performs all control and monitoring of the Allison 501 turbine, RIMSS turbine, generator, and all auxiliary support systems.

In order to start the GTG from completely dark conditions, the GTG enclosure can operate independent of ship support systems for a short period of time. To provide power for operation under such conditions, the GTG is equipped with a No Break Power Supply (NBPS), which simply put, is an Uninterruptible Power Supply (UPS) for the LOCOP. The NBPS receives 440 VAC from the ships electrical distribution system which maintains charge on the NBPS batteries. In addition, the 440 VAC is converted to 28VDC to power the FADC LOCOP. A block diagram of the NBPS is shown below in Figure 3-4.

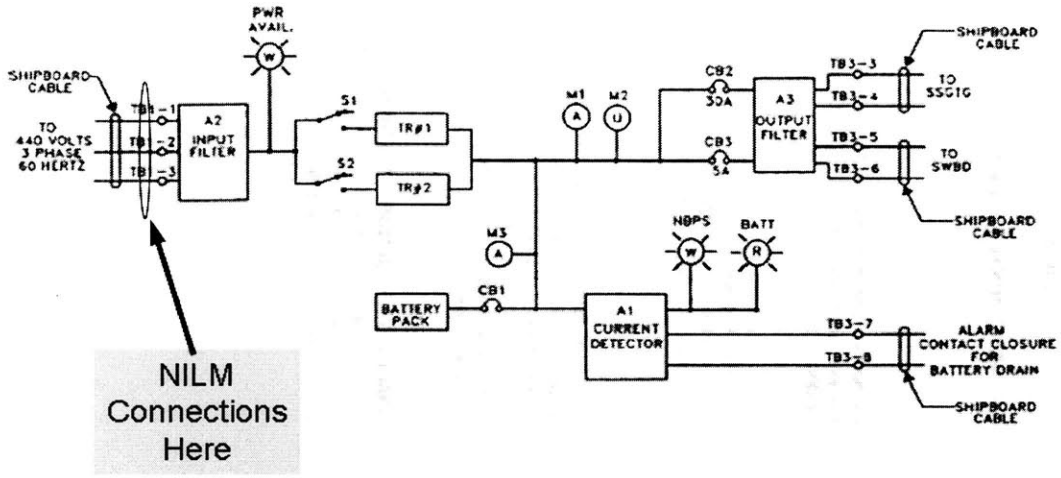

Figure 3-4: NBPS Block Diagram [46]

A NILM was installed on the 440 VAC input bus to the NBPS as shown in Figure 3-4. Specifically, the connections were made at the NBPS breaker in the 440VAC distribution panel that powers the NBPS. Because the GTG LOCOP receives power directly from the NBPS, the power drawn by the NBPS is, in essence, the power drawn by the GTG LOCOP. For the remainder of this thesis, this NILM will be referred to as the GTG NBPS NILM. Table 3-11 below is a summary of the GTG NBPS NILM setup. More detailed information about the functions and operations of the GTG and associated support equipment can be found in [25].

Table 3-11: NBPS NILM Configuration

NILM Channel	Measurement	Phase	Measurement Resistors (R_M)	Reference Resistors	Transducers	Gain Code
1	Voltage	B and C	110Ω	51Ω	LEM LV-25P	0
2	NBPS Current	A	147Ω	51Ω	LEM LA-55P	3

Chapter 4 Proven LBES Field Testing Results

In order to demonstrate the NILM's potential for a supervisory control system for integrated plant operations, each category of equipment, gas turbine controllers, pump motor controllers, and electromechanical support equipment, required individual study and analysis. NILM power data was collected over many days of integrated plant operations during DDG pre-commissioning crew training, as well as Machinery Control System (MCS) software testing and validation. This chapter presents the data analysis results that have proven to be consistent over the course of the research and are believed to correctly describe the operation of LBES equipment from the NILM perspective.

4.1 Controller NILM Results

A primary objective of this thesis is to correlate individual controller NILM data in order to determine equipment operating states. Over the course of the research, as NILM power data was collected, it was processed and analyzed looking for similarities in different power signatures of the same event (i.e. do all power signatures of GTM starts look the same, etc?). The power data for each piece of monitored equipment was systematically analyzed and a comprehensive event library was created and categorized by equipment and event type.

By creating the event library, it was established that some plant operations exhibit the same or nearly the same power signature each time they are performed. The first step in unlocking the potential of the NILM is to identify each power transition in the event signatures. One way to enable a NILM to track power transitions is to summarize them with a Finite State Machine (FSM). Using FSM models the NILM can determine if individual actuators are functioning properly and specific events (such as those required for a GTM start) are occurring in the appropriate sequence. Methods for tracking finite-state behavior are described in [24]. By using equipment technical manuals, LBES engineers, and the DDG 51 engineering plant operational experience of the author, engine controller power transitions were matched to specific commands and actuator operations performed by the controllers during plant events, and FSMs developed where applicable. The following sections detail the findings obtained for the UECs, SCU, and GTG NBPS.

4.1.1 UEC

Three GTM events consistently exhibited similar power signatures: start, motor, motor and fuel purge. When a GTM start is commanded by the operator, the SCU receives the start command from the console in control, usually the PACC. The SCU then sends a start command to the UEC which performs the necessary actions to start the GTM. Table 4-1 below outlines in detail the GTM start sequence.

Table 4-1: GTM Start Sequence

Speed Channel	Action/Event
"ON" Pushbutton Depressed Ngg = 0 RPM	SCU checks for start permissives: 1. MRB pressure greater than 13 psig 2. MRG turning gear not engaged 3. PLA/DFC at idle 4. Clutch cover in place

	SCU commands motor air regulator valve and start/masker air transfer valves to the start position, and waits 5 seconds to allow valves to shift position. SCU sends a UEC system reset command, followed by an auto start command. UEC verifies that PLA is at idle and that Ngg is less than 3500 RPM. UEC starts the following timers: 1. 20 seconds for Ngg to reach 1200 RPM 2. 45 seconds for L/O pressure to reach 10 psig 3. 90 seconds for Ngg to reach idle speed (4850-5150 RPM) **UEC commands the Starter Air Regulator Valve (SARV) to the open position.** "GTM __ TRANSITIONING TO ON" will be displayed on the AMLCD.
Ngg = 1200 RPM	**UEC opens (energizes) Fuel Oil Shutoff Valves (2) (FOSV)** ("FUEL ON" displayed) UEC energizes ignition system. UEC starts 40 second timer for T5.4 to reach 400 deg F (lightoff), and for FMP to reach 50 psig ("FLAME ON" displayed). If lightoff is achieved, the engine operating timer is started, and the engine start timer is incremented by one.
Ngg = 4500 RPM	UEC de-energizes ignition system. **UEC commands the starter air regulator valve to the close position.** UEC enables the L/O pressure low circuit
Ngg = idle speed (4850-5150 RPM)	SCU opens module vent damper and starts cooling fan. SCU commands start/masker air transfer valve to masker position, if masker air system is active. Icing alarm circuit is enabled. "GTM __ STATE ON" is displayed.

The items in bold font are the operations that are visible in the UEC power trace of a GTM start. The actuation of the Start Air Regulating Valve (SARV) and Fuel Oil Shut Off Valves (FOSVs) require a +28 VDC signal from the UEC, resulting in a rise in UEC power when the valves are actuated. To complete the FSM of the GTM start cycle, the GTM must return to its original (off) condition. This is referred to as "Normal Stop/Cool Down." In this state[1] the GTM runs at idle speed for 5 minutes to return to an acceptable operating temperature prior to turning off. Table 4-2 below outlines the GTM Normal Stop/Cool Down sequence.

[1] Refers to 1 of 4 engine states: OFF, ON, ONLINE, NORMAL STOP/COOLDOWN, which are not the same as UEC power states.

Table 4-2: GTM Normal Stop/Cooldown Sequence

Time	Action/Events
T = 0 "NORMAL STOP/COOLDOWN is depressed.	SCU drives PLA/DFC to idle, and issues a normal stop command to the UEC. UEC starts a 300-second (5 minutes). "GTM __ TRANSITIONING TO COOLDOWN" is displayed on the AMLCD. "NORM STOP/COOLDOWN pushbutton indicator illuminates.
T = +300 seconds	**UEC de-energizes FOSV** and starts a 90-second timer. If T5.4 and FMP is not less than 400 deg F and 50psig respectively, a "Normal Stop Failure" alarm occurs. When Ngg and FMP is less than 3500 RPM and 50 psig respectively, the "OFF" LED indicator on the SCU and PACC will illuminate. When Npt decreases to 500 RPM and FMP is less than 50 psig, the SCU commands the PT brake to engage. "GTM __ STATE OFF" will be displayed on the AMLCD.

The item in bold font is the operation visible in the UEC power trace, completing the GTM start FSM. The FOSVs as well as the SARV are commanded closed by the removal of the +28VDC signal used to open the valves, resulting in a drop in UEC power. Figure 4-1 below shows the typical power data obtained by the NILM during a GTM start.

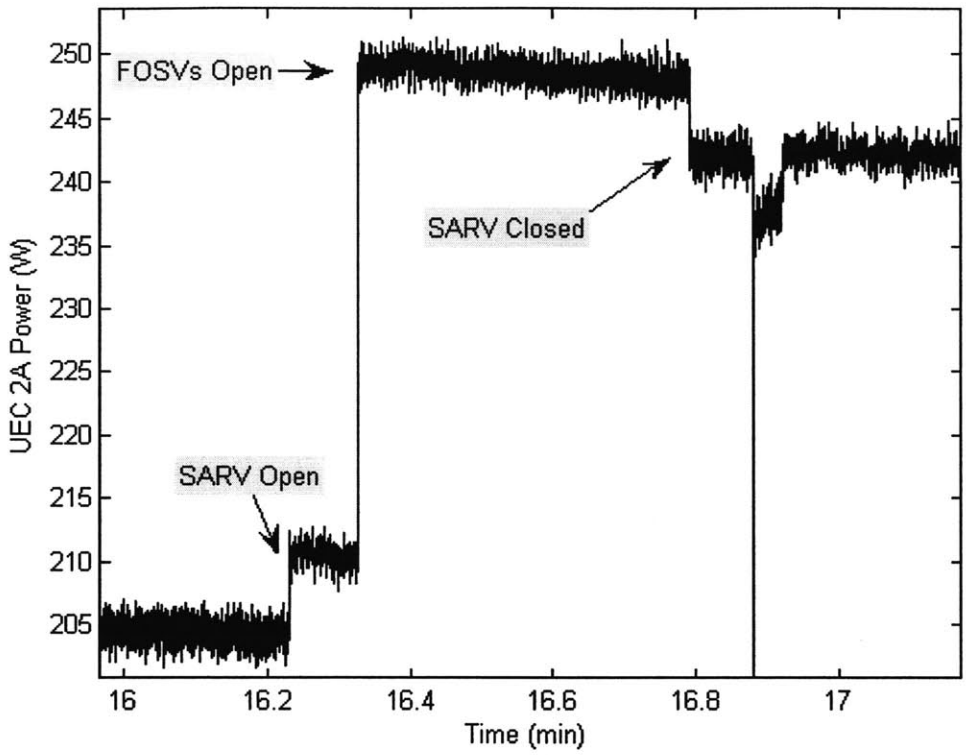

Figure 4-1: Power drawn by the UEC during a normal turbine start

Not shown in the figure is the drop in UEC power when the FOSVs are closed and the engine is stopped. When this occurs, the UEC power returns to the GTM off power level of approximately 205 W. The simple FSM developed for the UEC GTM start considers only power changes caused by the operation of electromechanical actuators controlled by the UEC and is shown below in Figure 4-2. Initially, the GTM is off and both the SARV and FOSVs are closed, so the UEC would be in the top most state shown in Figure 4-2. Once the SARV is opened, the UEC power increased triggering a transition to the next state. Similarly, other power level changes trigger other state transitions.

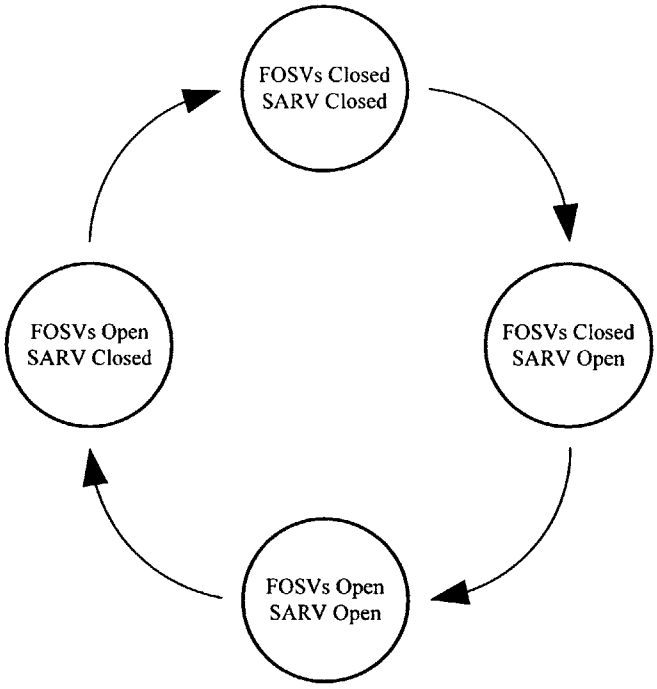

Figure 4-2: FSM model corresponding to the power transitions that occur on the UEC input bus during a normal turbine start

GTM motors and fuel purges are another event that can be easily recognized by the NILM and characterized by a simple finite state machine. During a GTM motor, the start air pressure is reduced to approximately 20 psig by actuation of the Motor Air Regulating Valve (MARV) to rotate the gas turbine at approximately 2200 rpm for maintenance and casualty response purposes. Fuel purges are performed during a GTM motor to purge old or cold fuel out of the GTM prior to a start. Figure 4-3 is the UEC power data collected by the NILM during a GTM motor. The only tasks performed by the UEC during a motor are opening and closing the SARV.

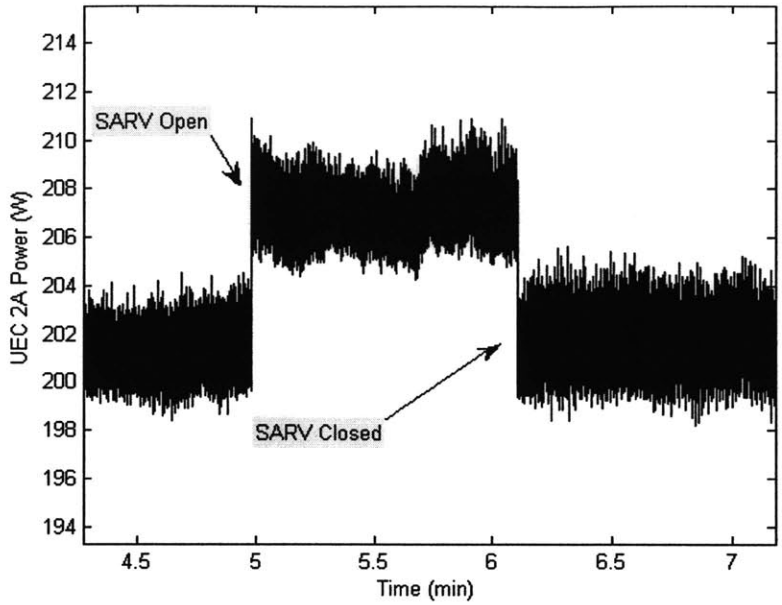

Figure 4-3: Power drawn by the UEC during a turbine motor

For a fuel purge, the fuel purge solenoid valve is not controlled by the UEC, but rather the SCU. Therefore, the UEC power trace for a fuel purge is the same as that for a motor, as shown in Figure 4-4 below.

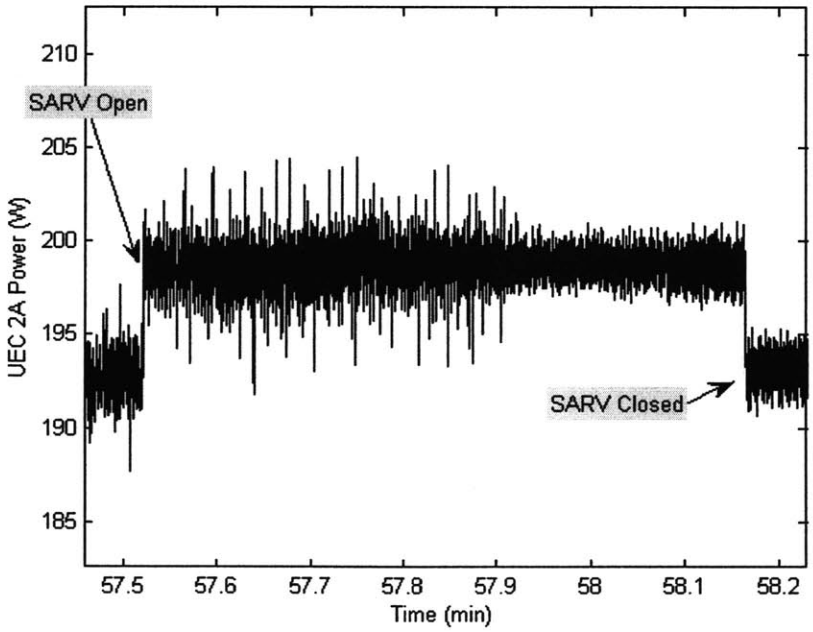

Figure 4-4: Power drawn by the UEC during a fuel purge

Note that even though Figure 4-3 and Figure 4-4 are power traces of the same UEC, UEC 2A, the initial power level is slightly different; approximately 202W in Figure 4-3 and approximately 193W in Figure 4-4. These "snapshots" are of different events on different days. It is unknown exactly why the power levels are different and the reason may ultimately be difficult to determine as many factors present in a complex system such as the LBES plant may affect the power drawn by a particular piece of equipment. Of importance to the NILM is not the aggregate level of power, but the power change. In this particular case, the power change for both operations is cause by the same event, actuation of the SARV, and the power change is consistent at approximately 6W.

The motor and fuel purge are treated as separate events even though in this case the actions are the same. For the purpose of the UEC FSM, however, the same model can be used for both events and is shown below in Figure 4-5.

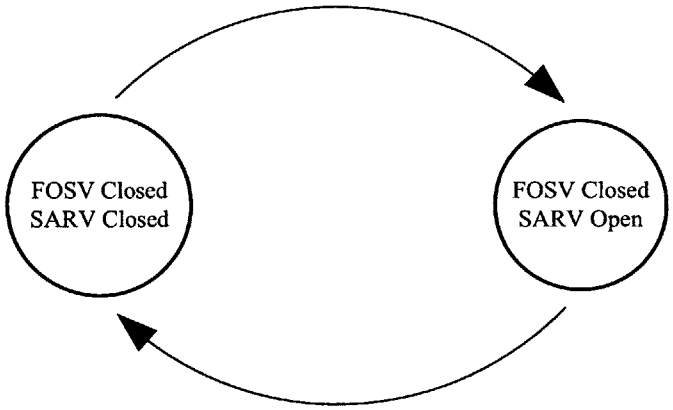

Figure 4-5: FSM model corresponding to a UEC motor and fuel purge

4.1.2 SCU

At this stage of data analysis three events have shown to exhibit consistent unique SCU power signatures: GTM start, motor and motor & fuel purge. Once the GTM start command is issued by the SCU, the next SCU function during a start is to open the GTM module cooling vent damper and issue start command to the module cooling fan (Table 4-1 refers). The module vent damper is opened and closed by an electrically controlled pneumatically operated actuator. Like the SARV and MARV, the vent damper requires a continuous +28VDC signal to remain open. This signal results in an increase in power drawn by the SCU as shown in Figure 4-6 below.

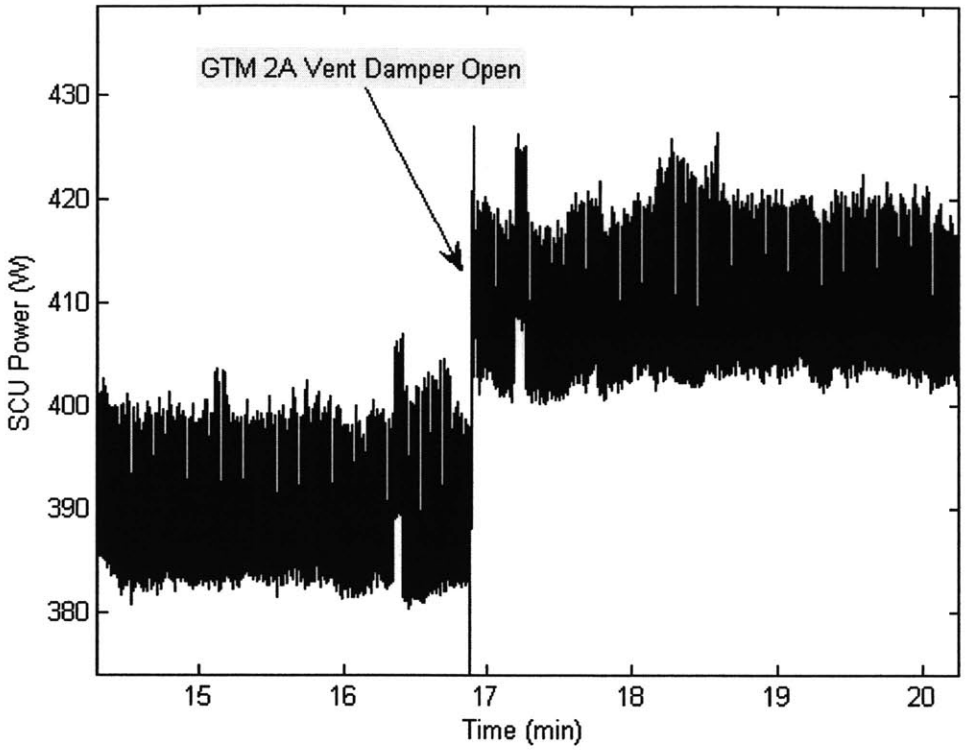

Figure 4-6: Power drawn by the SCU following a GTM start

The power drawn by the SCU increases by approximately 20W when the vent damper opens. Data analysis has shown the total SCU power drawn when both vent dampers are open increases by approximately 40W, 20W for each damper. The corresponding SCU FSM is shown below.

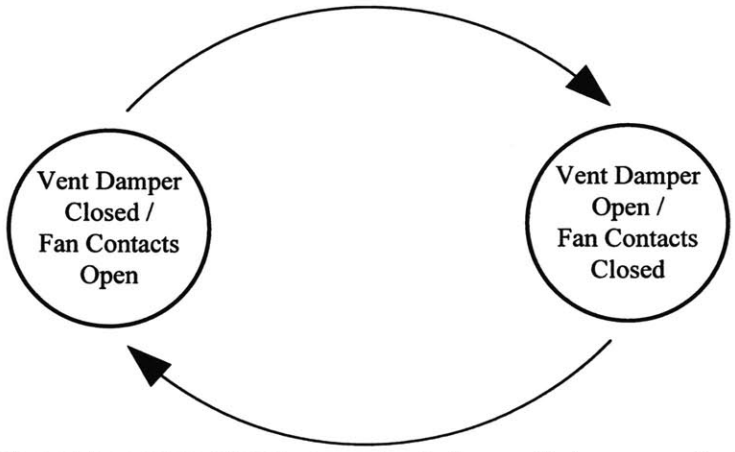

Figure 4-7: FSM model corresponding to power level changes that occur on the SCU input bus during a normal turbine start

This particular FSM model only considers power changes due to electromechanical actuators controlled by the SCU. The initial FSM state is shown on the left.

When performing a GTM motor, the SCU applies a continuous +28VDC signal to the MARV causing a rise in SCU power. The SCU motor power trace and corresponding FSM are below in Figure 4-8 and Figure 4-9 respectively.

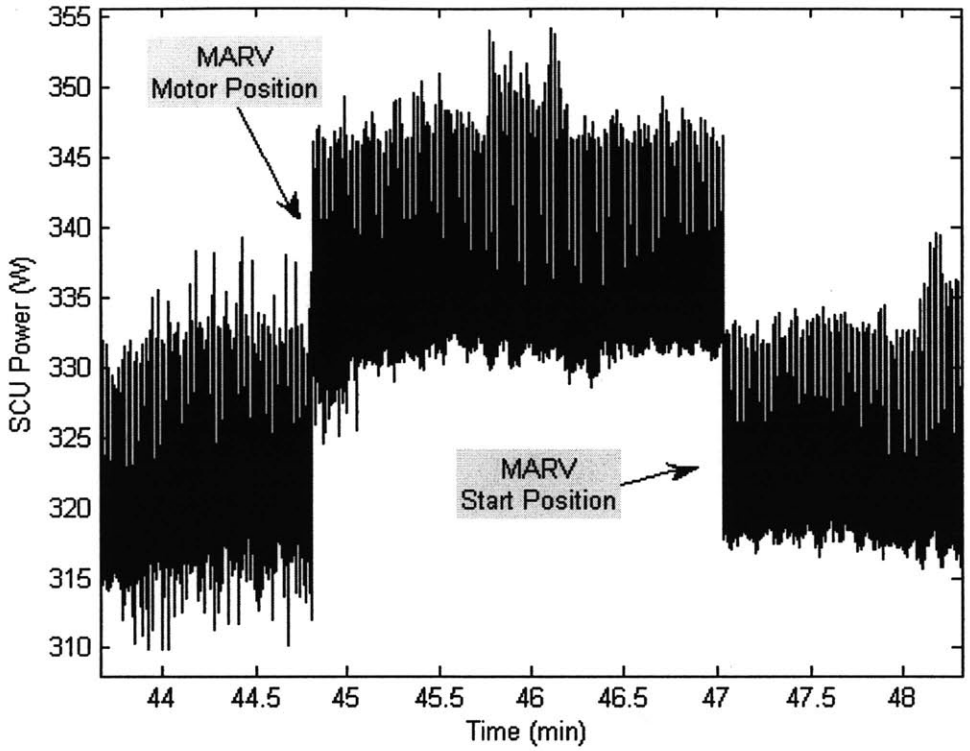

Figure 4-8: Power drawn by SCU during GTM motor

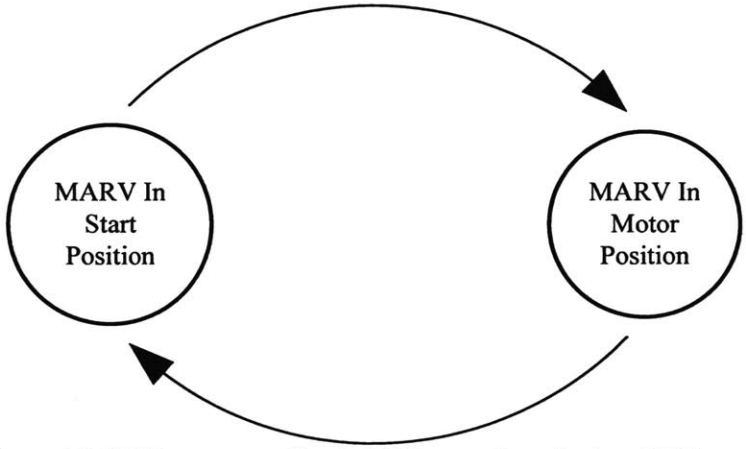

Figure 4-9: FSM corresponding to SCU operations during GTM motor

During a fuel purge, residual fuel present in the turbine is flushed out with fresh fuel during a motor. The fuel purge solenoid requires another continuous +28 VDC signal from the SCU to remain open and allow the purge causing an additional rise in SCU power as shown in Figure 4-10 below.

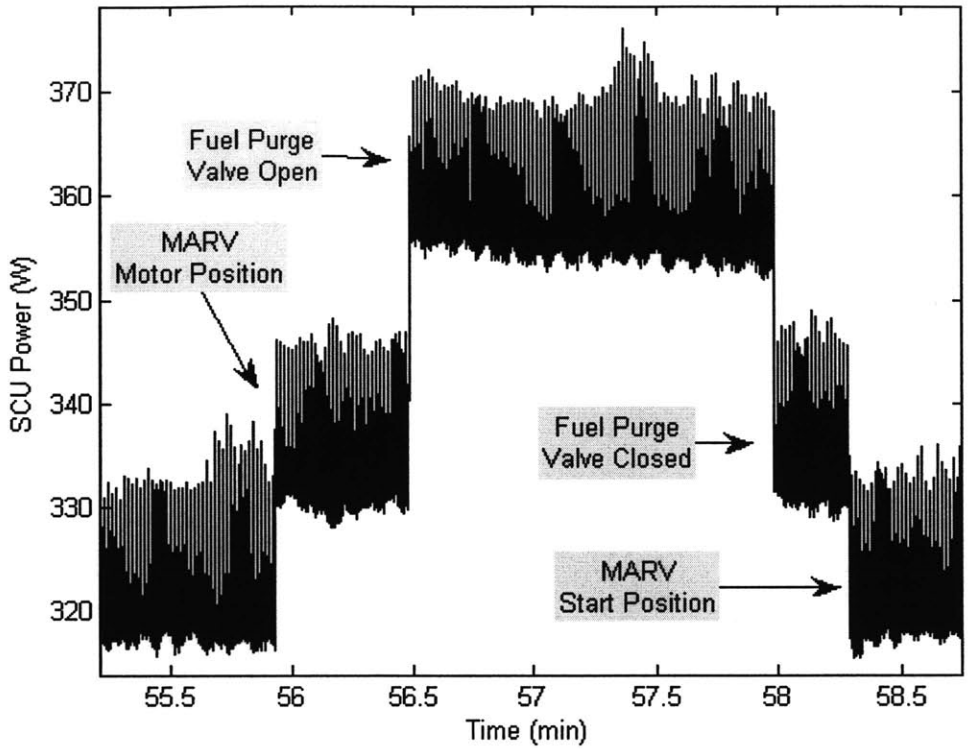

Figure 4-10: Power drawn by the SCU during a GTM motor and fuel purge

The corresponding FSM for is below in Figure 4-11. The initial state is shown at the top of the diagram.

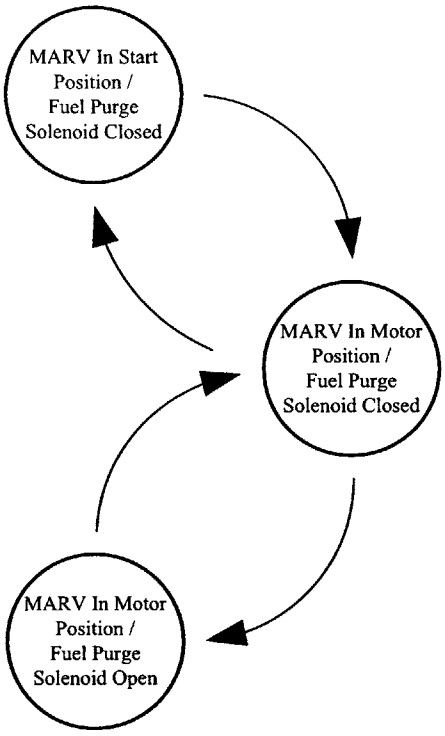

Figure 4-11: FSM corresponding to SCU motor and fuel purge

The motor and fuel purge is a manual evolution performed by the operator from either the PACC or the SCU. The operator must initiate the motor by depressing the motor button on the console. Once the turbine has reached "motor speed" of approximately 2200 rpm, the operator must press the "purge on" button on the console. The fuel purge solenoid remains open until the operator presses the "purge off" button. The operator then stops the motor by depressing the "Normal Stop/Cool Down" button; the turbine stops rotating and the evolution is complete. Although this is the correct procedure, it is possible to perform the evolution out of sequence. Due to the nature of the consistency of the power changes when the MARV and fuel purge solenoid are actuated, it is possible for the NILM to still recognize the evolution and more importantly, recognize that the evolution was performed out of sequence. Figure 4-12 below is the SCU power trace of an out-of-sequence motor and fuel purge. Note that the motor was stopped removing the +28 VDC MARV actuation signal before the fuel purge solenoid was closed. Figure 4-13 is the corresponding FSM.

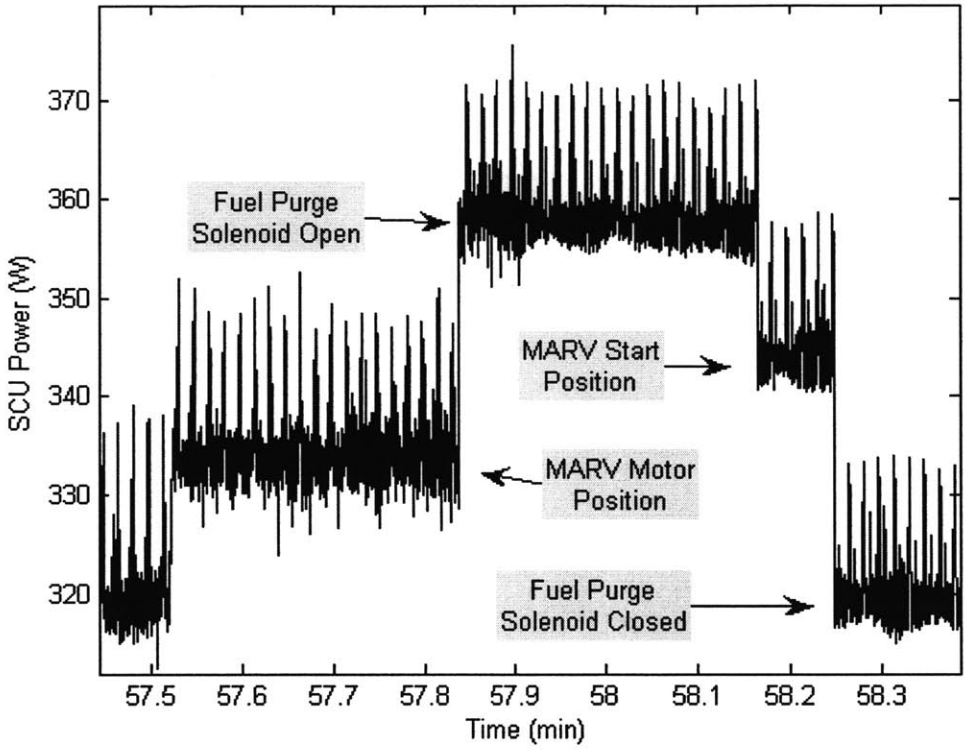

Figure 4-12: Power drawn by SCU by out of sequence fuel purge operation

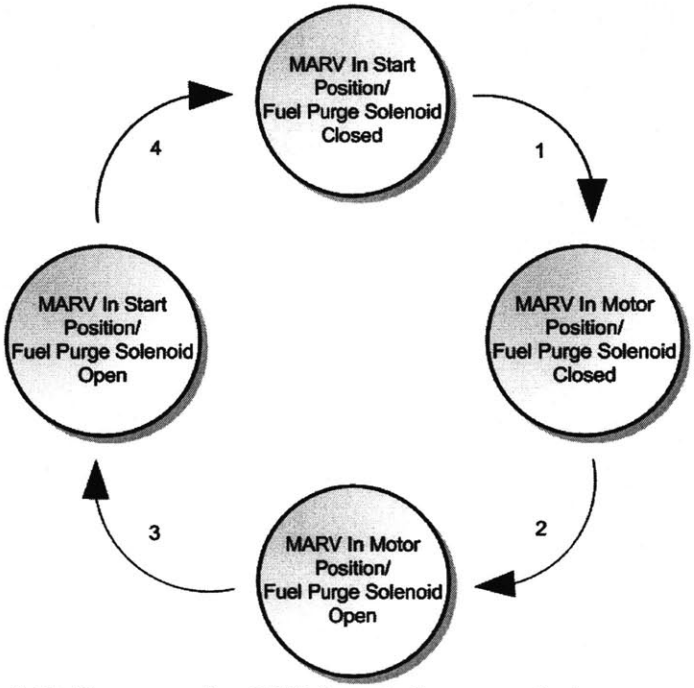

Figure 4-13: Corresponding FSM for out of sequence fuel purge operation

4.1.3 AG9140 GTG

The finite state behavior of the GTG LOCOP controller is similar to that observed for the GTM controllers. Figure 4-14 shows the real power drawn by the GTG NBPS. Recall that the GTG NBPS is the power supply for the LOCOP.

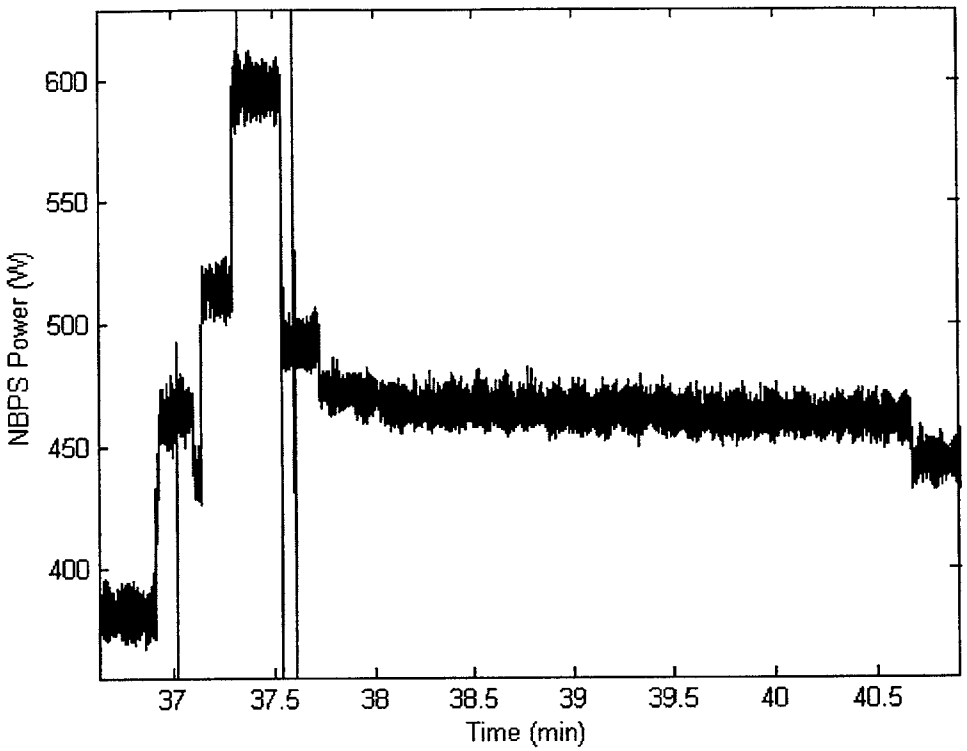

Figure 4-14: Power drawn by the NBPS during a normal GTG start

The GTG start sequence is somewhat more complicated that a GTM start, which explains the more complex power signature. Recall that the 9140RF GTG is equipped with the RIMSS for starting and motoring. The RIMSS itself is a small gas turbine engine, so the GTG start sequence and resulting power trace involves the start of two gas turbine engines. Each of the many transitions corresponds to actions of various relays and solenoids during the start. Note that the system progresses rapidly through many of the early states. Close examination of the power trace reveals 9 discernable states. The complex start sequence of the RIMSS start is shown in Table 4-3 below. In the table N1 refers to RIMSS turbine speed and K34 refers to main turbine speed.

Table 4-3: GTG RIMSS Start Sequence

Speed Channel	Actions/Events
Start Pushbutton Depressed K34 = 0 RPM N1 = 0 RPM **or** K34 ≤ 2000 RPM N1 ≤ 1215 RPM	1. RIMSS exhaust damper opens 2. GTG enclosure cooling air dampers open, and cooling fan starts 3. RIMSS starter motor energized (on) 4. The following circuits are armed: a. Cooling Fan Not On Alarm b. Cooling Air Damper Closed Alarm

	c. Exhaust Damper Closed Shutdown 5. RIMSS Start Attempts counter increments 6. RIMSS engine N1 accelerates
N1 = 4080 RPM	Igniter energized (on)
N1 = 6120 RPM	1. Fuel shut-off valve energized (open) 2. Flameout Shutdown circuit enabled
N1 = 25,000 RPM	Igniter de-energized
N1 = 27,500 RPM	Starter motor de-energized
N1 = 29, 500 RPM	Run Lube Oil Pressure Low Alarm and Shutdown circuit is enabled
N1 = 30,000 RPM **(idle speed)**	1. RIMSS cycle counter increments 2. RIMSS engine (N1) continues to accelerate
N1 = 32, 000 RPM	1. **501-K34 start sequence initiated** 2. Aux Lube Oil Pumps start 3. Fuel manifold drain valves energized (open) 4. 5th and 10th stage bleed valves and 14th stage diffuser bleed valves open 5. K34 Slow Start (2) and Start Overtemp shutdown circuits are armed 6. RIMSS engine (N1) continues to accelerate
N1 = 40,000 RPM	1. **RIMSS Power Turbine (N2) starts to rotate and engages 501 K34 thru the transfer gearbox** 2. RIMSS engine continues to accelerate (N1 approaches 50,000 RPM)
K34 = 2200 RPM	1. The following occur on the 501-K34: a. Igniters are energized (open) b. Fuel manifold drain valves de-energized (close) c. Fuel shut-off valves energized (open) d. Fuel paralleling valve energized (parallel operation) 2. K34 Fail to Fire Shutdown and remaining Slow Start Shutdown circuits are enabled
K34 = 7500 RPM	1. Igniters de-energize (off) 2. Fuel paralleling valve de-energized (series operation) 3. One 14th stage diffuser valve closes (actuated from CDP of 16-18 psig at approximately this speed channel)
K34 = 9231 RPM	**RIMSS engine decelerates to idle speed (N1 ≅ 30,000 RPM)**
K34 = 12,225 RPM **(K34 electronic run speed)**	1. ENGINE RUNNING indicator illuminates 2. Generator seawater cooling pump starts, and FM back-up cooling valve (MORPAC) opens 3. Aux lube oil pump stops 4. 14th stage customer bleed air valve circuitry is enabled 5. Total Starts counter increments 6. The following alarm and shutdown circuits are enabled: a. Run Overtemp Shutdown b. Underspeed Shutdown c. High Vibration Alarm d. Lube Oil Pressure Low Alarm and Shutdowm e. Fuel Oil Pressure Low Shutdown 7. **RIMSS 3-minute cooldown timer starts**
K34 = 12,780 RPM	1. 5th and 10th stage bleed air valves and the remaining 14th stage diffuser valve closes 2. Overspeed Shutdown circuit is enabled
K34 = 14,340 RPM	**501-K34 at normal run speed**

Of the approximately 40 events that take place during a GTG RIMSS start, less than half of them are evident in the NBPS power trace. By reviewing the events that occur in the sequence, relating them to the power changes in the power trace, and by comparing their timing in the sequence to speed timing data obtained during an actual start (provided by LBES engineers) shown in Figure 4-15, it was possible to relate the 9 discernable states of the power signature to events in the start sequence. Figure 4-16 is a power trace with states annotated and Table 4-4 lists the actions that occur in each state.

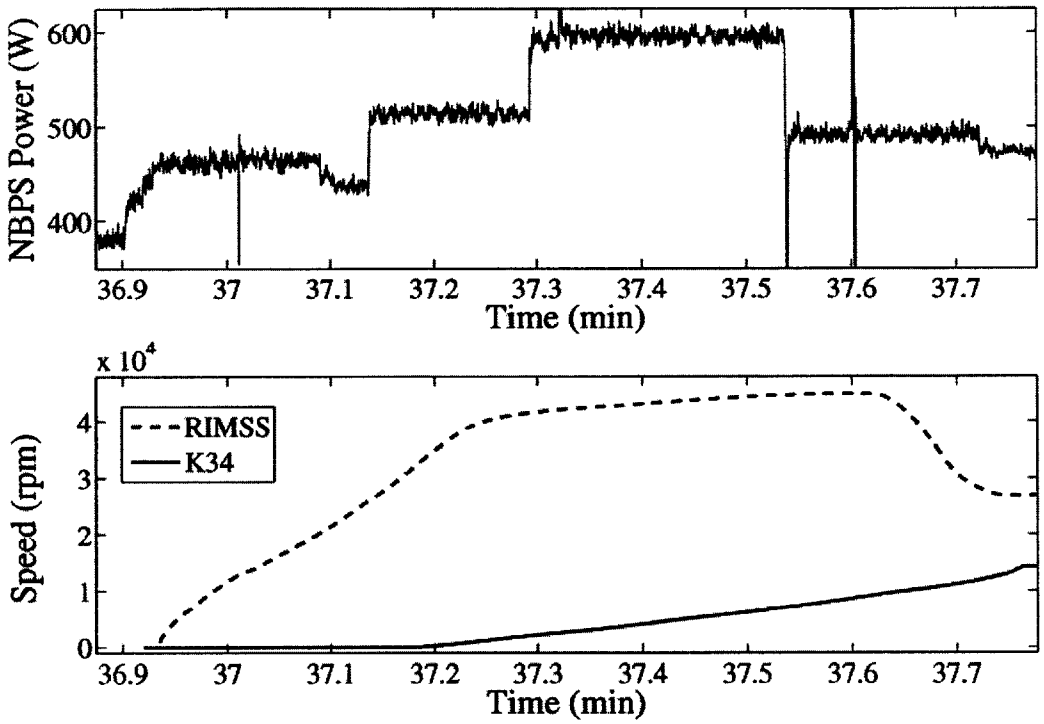

Figure 4-15: NBPS input power and turbine speeds during a GTG start. Note that the RIMSS accelerates rapidly during the early states.

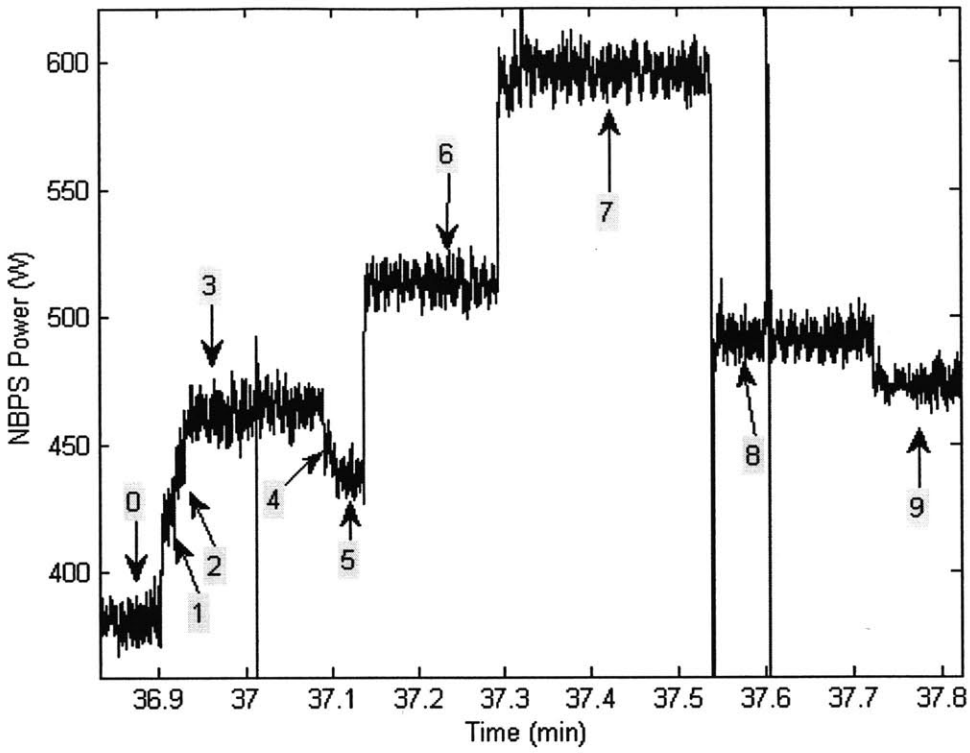

Figure 4-16: Power trace of GTG start with states annotated

Table 4-4: States of the GTG Start FSM

State Number	Actions That Trigger Transition Into State
0 (OFF)	N/A
1	1. RIMSS Exhaust Damper Opens 2. GTG Enc. Cooling Unit Dampers Open 3. RIMSS Starter Motor Energized
2	RIMSS Igniter Energized
3	RIMSS Fuel Shutoff Valve Energized (Open)
4	RIMSS Igniter De-energized
5	RIMSS Starter Motor De-energized
6	1. Aux. Lube Oil Pump Started 2. Fuel Manifold Drain Valves Energized (Open)
7	1. K34 Igniters Energized 2. Fuel Manifold Drain Valves De-energized (Closed) 3. Fuel Shutoff Valves Energized (Open) 4. Fuel Paralleling Valve Energized (Parallel Operation)
8	1. K34 Igniters De-Energized (Off) 2. Fuel Paralleling Valve De-Energized (Series Operation)
9	Aux Lube Oil Pump Stopped (K34 Electronic Run)

The final event in the start sequence is known as the "RIMSS time out" which is when the RIMSS gas turbine actually stops. It is not shown in Figure 4-16 but is clearly discernable in Figure 4-17 at approximately minute 21 and Figure 4-18 at approximately minute 16.

Many other operations performed by the LOCOP manifest themselves in the power drawn by the GTG NBPS. These include GTG stops, GTG motors, and customer Bleed Air Valve (BAV) operation.

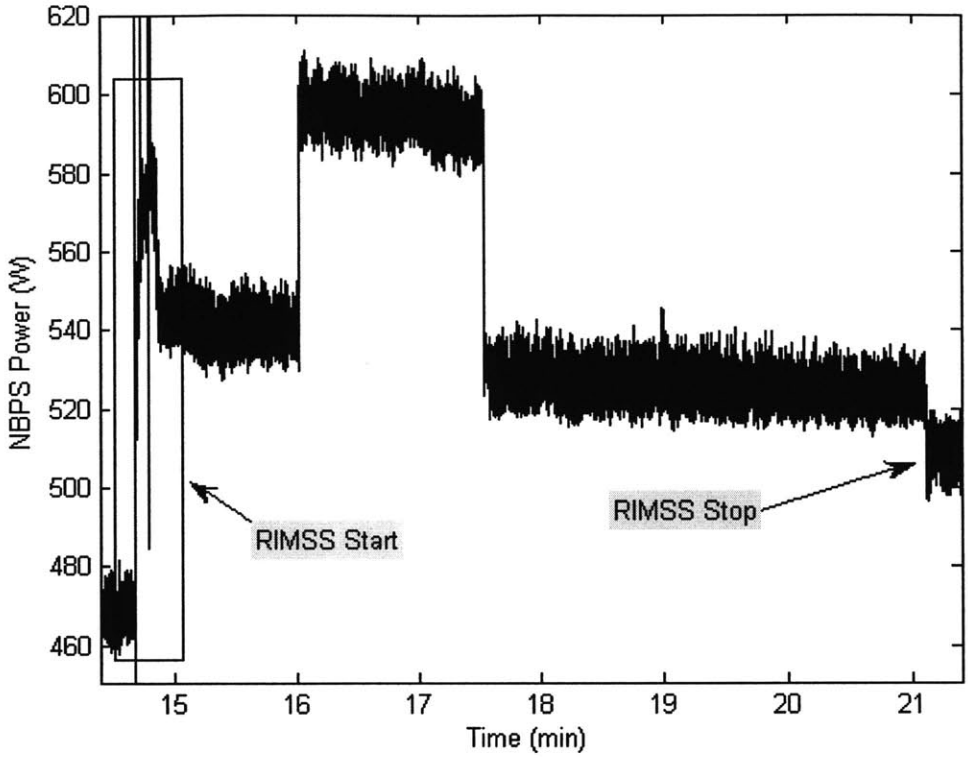

Figure 4-17: Power drawn by the GTG NBPS during a GTG motor

Figure 4-17 above shows the power trace of a GTG motor. The RIMSS start signature can clearly be seen occurring just before minute 15. The RIMSS time out (stop) can be seen at minute 21. This signature is consistent for all GTG motor events analyzed. The 60W increase in power starting at about minute 16.2 is unexplained. It does not correlate to any logged event and [25] does not describe specific events or a sequence incident to a GTG motor. It is perhaps related to the length of time of the motor (i.e. a 2 minute motor of the GTG) but this was not logged in the LBES log for any of the GTG motors thus, making the correlation and identification difficult. As a result, an FSM was not developed for the GTG motor due to the unknown events and their timing that occur during a RIMSS motor.

The actuation of the BAV on the GTG requires a continuous +28VDC signal from the LOCOP and therefore can be seen in the NBPS power trace. The application of the signal causes an increase in NBPS power by approximately 50W (see Figure 4-18 below). The power decreases by the same amount when the actuation signal is removed closing the valve. The BAV FSM (not shown) consists of two states: BAV Open and BAV closed.

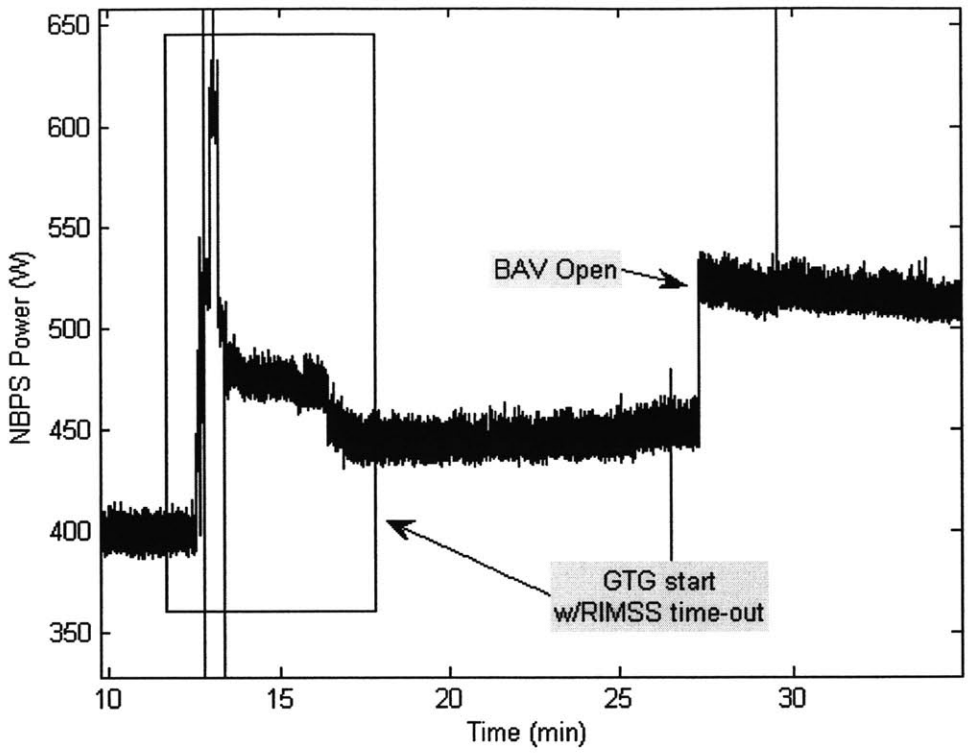

Figure 4-18: Power drawn by the GTG NBPS during a GTG start and BAV open operation

Another consistent power trace is that of a GTG stop. All GTG stops analyzed exhibited similar power signatures to Figure 4-19 below. Like the GTG motor however, it so far has not been possible to correlate the changes in GTG NBPS power with any specific event that occurs when the GTG shuts down.

The GTG is a complex device, even more so than the GTM. Several hours of data was analyzed and reviewed looking for evidence of power load changes, load sharing, manual governor and voltage regulation operations, etc. None of these were positively identified in the NILM power data. As already indicated, some power changes are so far unexplained and there are other unexplained consistent power signatures which are not shown.

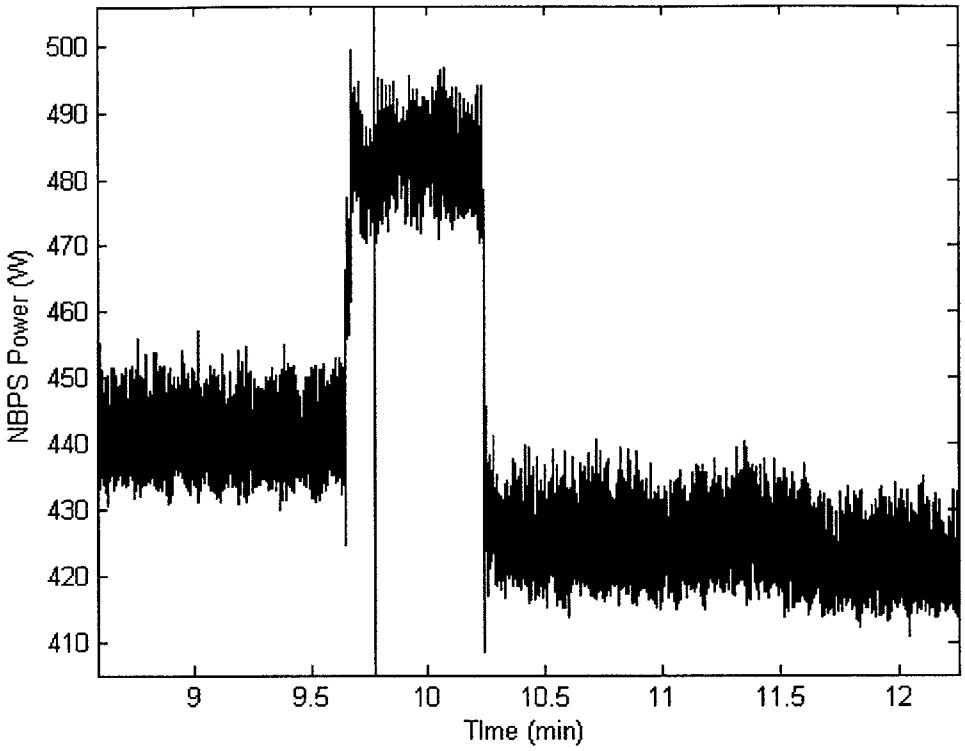

Figure 4-19: Power drawn by the GTG NBPS during a GTG Stop

Chapter 5 Recent LBES Field Testing Results

The most recent LBES crew training session conducted in April 2007 has yielded some results not detected in the analysis of previous LBES operations. This is due in part to NILM equipment improvements and the acquisition of the LBES MCS data log. The MCS data log is a more comprehensive description of plant events than the LBES test manager's written log previously used to correlate NILM power changes to plant events. The addition of this log to NILM data analysis enabled correlation of power changes to plant events that were not possible in the past. This chapter presents some of the findings from the most recent LBES data.

5.1 2A FOSP

FOSP events easily detected in NILM power data include starting, stopping, and the change in pump speed (recall the FOSP has 2 operating speeds). Through careful analysis and comparison to LBES MCS data logs it has been discovered that starts and stops of the other, non-monitored pump can be seen in the monitored FOSP power trace. Notice Figure 5-1 below. While 2A FOSP was running in slow speed 2B FOSP was started at approximately minute 27. The 2A pump was stopped shortly thereafter at approximately minute 27.5. It is important to note that the NILM computer time and the LBES MCS time are not synchronized. The events were correlated by the elapsed time between them and the absence of any other logged events at the time of the change in the power trace.

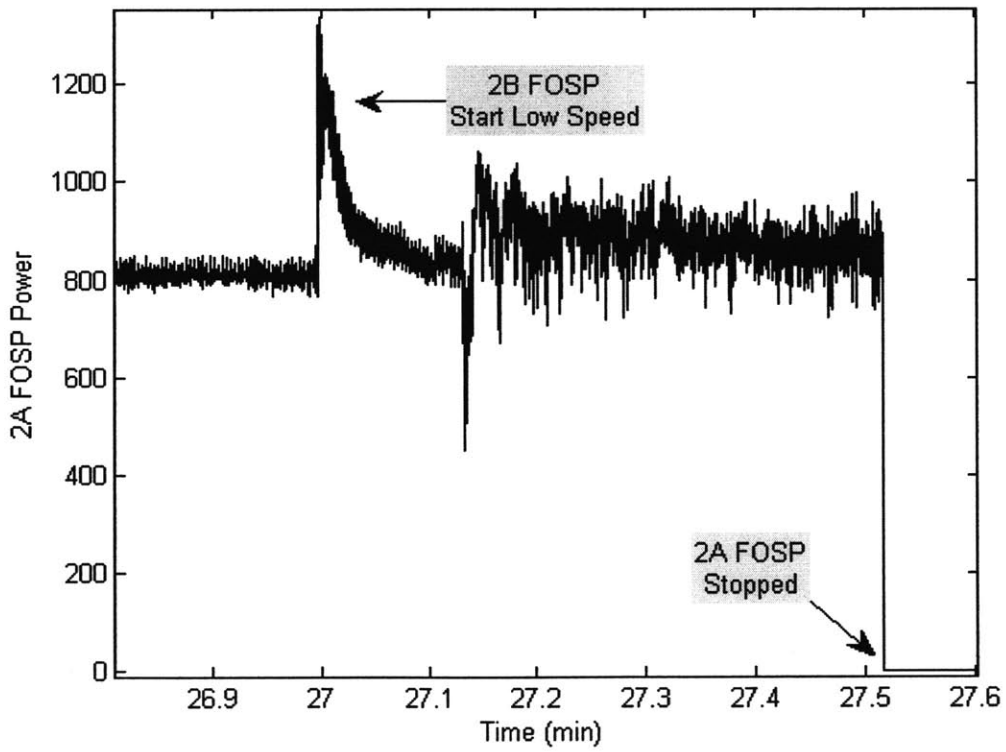

Figure 5-1: 2A FOSP Power Trace

Figure 5-2 below is another example of this phenomenon. The 2A FOSP was started in slow speed just before minute 9. At approximately minute 9.8, the 2A pump was shifted to fast speed as evidenced by the increase in power drawn by the pump. While the 2A pump was running in fast speed, the 2B pump was stopped (it had been running in slow speed). 2A FOSP was then shifted back to slow speed just after minute12.

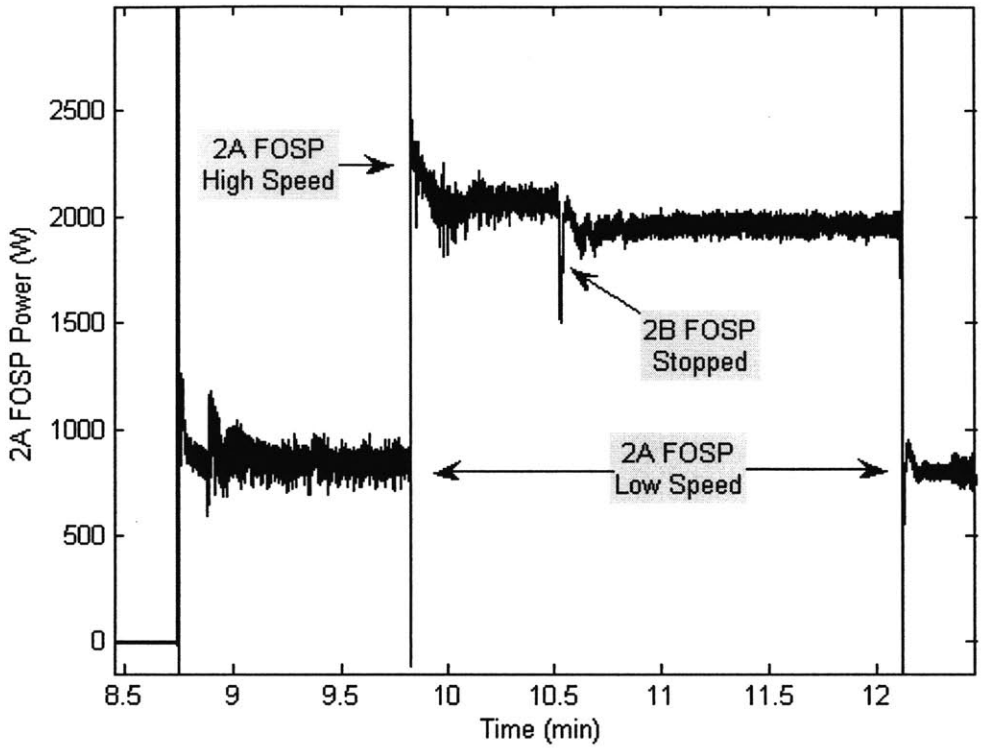

Figure 5-2: Power drawn by 2A FOSP during a FOSP pump shift evolution.

The cause of this power change is not known. Speculation indicates that this may be due to the fact that both FOSPs are positive displacement pumps piped to the same header. Therefore, the online pump motor reacts to the change in fuel flow rate caused by the state change of the offline pump. Further research is needed to validate this theory.

In addition to the starts and stops, bell orders (propulsion shaft speed changes) are also evident in the fuel pump power trace. Figure 5-3 shows the fuel pump response to the following large and rapid speed changes on 13 April 2007 (times are LBES hand-written log times):

- 0902 Ahead Full
- 0905 Ahead Flank
- 0907 Crashback (Back Full)
- 0909 Ahead Flank (logged crash ahead)
- 0911 All Stop

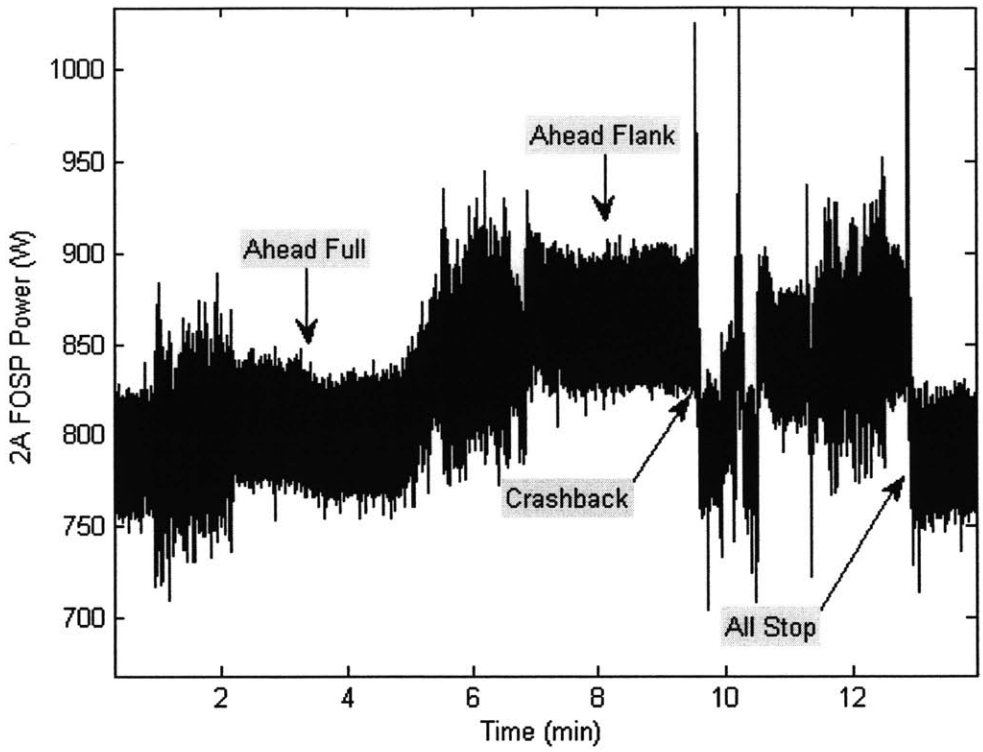

Figure 5-3: Power drawn by 2A FOSP in response to speed changes

When Ahead Full (representing about 20 knots ship speed) was ordered and steady state achieved, the FOSP responded with an increase in power which is annotated Ahead Full in Figure 5-3 and Figure 5-4. FOSP power again increased when Ahead Flank (representing about 30 knots ship speed) steady state was reached, also annotated on the figures. The significant event in annotated in Figure 5-3 is the crashback. A crashback is performed to stop the ship in the shortest distance possible from Ahead Flank (maximum ahead speed) by quickly ordering Back Full (maximum astern speed). When the crashback is ordered, the engine throttle (known as the Programmed Control Lever (PCL)) is moved in one continuous motion from Ahead Flank to Back Full. When the crashback is ordered, the engine power is immediately reduced and on an actual ship the propeller pitch begins the transition from full ahead (+100% pitch) to full astern (-44% pitch). Recall the LBES shaft does not have a controllable pitch propeller; the water brake performs that function and provides a similar response. The corresponding drop in FOSP power is a direct result of the reduced engine power. When the propeller pitch has reached its full astern pitch, engine power is increased to answer the Back Full ordered bell.

Figure 5-4 below is a zoomed in view of Figure 5-3, starting about minute 8.5. In this particular sequence, once full astern speed was attained (represented by the increase in FOSP power from approximately minute 9.5 to minute 10.2) Ahead Flank (logged as crash ahead in the LBES test manger's hand written log) was ordered. Note that based on the power trace, the plant did not reach steady state during the full astern bell. The resulting plant response from this maneuver is the reverse of the crashback. Engine power

is reduced to slow the propulsion shaft while the propeller transitions from full astern to full ahead pitch. Once the propeller is at full ahead pitch, engine power is increased to answer the Ahead Flank bell. The FOSP responded in a similar fashion reaching steady state in the full ahead bell at approximately minute 10.5. Finally, at approximately minute 13, All Stop is ordered. Engine power is reduced to idle as the propeller pitch transitions to zero thrust and the FOSP responded accordingly.

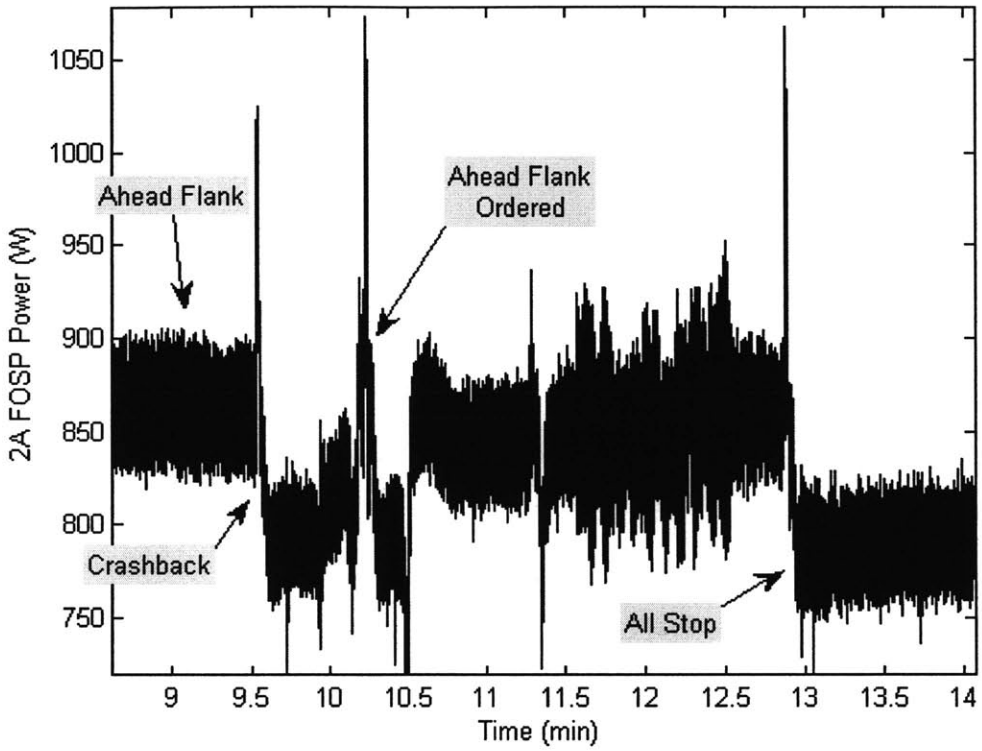

Figure 5-4: Close up of power drawn by 2A FOSP during speed changes

It is important to note that the speed change sequence and FOSP response describe above is a theory based on the data available and the extensive operational experience of the author. Review of other FOSP data collected during propulsion shaft speed changes revealed that not all speed changes manifest themselves in the FOSP power trace. The reason for this is believed to be that small, gradual changes do not put enough demand on the system to elicit a power response from the pump. However, large, rapid changes such as a crashback can be detected in the power trace, as the fuel pump responds to the rapid changes in fuel demand. Additionally, it appears that as speed increases (and therefore engine power also) so does the FOSP power demand. Although not enough significant speed changes are were analyzed for this thesis, they do represent a noticeable deviation from the normal steady state FOSP power trace, which remains relatively constant during most plant evolutions. More analysis of this type is needed to validate these conclusions.

5.2 2A LOSP

Similar to the FOSP, LOSP starts, stops, and pump speed changes can be easily detected in the LOSP power trace. Starts and stops of the unmonitored pump also are

evident. Figure 5-5 below shows the 2A LOSP power trace while operators are shifting pumps from 2B LOSP to 2A LOSP. LOSP states are annotated on the figure.

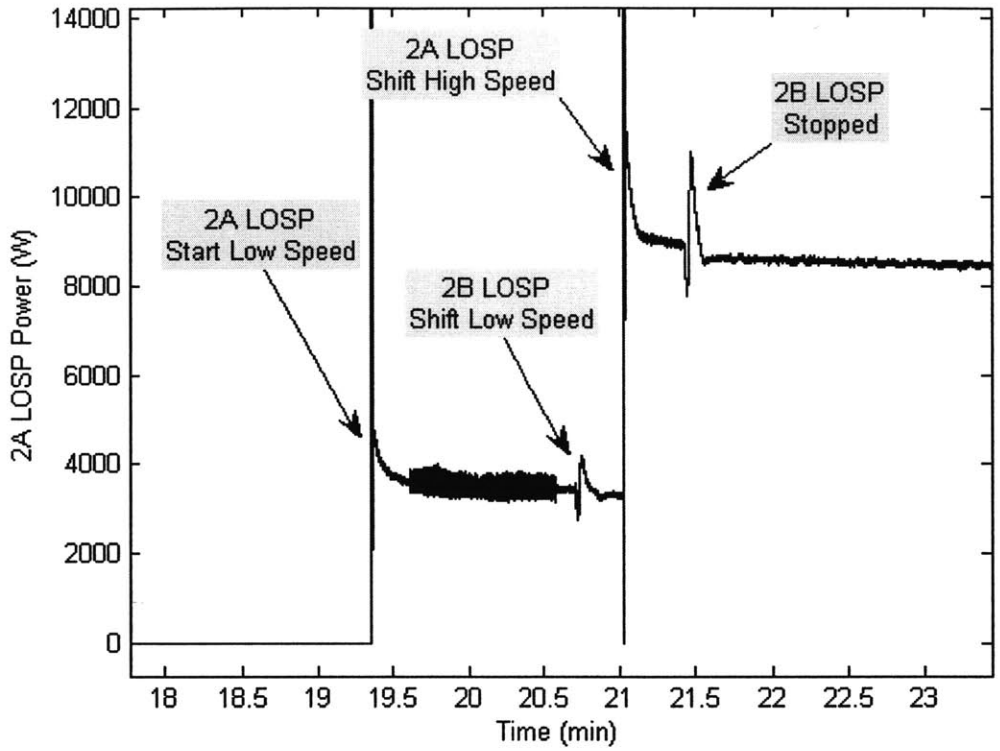

Figure 5-5: Power drawn by 2A LOSP during an LOSP pump shift evolution

The LOSPs are positive displacement pumps piped to the same header. This is believed to be the reason why the unmonitored LOSP state changes are present in the monitored LOPS power trace. Again, further research is required to validate the theory.

Also like the FOSP, the LOSP exhibits a power response to speed changes. The demand for lubrication oil provided by the electric LOSP changes with the speed of the propulsion shaft and MRG. Figure 5-6 is the LOSP power data collected during the same speed change sequence described in Section 5.1.

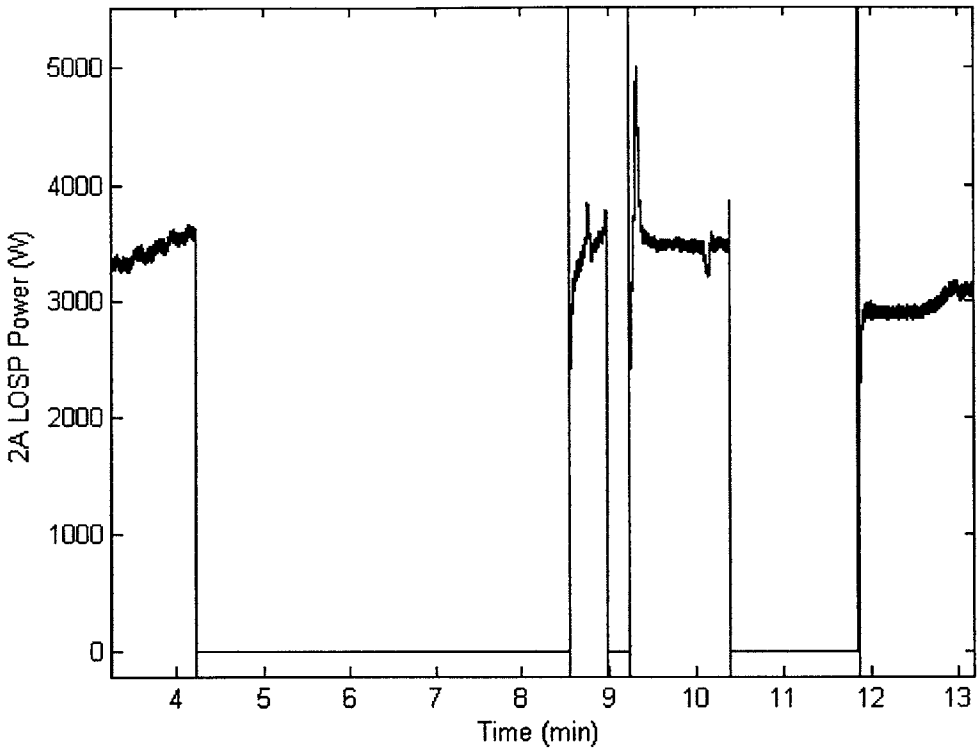

Figure 5-6: Power drawn by the LOSP during speed changes

It can clearly be seen where the LOSP was stopped during this high speed run of the LBES plant. Recall that the Lube Oil Service System is equipped with an attached mechanical lube oil pump. At sufficient speeds this mechanical pump provides sufficient lubrication and the electric LOSP is not needed. Therefore, the electric LOSP is stopped by the operator. Pump logics operating from mechanical pressure switches automatically start the electric LOSP when lube oil pressure drops below a certain set point. Further details are located in [40]. The automatic starts can be seen at approximately minutes 8.6, 9.2, and 11.9. LOSP power isn't as closely related to engine speed as FOSP power. Therefore it is much more difficult to specifically match LOSP power changes with propulsion shaft speed changes. Because of the uncertainty involved, annotating the power trace with the bell orders from the LBES log was not attempted.

5.3 LPAC

LPAC NILM data analysis presented in [6] revealed that the LPAC power response to load and unload cycle times was related to plant events. Figure 5-7 below is a snapshot of LPAC data captured during a Nr 2 GTG start. The start is annotated "Air Start" because the Nr 2 GTG is not equipped with RIMSS and thus air starts are the only alternative.

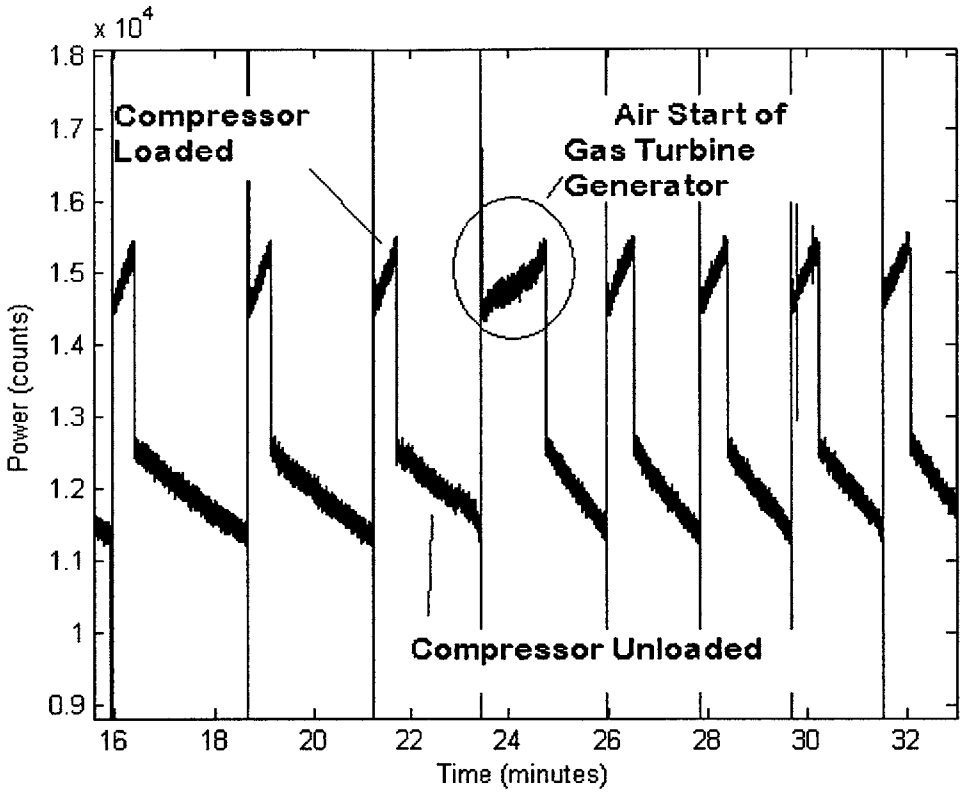

Figure 5-7: Plot of the real power drawn by the LPAC before, during, and after an air start of Nr 2 GTG. The units of real power are shown here to be counts, and they reflect the scale factors introduced by the NILM and were not converted to Watts [6].

The time of the GTG start is annotated on the figure. Note the increase in LPAC load time as a result. This is due to the use of LP air in the actuation of a pneumatic vent damper and other events that occur during a GTG start [25].

The same LPAC response was not observed in the recent LPAC NILM data collected from February to April 2007. In fact, this LPAC data revealed a power response indicative of some erratic behavior exhibited by the LPAC. Figure 5-8 and Figure 5-9 below show the inconsistencies in LPAC behavior from April 2005 to April 2007.

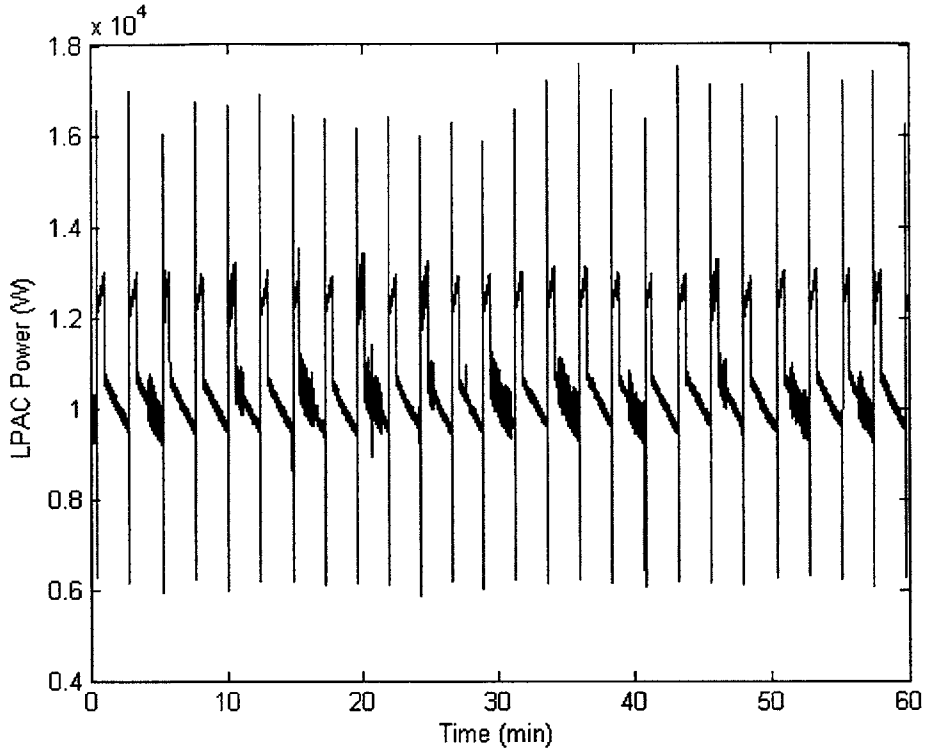

Figure 5-8: Power drawn by the LPAC during plant operations on 20 April 2005

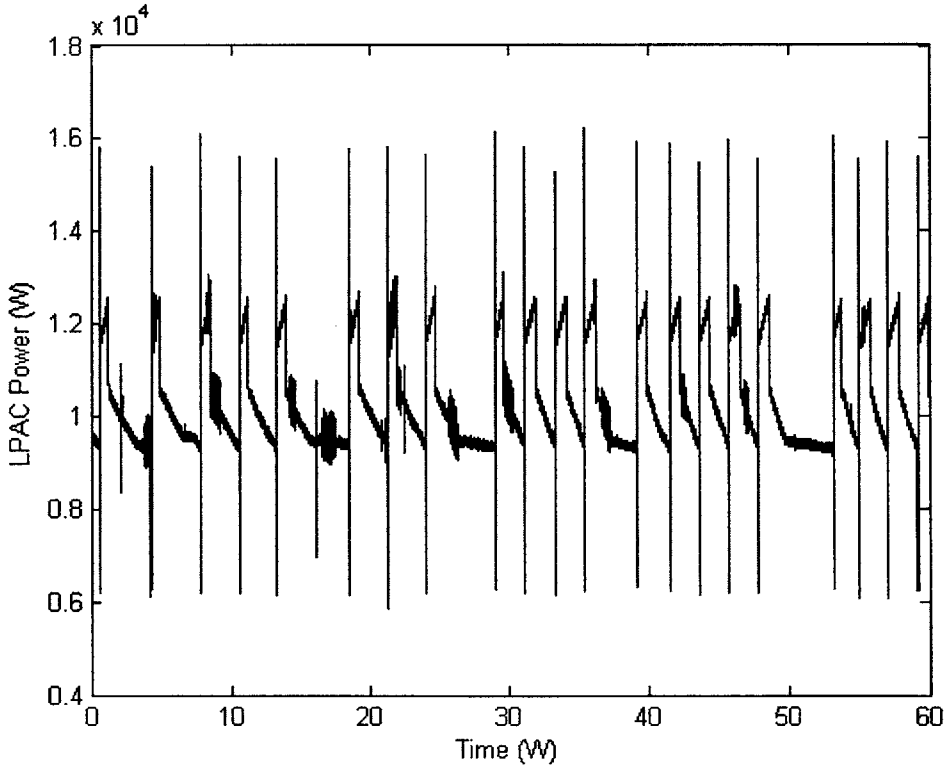

Figure 5-9: Power drawn by the LPAC during plant operations on 16 April 2007

Note that the LPAC load and unload cycles shown in the power trace in Figure 5-8 are fairly consistent throughout the hour. This figure is representative of LPAC behavior around this particular time (April 2005). In contrast, the load times in Figure 5-9 appear to be fairly consistent, but the unload cycles shown do not. Several times during this hour there is a significant change in the slopes of the unload cycles in the power trace, indicating a change in unload cycle time. This is representative of LPAC behavior in April 2007 and was first noticed in data collected in February 2007.

It is unknown what may have caused the change in LPAC behavior. It is believed that something either in the LBES LP Air system configuration or the LPAC itself has changed to cause the change in response. Whether or not the change is due to some sort of failure or imminent failure is also not known. In order better understand this behavior a pressure sensor was installed on the LPAC to measure the LP Air pressure (see Section 3.2.3 for sensor details). Figure 5-10 below shows the LP Air Pressure as it relates to the power drawn by the LPAC during operation. Note that during the unload cycle beginning at approximately minute 48.5, the reduction rate of LP Air pressure slows significantly at about minute 49.5. The cause of this change is unknown.

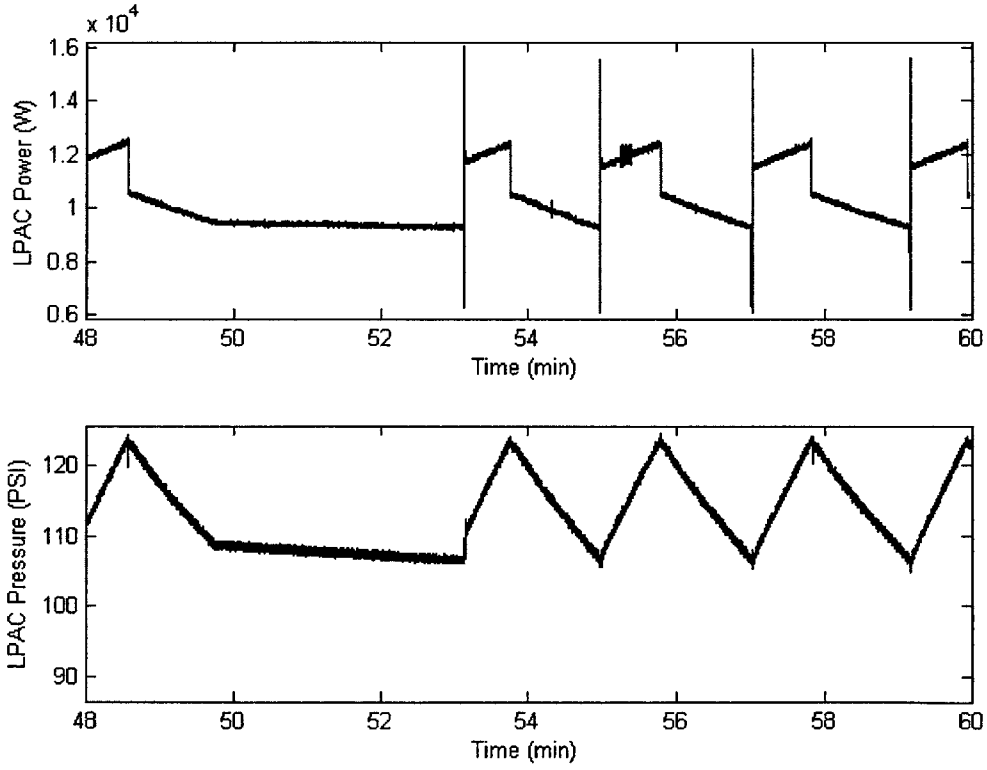

Figure 5-10: LPAC Power and Pressure Trace

5.4 New Trends

As the research for this thesis progressed, some new NILM experiments were conducted which yielded some new insights. The initial results presented below further highlight the NILM's potential as an effective, low cost supervisory monitoring and control device.

5.4.1 Power Panel 1-282-1

An ongoing project is the development of a system that minimizes the overall level of intrusion. Recall that a NILM has been installed on Power Panel 1-282-1, the distribution panel that feeds all of the GTM controllers and several critical support loads. The monitored loads include the following:

- UEC2A
- UEC2B
- SCU
- Igniters for the 2A GTM
- Igniters for the 2B GTM
- Lighting and heating for the various turbine modules and controllers

Figure 5-11, Figure 5-13, Figure 5-13, and Figure 5-14 all show some results from the initial tests. The data presented in these figures was recorded during GTM starts. Note that the level transitions in each of the component streams are still visible in the aggregate. Furthermore, note that we are now able to monitor the behavior of the igniters, as detailed in close up Figure 5-12 and Figure 5-14. It is worth noting from Figure 5-12 that the igniters inside the 2A turbine draw power waveforms that display a significant amount of high frequency content. This is not the case for the 2B turbine, as evidenced Figure 5-14, suggesting that there may be opportunities to develop new and critical diagnostic indicators.

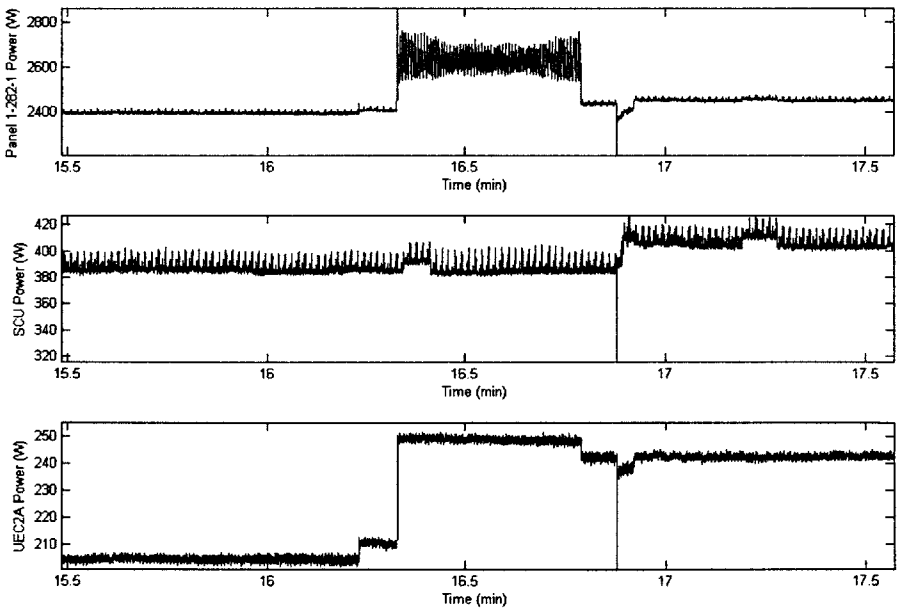

Figure 5-11: Power drawn during start of GTM 2A

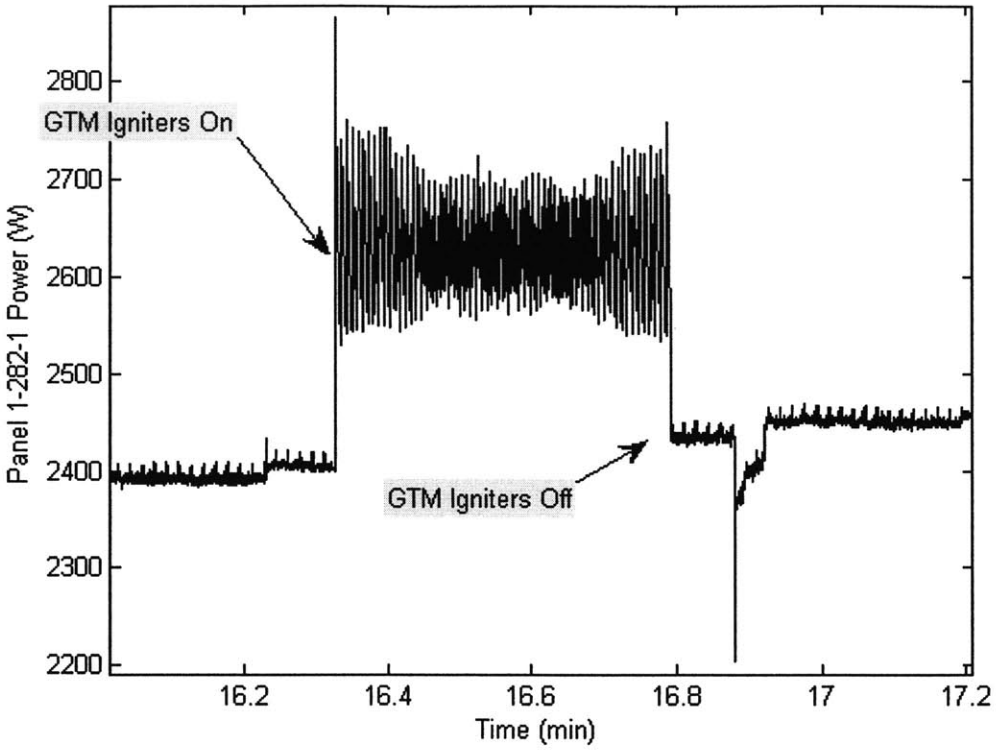

Figure 5-12: Close up of panel power drawn during the GTM 2A start shown in Figure 39

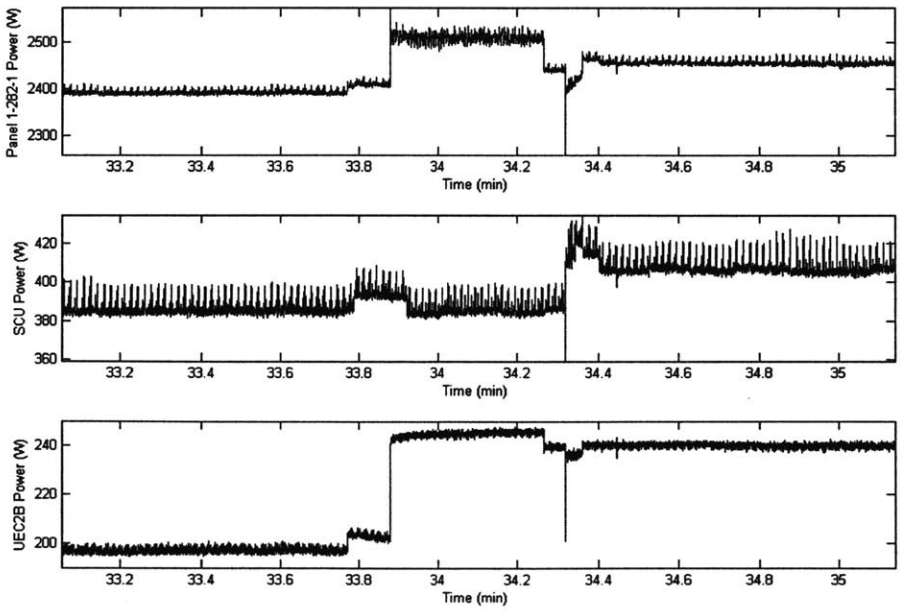

Figure 5-13: Power drawn during start of GTM 2B

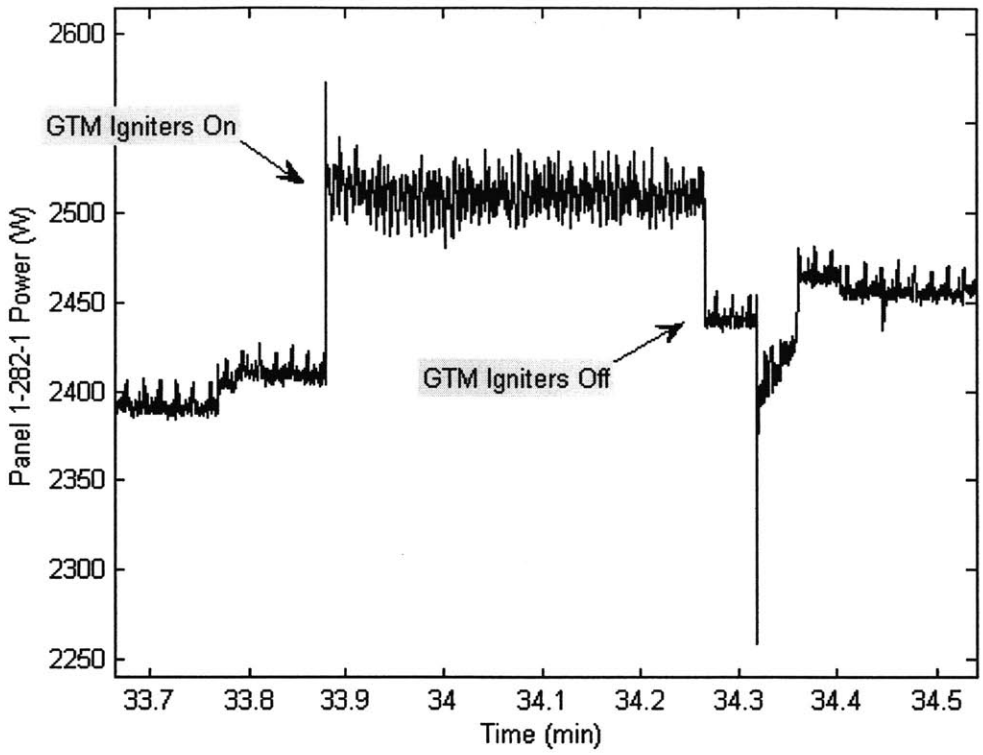

Figure 5-14: Close up of panel power drawn during the GTM 2B start shown in Figure 41

5.4.2 GTM Cooling Fan

Figure 5-11 and Figure 5-13 highlight another potential benefit of the NILM. Note the disturbance located in each of the data streams at approximately minute 16.9 and 34.3. This disturbance is the result of a sub-transient voltage sag. Field tests and data analysis has shown that this sag, which is visible throughout the plant, occurs at the same time that the SCU commands the large GTM cooling fan with a 130 HP motor to energize. Figure 5-15 below highlights another example of the cooling fan start and its presence in the power trace of the non-starting UEC as well as the distribution panel aggregate power trace. The ability to identify the source and effects of these power-quality disturbances could make the NILM indispensable to the all-electric warships of the future.

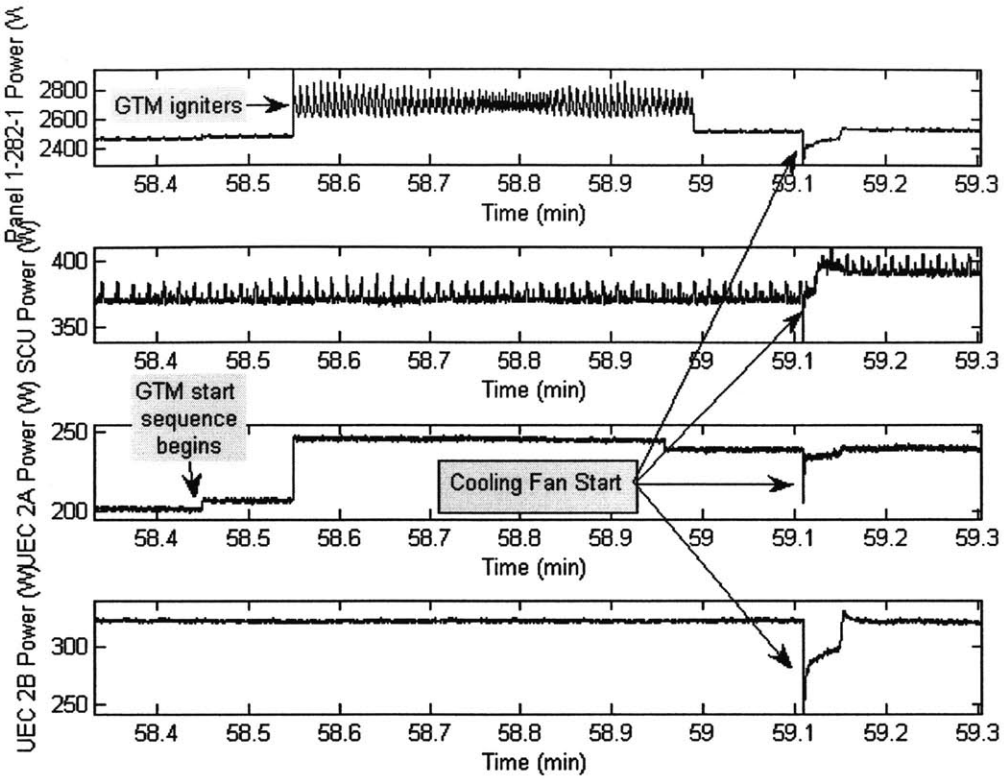

Figure 5-15: GTM Cooling Fan Starts

5.4.3 Event Detection in Reactive Power

In addition to Real Power (P) the NILM software computes Reactive Power (Q) and other harmonics. Therefore, it is possible for the NILM to detect events in the reactive power trace. Figure 5-16 below is a snapshot of 2 GTM starts. The SCU real power trace is on top with the FOSP real power in the center, and the FOSP reactive power is on the bottom. The sub-transient voltage sag caused by the cooling fan starts can easily be seen in the Q trace. There exists, in fact, a power spike in the FOSP P trace, but when viewed separately this spike is difficult to correspond to the fan start, and is sometimes non-existent.

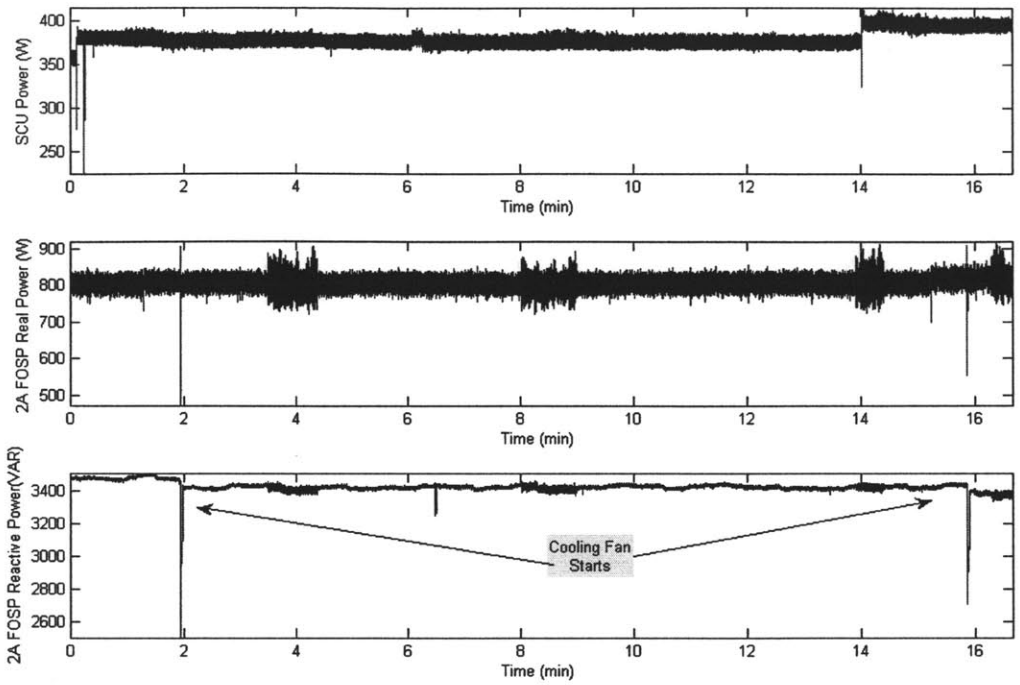

Figure 5-16: Power traces of SCU real power and FOSP real and reactive power captured during GTM starts

It can easily be seen that the SCU and FOSP data is not exactly time aligned with the FOPS start signatures occurring almost 2 minutes after the SCU signatures. This is due to a processing error in which the SCU data files contain less data points than the FOSP data files.

It is also important to note that this particular response is not present in FOSP data for all GTM starts. It is not yet known what factors in either NILM operations or plant operations affect the power response of the equipment.

The Q trace response to GTM cooling fan starts is also present in the LOSP power data. Figure 5-17 below highlights 2 GTM cooling fan starts one at approximately minute 38.5 and the other at approximately minute 43.5. The distinctive shape of the voltage sag is clearly evident in the reactive power trace. In this particular case, there is also a change in the real power as well, but like the FOSP, this is not always the case. Also annotated is the LOSP real power response to the operator placing GTM 2A online. That is, releasing the power turbine brake and allowing the engine to turn the propulsion shaft.

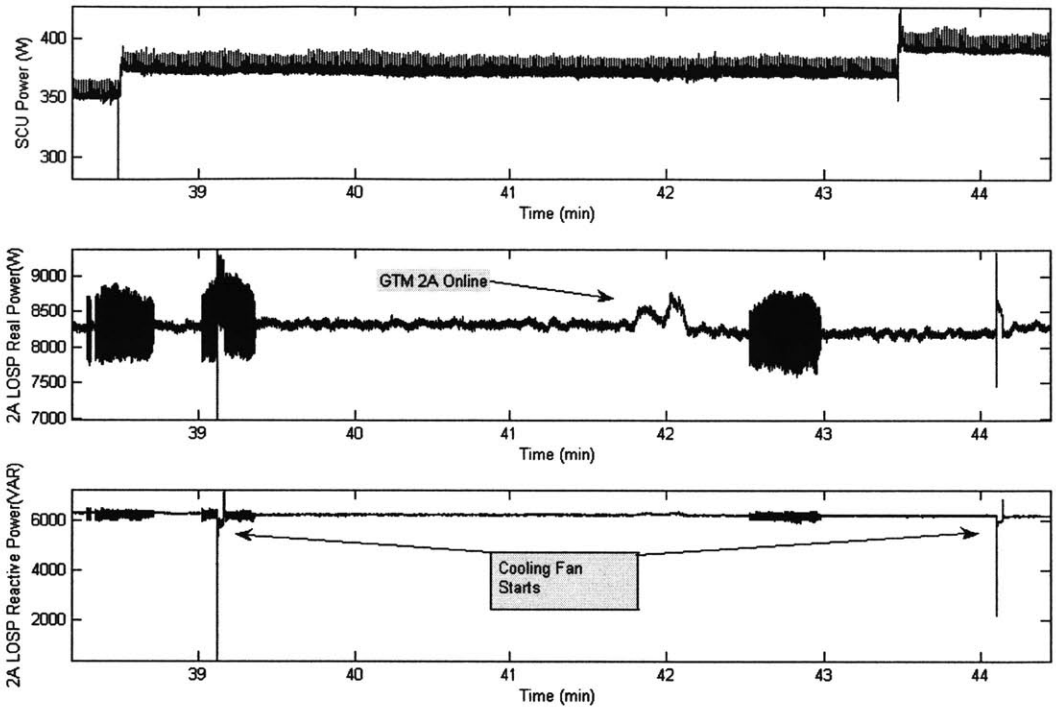

Figure 5-17: Power traces of SCU real power and LOSP real and reactive power captured during GTM starts

Also like the FOSP figure above, it is evident that the SCU and LOSP data is not exactly time aligned, with the LOSP data about 30 seconds behind the SCU data. In this case, all files contained the same amount of data points. The error is due to the algorithm used to time synchronize the computers discussed in the section below.

In order to establish a pattern of responses and to fully understand complex integrated plant operations from a NILM perspective, further analysis is required of the reactive power traces of the FOSP and LOSP. Many more GTM start events need to be analyzed to determine the frequency of these particular events and the factors that affect whether or not they are visible in the power trace. Nonetheless, these initial results presented here are promising and showcase the enormous potential of the NILM.

5.5 Time Synchronization

The real utility and potential of the NILM as a supervisory control device is manifested at the system level. That is, all installed NILMs working together to analyze the LBES plant as a whole. In order to better understand and analyze integrated plant operations using just the NILM power data, the five NILM computers were networked and synchronized in December 2006. Even though the concept is still in its infancy, the initial field results have been promising. It is now possible to view the cascading effects of plant evolutions.

The synchronization works in the following fashion. The SCU computer serves as the master clock and at predetermined set intervals, the other NILM computers "check

in" with the master computer and compare their clocks with the master clock. At that time, clock errors are corrected based on the difference between the two clocks. It is possible, as evidenced by Figure 5-17, that between "check ins" the slave clocks may slightly wander.

Even so, the synchronized NILM network is a vast improvement in analysis of integrated plant operations. Prior to the synchronization, it was nearly impossible in some cases to correlate events detected in NILM power traces with actual events in the LBES plant.

The following figures contain close ups of events during the day on 16 Aril 2007 highlight data analysis and demonstrate the potential if the NILM. Annotated on Figure 5-18 is the LOSP response to the speed changes ordered at approximately 0930 to 0934. Even though the speed orders aren't readily apparent in the SCU or UEC, they can easily be detected by a NILM monitoring the LOSP. During this particular hour the 2A FOSP was off, but it is expected based on previous findings (see section 5.1) that a similar response may be noticeable.

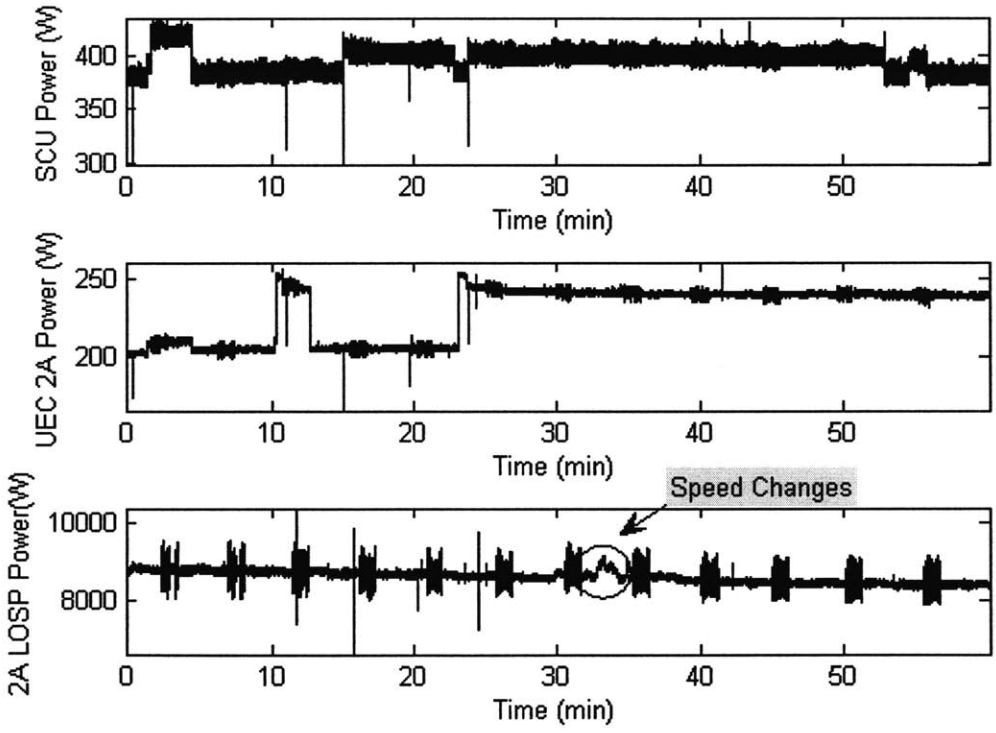

Figure 5-18: Time aligned power traces of the SCU, UEC and LOSP 16 April 2007 0900-1000

One utility of the NILM is fault diagnosis and analysis of time synchronized data can prove beneficial when a problem occurs. As plant equipment cycles through operating states, the NILM can track the state transitions and immediately recognize when a component fails to transition to an expected state. Figure 5-19 below, demonstrates an example. A GTM 2A start was initiated at 0910. Approximately 1 minute later, the GTM cooling fan started, but the associated vent damper did not open, resulting in a cooling system failure casualty, mandating an emergency stop of the engine, which was executed

at 0912. Reviewing the SCU power trace from the figure, the transition to the vent damper open state indicated by a rise in power drawn did not occur. Knowing a GTM start was in progress from the UEC data, the NILM would be "looking" for associated state transition changes in other equipment, such as the SCU. In this particular case, the NILM could have alerted the operator that a problem had occurred with the GTM vent damper. The cause of the failure was remedied and further review of the power data shows the operation of the cooling fan and vent damper, followed by another start attempt at minute 0923 where the vent damper operated correctly.

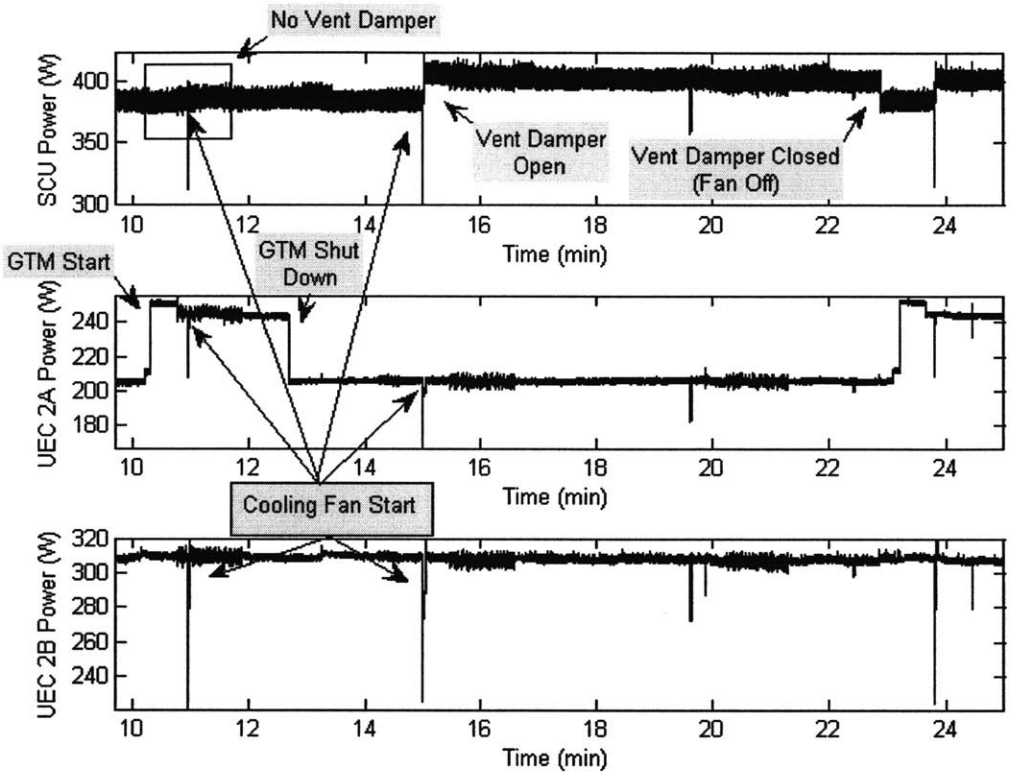

Figure 5-19: Vent Damper Failure Sequence

Putting it all together, Figure 5-20 below shows the power traces of the SCU, UEC 2A, UEC 2B, GTG NBPS, and 2A LOSP on April 16 2007 from 0900 to 1000. The 2A FOSP was stopped during this time so it is not shown in the figure. During this hour the following events can be seen in the power traces and are annotated in the Figure 5-20:

Table 5-1: LBES Plant events on 16 April 2007 from 0900 to 1000

Event	Time	Description
A	0901	Motor & Fuel Purge 2A
B	0910	GTM 2A Start
C	0912	Emergency Stop GTM 2A
D	0923	GTM 2A start
E	0927	Stop 9140 GTG
F	0930	Ahead 2/3
G	0932	Ahead Standard

H	0933	Back 1/3
I	0934	Ahead 1/3
J	0942	Normal Stop Complete GTM 2B
K	0950	RIMSS Start of 9140 GTG
L	0952	GTM 2B Vent Damper closed
M	0954	60 second motor GTM 2B
N	0954	RIMSS Stopped

Events and times were excerpted from the LBES test manager's written log; therefore times do not exactly match up with NILM computer times.

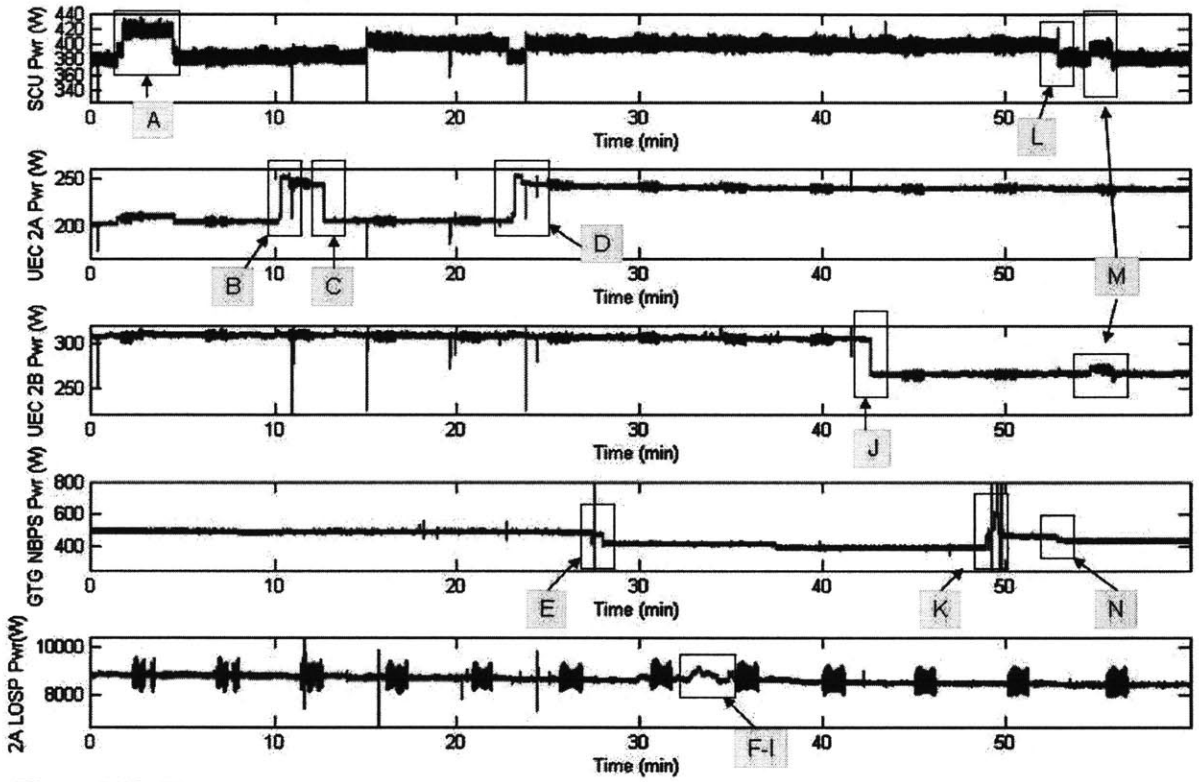

Figure 5-20: Time Aligned Plot showing power traces of SCU, UEC 2A, UEC 2B, GTG NBPS, & 2A LOSP captured on 16 April 2007 0900-1000

Chapter 6 Conclusions and Future Work

The analysis of twelve months worth of NILM experiments and associated data were presented in this thesis. The results clearly demonstrate the ability of the NILM to recognize equipment state changes from simple current and voltage measurements. In addition, the synchronized computer network further demonstrates the potential of the NILM to perform supervisory monitoring and control on a complex shipboard engineering plant. Indeed, the NILM has proven potential as a viable and inexpensive alternative for shipboard automation and control.

Even so, much work remains before the NILM is "shipboard ready." The results presented here represent a fraction of the data collected over three LBES DDG pre-commissioning crew training weeks and numerous other days of hot plant operations. Further analysis of many more plant operations is needed to fully understand complex integrated plant sequences and evolutions. Consider Figure 6-1 below. This snapshot of UEC 2B power data was taken during a Digital Fuel Control Fuel Metering Valve calibration. Much information can be obtained from NILM power data and for the NILM to serve as a supervisory control system, it must be able to recognize and diagnose complex sequences like the one shown in the figure.

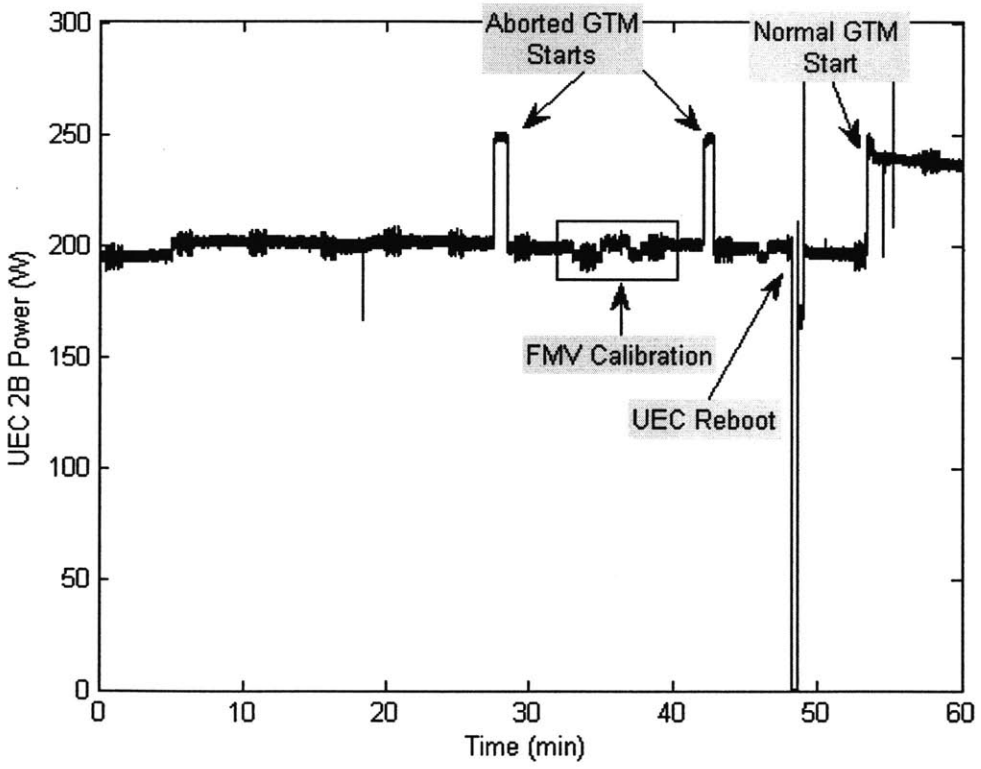

Figure 6-1: Power Drawn by UEC 2B during FMV Calibration and other operations.

To further the development of a NILM-based supervisory control system, several new projects are currently underway. The NILM software suite is being expanded so that

the NILM can log several critical electrical parameters. Example quantities include the following:

- Generator load
- Line frequency
- Voltage amplitude
- Harmonic distortion

By logging these features, a NILM placed on the generator output bus could potentially perform many of the monitoring and control functions that are now performed by the LOCOP[2]. The benefit of this approach would be that the NILM could simultaneously evaluate the status of loads downstream from the generator.

6.1 Future Work

To continue the development of the NILM as a supervisory control system, the next steps should be immediately accomplished.

- The LPAC requires further experiments and data analysis. The change in behavior from 2005 to 2007 must be diagnosed and understood. Install a NILM on the LBES Nr 1 LPAC for data comparison.
- The FOSP and LOSP responses to bell orders require further analysis. Review other data collected during LBES plant speed changes for similar responses.
- FOSP and LOSP responses to GTM starts and other GTM operations have been inconsistent and also require further analysis. More GTM evolutions should be studied to establish a patter of similar responses.
- Continue to review the reactive power (Q) and other harmonic data for responses to plant events.
- Continue to improve the time synchronization of the LBES NILM computers.

Other work includes experiments furthering development of a NILM capable of monitoring a large aggregate power signal, such as the generator output bus discussed above. The installation of the NILM on Power Panel 1-282-1 was the first step and more preliminary experiments are required. Placements for new NILMs to be considered:

- Main load center powering Panel 1-282-1
- A main distribution panel feeding more than one 44VAC load (i.e. the panel feeding both an FOSP and LOSP and other 440 VAC loads)
- One of the two main load centers on the LBES 24 foot level

By "zooming" out to larger load centers, it will be easier to determine the feasibility of the NILM to monitor aggregate plant loads before operating from the generator output bus.

[2] It is important to note that the NILM already has the ability to measure the key electrical quantities described here. The features that need to be incorporated into the NILM are the real-time control activities that rely on this information.

The NILM has proven to be a potential useful tool capable of performing shipboard supervisory control. This is a key to the development of such a system for the all electric warship of the future. The simple COTS technology used by the NILM for supervisory control can save the U.S. Navy millions of dollars in research & development, ship acquisition, and lifecycle costs for the next class of warships.

References

[1] R. W. Cox, J. P. Mosman, D. McKay, S. B. Leeb, and T. J. McCoy, "Diagnostic indicators for shipboard cycling systems using non-intrusive load monitoring," in *Proc. ASNE Day 2006*, Arlington, VA.

[2] T. DeNucci, R. W. Cox, S. B. Leeb, J. Paris, T. J. McCoy, C.R. Laughman, and W. C. Greene, "Diagnostic indicators for shipboard systems using non-intrusive load monitoring," in *Proc. 1st IEEE Electric Ship Technologies Symposium*. Philadelphia, PA.

[3] R. W. Cox, G. Mitchell, J. Paris, and S. B. Leeb, "Shipboard fluid system diagnostic indicators using non-intrusive load monitoring," to appear in *Proc. ASNE Day 2007*, Arlington VA.

[4] R. W. Cox, G. Mitchell, P. Bennett, M. Piber, J. Paris, W. Wichakool, and S. B. Leeb, "Improving shipboard maintenance practices using non-intrusive load monitoring," to appear in *Proc. ASNE Intelligent Ships VII* , Philadelphia, PA.

[5] J. S. Ramsey, S. B. Leeb, T. DeNucci, J. Paris, M. Obar, R. W. Cox, C. R. Laughman, and T. J. McCoy, "Shipboard applications of non-intrusive load monitoring," in *Proc. ASNE Reconfiguration and Survivability Symposium,* Atlantic Beach, FL, 15-18 Feb. 2005.

[6] T. D. McKay, "Diagnostic indicators for shipboard mechanical systems using non-intrusive load monitoring," S.M./N.E. Thesis, Mech. Eng., MIT, 2006.

[7] H. J. Kozuhowski, M. G. Hoffman, C. D. Mako, L. L. Overton, and W. E. Masincup, "Integrated testing of the full authority digital control and redundant independent mechanical start system for the U.S. Navy's DDG-51 ship service gas turbine generator sets," in *Proc. ASME TURBO EXPO*, Stockholm, 1998.

[8] M. DiUlio, C. Savage, and E. Schneider, "Taking the integrated condition assessment system to the year 2010," in *Proc. 13th International Ship Control Systems Symposium*, Orlando, FL, Apr. 2003.

[9] R. J. Bost, J. G. Mellis, and P. A. Dent, "Is the Navy serious about reducing manning on its ships?" Office of Naval Research, 1999.

[10] R. L. Lopushansky, "All optical shipboard sensing system," in *Proc. 45th International Instrumentation Symposium,* Albuquerque, NM, May 1999.

[11] R. W. Cox, "Minimally intrusive strategies for fault detection and energy monitoring," Ph.D. dissertation, EECS, MIT, Aug 2006.

[12] S. B. Leeb, S. R. Shaw, and J. L. Kirtley, "Transient event detection in spectral envelope estimates for nonintrusive load monitoring," *IEEE Trans. on Power Delivery*, vol. 10, no. 3, pp. 1200–1210, July 1995.

[13] S. R. Shaw, "System identification techniques and modeling for non-intrusive load diagnostics," Ph.D. dissertation, EECS, MIT, Feb. 2000.

[14] S. R. Shaw, C. B. Abler, R. F. Lepard, D. Luo, S. B. Leeb, and L. K. Norford, "Instrumentation for high performance nonintrusive electrical load monitoring," *ASME Journal of Solar Energy Engineering*, vol. 120, pp. 224-229, Aug 1998.

[15] A. V. Oppenheim, A. S. Willsky, and I. T. Young, Signals and Systems. Prentice Hall Signal Processing Series, Englewood Cliffs, New Jersey: Addison Wellesley, 1988.

[16] K. D. Lee, "Electric load information system based on non-intrusive power monitoring," Ph.D. dissertation, Mech.. Eng, MIT, May 2003.
[17] S. B. Leeb, "A conjoint pattern recognition approach to nonintrusive load monitoring," Ph.D. dissertation, EECS, MIT, Feb. 1993.
[18] P. R. Armstrong, C. R. Laughman, S. B. Leeb, and L. K. Norford, "Detection of rooftop cooling unit faults based on electrical measurements," HVAC+R Research Journal, vol. 12, no. 1, pp. 151–175, Jan. 2006.
[19] D. Luo, "Detection and diagnosis of faults and energy monitoring of HVAC systems with least- intrusive power analysis," Ph.D. dissertation, Dept. Arch., MIT, Feb. 2001.
[20] C. R. Laughman, P. R. Armstrong, L. K. Norford, and S. B. Leeb, "The detection of liquid slugging phenomena in reciprocating compressors via power measurements," in *Proc. International Compressor Engineering Conference at Purdue*, pp 1-8, West Lafayette, IN, Jul 2006.
[21] J. Paris, "A framework for non-intrusive load monitoring and diagnostics," M.Eng. Thesis, EECS, MIT, Feb. 2006.
[22] *Technical Manual for LM2500 Propulsion Gas Turbine*, Naval Sea Systems Command, S9234-AD-MMO-010/LM2500, 26 May 2000.
[23] *Technical Manual for Universal Engine Controller*, Naval Sea Systems Command, S6263-B7-MMA-010, 25 Nov 2002.
[24] G. W. Hart, "Nonintrusive appliance load monitoring," *Proc. of the IEEE*, vol. 80, no. 12, pp. 1870-1890, Dec 1992.
[25] *Technical Manual for AG9140RF Ship Service Gas Turbine Generator (SSGTG)*, Naval Sea Systems Command, S9311-XX-MMO-010, Mar 2003.
[26] McCoy, Timothy J.Manning and Automation. 2005. Masschusetts Institute of Technology. PowerPoint. 30 March 2007
[27] "Assistant Secretary of the Navy Financial Management and Comptroller Web Site.", 30 March 2007 <http://www.finance.hq.navy.mil/fmc/>
[28] Department of the Navy. "Supporting Exhibits Book." President's Budget FY 2007. 2006 Assistant Secretary of the Navy Financial Management and Comptroller Web Site 30 March 2007. <http://www.finance.hq.navy.mil/fmb/07pres/SUPP/Supporting_Exhibits_Book_PB07.pdf>
[29] Department of the Navy. Fiscal Year 2008/2009 Budget Estimates. 2007. Assistant Secretary of the Navy Financial Management and Comptroller Web Site 30 March 2007 <http://www.finance.hq.navy.mil/fmb/08pres/pers/MPN_Book.pdf>
[30] Department of the Navy. "Supporting Exhibits Book." President's Budget FY 2008. 2007 Assistant Secretary of the Navy Financial Management and Comptroller Web Site <http://www.finance.hq.navy.mil/fmb/08pres/SUPP/Supporting_Exhibits_Book.pdf>
[31] Department of the Navy. Department of the Navy FY08 President's Budget. 2007.Department of the Navy. PowerPoint 30 March 2007 <http://www.finance.hq.navy.mil/fmb/08pres/highbook/FY08_PB_press_brief_final.pdf>
[32] "Program Executive Office Ships – DDG 1000." 3 April 2007 <http://peoships.crane.navy.mil/DDG1000/>

[33] "DDG-1000 Zumwalt / DD(X) Design." GlobalSecurity.org. 3 April 2007. <http://www.globalsecurity.org/military/systems/ship/dd-x-design.htm>
[34] "Fact File Destroyers – DDG." Navy.mil. 3 April 2007. <http://www.navy.mil/navydata/fact_display.asp?cid=4200&tid=900&ct=4>
[35] United States General Accounting Office. Navy Actions Needed to Optimize Ship Crew Size and Reduce Total Ownership Costs. 2003. 3 April 2007. <http://www.globalsecurity.org/military/library/report/gao/d03520.pdf>
[36] Gilmore, J. Michael. "The Navy's DD(X) Destroyer Program." Congressional Budget Office Testimony. 2005 <http://www.cbo.gov/ftpdocs/65xx/doc6561/07-19-NavyDDX.pdf> 3 April 2007
[37] Naval Research Advisory Committee. Optimized Surface Ship Manning. 2000. <http://www.onr.navy.mil/nrac/docs/2000_rpt_optimizing_surface_ship_manning.pdf > 5 April 2007
[38] "DDG 1000." 5 April 2007 <http://www.ddg1000.com/overview/ddg1000_brief.php>
[39] *Draft Technical Manual for Universal Engine Controller Plus*, Naval Sea Systems Command, SXXXX-XX-MMA-010, 1 Oct 2004.
[40] William C. Greene, "Evaluation of Non-Intrusive Monitoring for Condition Based Maintenance Applications on US Navy Propulsion Plants", S.M./N.E. Thesis, Mech. Eng., MIT, 2005.
[41] *Technical Manual for Machinery Control System, Shaft Control Unit, P/N 63E915603G1, Volume 2*, Naval Sea Systems Command, S9202-AN-MMF-020, 09 Oct 1998
[42] "Machinery Control System (MCS) – DDG 83AF," LBES Trainee Guide,T7200-1-01, June 2003.
[43] *Technical Manual for Fuel Service Pump*, Naval Sea Systems Command, S6226-DE-MMA-010/07524, 05 July 2000.
[44] *Technical Manual for Air Compressor Low Pressure, Oil Free*, Naval Sea Systems Command, S6220-DQ-MMA-010, 01 Nov 1992.
[45] J. Steven Ramsey, "Shipboard Applications of Non-Intrusive Load Monitoring", S.M./N.E. Thesis, Mech. Eng., MIT, 2004.
[46] *Technical Manual for No Break Power Supply, 28 VDC, 840W, 3 Phase, 60 Hertz*, Naval Sea Systems Command, S9314-DC-MMA-010, 01 Jul 1992.

Appendix A NILM Parts List

Nomenclature	Manufacturer	Part Number	Quantity
NEMA Enclosure	Rittal Corporation www.rittal-corp.com	E-1210CH	1
Backplane	Rittal Corporation www.rittal-corp.com	E-12P10	1
Power Supply	Mean Well www.meanwell.com	Model PD-2512	1
Voltage Transducer	LEM www.lem.com	LV25-P	1
Current Transducer	LEM www.lem.com	Various	As Needed
Voltage Board	LEES[3]	N/A	1
Resistor Board	LEES	N/A	1
Fuse Holder	Littelfuse www.littelfuse.com	L60030C-3PQ	1
Fuse	Littelfuse www.littelfuse.com	KLKR Series	1
68-Pin SCSI-II Wiring Terminal Board, DIN Rail Mount	B&B Electronics Manufacturing Co. www.bb-elec.com	ADAM-3968	1
0.25W Carbon Film Resistors (R_m and Reference)	DigiKey www.digikey.com	Various	As Needed
3W Metal Film Resistors	DigiKey www.digikey.com	BC100KW-3CT-ND	3
KK© Crimp Terminal Housing	Molex www.molex.xom	41695 Series	As Needed
KK© Crimp Terminal	Molex www.molex.xom	2478 Series	As Needed
Hand Crimp Tool	Molex www.molex.xom	63811-2300	1
.250 Hex Male-Female Standoff (6-32 Threads), for Power Supply and Resistor Board	Keystone Electronics www.keyelco.com	8414	As Needed
.375 Hex Male Female Standoff (10-32 Threads), for Voltage Board	Keystone Electronics www.keyelco.com	Custom Build (See Below)	4
.375 Machine Screws, 10-	Various	Various	6

[3] Laboratory for Electromagnetic and Electronic Systems at the Massachusetts Institute of Technology

32 Threads			
.250 Machine Screws, 6-32 Thread	Various	Various	As Needed
Nut, 10-32 Thread	Various	Various	As Needed
Nut, 6-32 Thread	Various	Various	As Needed
¾" Clamp Connector	Halex www.halexco.com	05107B	As Needed
DIN Rail	B&B Electronics Manufacturing Co. www.bb-elec.com	ERS35	As Needed
68-pin SCSI-II Shielded Cable, 2m	B&B Electronics Manufacturing Co. www.bb-elec.com	PCL-10168-2	1
CT Cable, Multi-Conductor, Foil Shield	General Cable www.generalcable.com	C2537	As Needed
Voltage Cable, Carolprene® Jacketed Type SOOW	General Cable www.generalcable.com	02766	As Needed
18 AWG Copper Braided Wire	Various	Various	As Needed

Voltage Board Standoff Specifications:

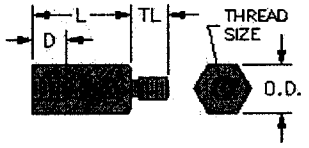

O.D. = 0.375 in
L = 0.375 in
TL = 0.375 in
D = 0.250 in

Appendix B NILM Electrical Connection Scheme

Component	Terminal
120 VAC in	Power Supply In
Power Supply +12V	Voltage Board +12V, CT +12V, Voltage Board +12V
Power Supply -12V	Voltage Board -12V, CT -12V, Voltage Board -12V
Power Supply COMMON	"Ground + Bottom SCSI Row" on Resistor Board, Terminals 68-61 on ADAM-3968
Voltage Board +12V	Power Supply +12V
Voltage Board -12V	Power Supply -12V
Voltage Tap In	One lead to A in on Voltage Board, the other to N on the Voltage Board
Current Transducer +12V	Power Supply +12V
Current Transducer-12V	Power Supply -12V
Current Transducer Output	"Transducers + Top SCSI Row" On Resistor Board, Terminals 27-33 on ADAM-3968
Voltage Transducer Output	Transducers + Top SCSI Row" On Resistor Board, Terminal 34 on ADAM-3968
Measuring Resistors (R_m)	Top Resistor connections on Resistor Board
Ground (Reference Resistors)	Bottom Resistor Connections on Resistor Board
Resistor Board GND	Terminal 26 on ADAM-3968

Appendix C NILM Transducer Data Sheets

LEM

Voltage Transducer LV 25-P

I_{PN} = 10 mA
V_{PN} = 10 .. 500 V

For the electronic measurement of voltages : DC, AC, pulsed..., with a galvanic isolation between the primary circuit (high voltage) and the secondary circuit (electronic circuit).

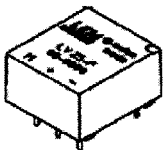

18084

Electrical data

I_{PN}	Primary nominal r.m.s. current		10		mA
I_P	Primary current, measuring range		0 .. ± 14		mA
R_M	Measuring resistance		$R_{M\,min}$	$R_{M\,max}$	
	with ± 12 V	@ ± 10 mA$_{max}$	30	190	Ω
		@ ± 14 mA$_{max}$	30	100	Ω
	with ± 15 V	@ ± 10 mA$_{max}$	100	350	Ω
		@ ± 14 mA$_{max}$	100	190	Ω
I_{SN}	Secondary nominal r.m.s. current		25		mA
K_N	Conversion ratio		2500 : 1000		
V_C	Supply voltage (± 5 %)		± 12 .. 15		V
I_C	Current consumption		10 (@ ± 15 V) + I_S		mA
V_d	R.m.s. voltage for AC isolation test [1], 50 Hz, 1 mn		2.5		kV

Accuracy - Dynamic performance data

X_G	Overall Accuracy @ I_{PN}, T_A = 25°C	@ ± 12 .. 15 V	± 0.9		%
		@ ± 15 V (± 5 %)	± 0.8		%
ε_L	Linearity error		< 0.2		%
			Typ	Max	
I_O	Offset current @ I_P = 0, T_A = 25°C			± 0.15	mA
I_{OT}	Thermal drift of I_O	0°C .. + 25°C	± 0.06	± 0.25	mA
		+ 25°C .. + 70°C	± 0.10	± 0.35	mA
t_r	Response time [2] @ 90 % of V_{PN}		40		µs

General data

T_A	Ambient operating temperature	0 .. + 70	°C
T_S	Ambient storage temperature	- 25 .. + 85	°C
R_P	Primary coil resistance @ T_A = 70°C	250	Ω
R_S	Secondary coil resistance @ T_A = 70°C	110	Ω
m	Mass	22	g
	Standards	EN 50178 : 1997	

Notes : [1] Between primary and secondary
[2] R_1 = 25 kΩ (L/R constant, produced by the resistance and inductance of the primary circuit).

Features

- Closed loop (compensated) voltage transducer using the Hall effect
- Insulated plastic case recognized according to UL 94-V0.

Principle of use

- For voltage measurements, a current proportional to the measured voltage must be passed through an external resistor R_1 which is selected by the user and installed in series with the primary circuit of the transducer.

Advantages

- Excellent accuracy
- Very good linearity
- Low thermal drift
- Low response time
- High bandwidth
- High immunity to external interference
- Low disturbance in common mode.

Applications

- AC variable speed drives and servo motor drives
- Static converters for DC motor drives
- Battery supplied applications
- Uninterruptible Power Supplies (UPS)
- Power supplies for welding applications.

Application domain

- Industrial.

060330/15

Current Transducer LA 55-P

I_{PN} = 50 A

For the electronic measurement of currents : DC, AC, pulsed..., with a galvanic isolation between the primary circuit (high power) and the secondary circuit (electronic circuit).

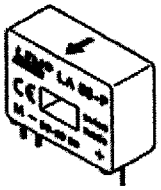

16019

Electrical data

I_{PN}	Primary nominal current rms			50			A
I_{PM}	Primary current, measuring range			0 .. ± 70			A
R_M	Measuring resistance @		T_A = 70°C		T_A = 85°C		
			$R_{M\,min}$	$R_{M\,max}$	$R_{M\,min}$	$R_{M\,max}$	
	with ± 12 V	@ ± 50 A_{rms}	10	100	60	95	Ω
		@ ± 70 A_{rms}	10	60	60[1]	60[1]	Ω
	with ± 15 V	@ ± 50 A_{rms}	50	160	135	155	Ω
		@ ± 70 A_{rms}	50	90	135[2]	135[2]	Ω
I_{SN}	Secondary nominal current rms			50			mA
K_N	Conversion ratio			1 : 1000			
V_C	Supply voltage (± 5 %)			± 12 .. 15			V
I_C	Current consumption			10 @ ±15 V) + I_S			mA
V_d	Rms voltage for AC isolation test, 50 Hz, 1 min			2.5			kV

Accuracy - Dynamic performance data

X	Accuracy @ I_{PN}, T_A = 25°C	@ ± 15 V (± 5 %)		± 0.65	%
		@ ± 12 .. 15 V (± 5 %)		± 0.90	%
ε_L	Linearity error			< 0.15	%
			Typ	Maxi	
I_O	Offset current @ I_P = 0, T_A = 25°C			± 0.2	mA
I_{OM}	Magnetic offset current[3] @ I_P = 0 and specified R_M after an overload of 3 x I_{PN}			± 0.3	mA
I_{OT}	Temperature variation of I_O	0°C .. + 70°C	± 0.1	± 0.5	mA
		- 25°C .. + 85°C	± 0.1	± 0.6	mA
t_{ra}	Reaction time @ 10 % of I_{PN}			< 500	ns
t_r	Response time @ 90 % of I_{PN} Step			< 1	µs
di/dt	di/dt accurately followed			> 200	A/µs
BW	Frequency bandwidth (- 1 dB)			DC .. 200	kHz

General data

T_A	Ambient operating temperature		- 25 .. + 85	°C
T_S	Ambient storage temperature		- 40 .. + 90	°C
R_S	Secondary coil resistance @	T_A = 70°C	80	Ω
		T_A = 85°C	85	Ω
m	Mass		18	g
	Standards		EN 50178: 1997	

Notes: [1] Measuring range limited to ± 60 A_{rms}
[2] Measuring range limited to ± 55 A_{rms}
[3] Result of the coercive field of the magnetic circuit.

Features

- Closed loop (compensated) current transducer using the Hall effect
- Printed circuit board mounting
- Isolated plastic case recognized according to UL 94-V0.

Advantages

- Excellent accuracy
- Very good linearity
- Low temperature drift
- Optimized response time
- Wide frequency bandwidth
- No insertion losses
- High immunity to external interference
  Current overload capability.

Applications

- AC variable speed drives and servo motor drives
- Static converters for DC motor drives
- Battery supplied applications
- Uninterruptible Power Supplies (UPS)
- Switched Mode Power Supplies (SMPS)
- Power supplies for welding applications.

Application Domain

- Industrial.

Current Transducer LA 205-S

I_{PN} = 200 A

For the electronic measurement of currents : DC, AC, pulsed..., with a galvanic isolation between the primary circuit (high power) and the secondary circuit (electronic circuit).

18137

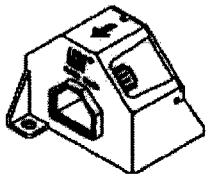

Electrical data

				T_A = 70°C		T_A = 85°C		
				$R_{M\,min}$	$R_{M\,max}$	$R_{M\,min}$	$R_{M\,max}$	
I_{PN}	Primary nominal r.m.s. current			200				A
I_P	Primary current, measuring range			0 .. ± 300				A
$I_{P\,max}$	Measuring overload [1]			600				A
R_M	Measuring resistance @							
	with ± 12 V	@ ± 200 A_{max}		0	68	0	66	Ω
		@ ± 300 A_{max}		0	33	0	30	Ω
	with ± 15 V	@ ± 200 A_{max}		5	95	5	93	Ω
		@ ± 300 A_{max}		5	50	5	49	Ω
I_{SN}	Secondary nominal r.m.s. current			100				mA
K_N	Conversion ratio			1 : 2000				
V_C	Supply voltage (± 5 %)			± 12 .. 15				V
I_C	Current consumption			20 (@ ± 15V) + I_S				mA
V_b	R.m.s rated voltage [2], safe separation			1625				V
	basic isolation			3250				V

Accuracy - Dynamic performance data

X_G	**Overall accuracy @ I_{PN}, T_A = 25°C**		± 0.8		%
ε_L	Linearity error		< 0.1		%
			Typ	Max	
I_O	Offset current @ I_P = 0, T_A = 25°C			± 0.15	mA
I_{OM}	Residual current [3] @ I_P = 0, after an overload of 3 x I_{PN}			± 0.50	mA
I_{OT}	Thermal drift of I_O	- 10°C .. + 85°C	± 0.15	± 0.30	mA
t_{ra}	Reaction time @ 10 % of I_{PN}		< 500		ns
t_r	Response time [4] @ 90 % of I_{PN}		< 1		µs
di/dt	di/dt accurately followed		> 100		A/µs
F	Frequency bandwidth (- 3 dB)		DC .. 100		kHz

General data

T_A	Ambient operating temperature		- 10 .. + 85	°C
T_S	Ambient storage temperature		- 40 .. + 90	°C
R_S	Secondary coil resistance @	T_A = 70°C	35	Ω
		T_A = 85°C	37	Ω
m	Mass		110	g
	Standards		EN 50178 : 1997	

Notes : [1] 3 mn/hour @ V_C = ± 15 V, R_M = 5 Ω
[2] Pollution class nr 2. With a non insulated primary bar which fills the through-hole
[3] The result of the coercive field of the magnetic circuit
[4] With a di/dt of 100 A/µs.

Features

- Closed loop (compensated) current transducer using the Hall effect
- Insulated plastic case recognized according to UL 94-V0
- Patent pending.

Advantages

- Excellent accuracy
- Very good linearity
- Low temperature drift
- Optimized response time
- Wide frequency bandwidth
- No insertion losses
- High immunity to external interference
- Current overload capability.

Applications

- AC variable speed drives and servo motor drives
- Static converters for DC motor drives
- Battery supplied applications
- Uninterruptible Power Supplies (UPS)
- Switched Mode Power Supplies (SMPS)
- Power supplies for welding applications.

060531/7

Current Transducer LA 305-S

I_{PN} = 300 A

For the electronic measurement of currents : DC, AC, pulsed..., with a galvanic isolation between the primary circuit (high power) and the secondary circuit (electronic circuit).

16173

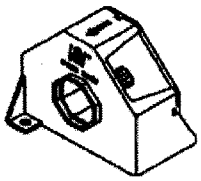

Electrical data

I_{PN}	Primary nominal r.m.s. current			300			A
I_P	Primary current, measuring range			0 .. ± 500			A
R_M	Measuring resistance @		T_A = 70°C		T_A = 85°C		
			R_{Mmin}	R_{Mmax}	R_{Mmin}	R_{Mmax}	
	with ± 12 V	@ ± 300 A$_{max}$	0	52	0	50	Ω
		@ ± 500 A$_{max}$	0	17	0	15	Ω
	with ± 15 V	@ ± 300 A$_{max}$	0	75	5	73	Ω
		@ ± 500 A$_{max}$	0	31	5	29	Ω
I_{SN}	Secondary nominal r.m.s. current			120			mA
K_N	Conversion ratio			1 : 2500			
V_C	Supply voltage (± 5 %)			± 12 .. 15			V
I_C	Current consumption			20 @ ± 15 V) + I_S			mA
V_b	R.m.s. rated voltage [1], safe separation			1750			V
	basic isolation			3500			V

Accuracy - Dynamic performance data

X_G	Overall accuracy @ I_{PN}, T_A = 25°C		± 0.8		%
ε_L	Linearity		< 0.1		%
			Typ	Max	
I_O	Offset current @ I_P = 0, T_A = 25°C			± 0.20	mA
I_{OM}	Residual current [2] @ I_P = 0, after an overload of 3 x I_{PN}			± 0.40	mA
I_{OT}	Thermal drift of I_O	- 10°C .. + 85°C	± 0.12	± 0.30	mA
t_{ra}	Reaction time @ 10 % of I_{PN}		< 500		ns
t_r	Response time [3] @ 90 % of I_{PN}		< 1		µs
di/dt	di/dt accurately followed		> 100		A/µs
f	Frequency bandwidth (- 3 dB)		DC .. 100		kHz

General data

T_A	Ambient operating temperature		- 10 .. + 85	°C
T_S	Ambient storage temperature		- 40 .. + 90	°C
R_S	Secondary coil resistance @	T_A = 70°C	35	Ω
		T_A = 85°C	37	Ω
m	Mass		200	g
	Standards [4]		EN 50178	

Notes : [1] Pollution class 2. With a non insulated primary bar which fills the through-hole
[2] The result of the coercive field of the magnetic circuit
[3] With a di/dt of 100 A/µs
[4] A list of corresponding tests is available.

Features

- Closed loop (compensated) current transducer using the Hall effect
- Insulated plastic case recognized according to UL 94-V0
- Copyright protected.

Advantages

- Excellent accuracy
- Very good linearity
- Low temperature drift
- Optimized response time
- Wide frequency bandwidth
- No insertion losses
- High immunity to external interference
- Current overload capability.

Applications

- AC variable speed drives and servo motor drives
- Static converters for DC motor drives
- Battery supplied applications
- Uninterruptible Power Supplies (UPS)
- Switched Mode Power Supplies (SMPS)
- Power supplies for welding applications.

060628/8

Appendix D NILM Data Processing Scripts

```
Unix script used to process LBES GTM Controller NILM data.
Robert W. Cox
Patrick L. Bennett
February 2007

#!/bin/bash

mount /cdrom
cp /cdrom/*.gz .
for i in *.1.gz
do
      if [ -e ${i/.1.gz/.2.gz} ] && [ -e ${i/.1.gz/.3.gz} ]
            then

      echo $i;
      gunzip -c $i > tempfile1;
      echo ${i/.1.gz/.2.gz};
      gunzip -c ${i/.1.gz/.2.gz} > tempfile2;
      echo ${i/.1.gz/.3.gz};
      gunzip -c ${i/.1.gz/.3.gz} > tempfile3;
      grep -v ^# tempfile1 > tempfile1a;
      rm -f tempfile1;
      grep -v ^# tempfile2 > tempfile2a;
      rm -f tempfile2;
      grep -v ^# tempfile3 > tempfile3a;
      rm -f tempfile3;
      paste tempfile1a tempfile2a tempfile3a > tempfile;
      cat tempfile | chansift2_12bit.pl 1 2 | /home/nilm/bin/prep stdin
-p /home/nilm/UEC/prep-msufp-text.so > UEC2A_fullprep${i/.gz/.txt}
      cat tempfile | chansift2_12bit.pl 1 3 | /home/nilm/bin/prep stdin
-p /home/nilm/UEC/prep-msufp-text.so > UEC2B_fullprep${i/.gz/.txt}
      cat tempfile | chansift2_12bit.pl 1 4 | /home/nilm/bin/prep stdin
-p /home/nilm/UEC/prep-msufp-text.so > SCU_fullprep${i/.gz/.txt}
      cat tempfile | chansift2_12bit.pl 1 5 | /home/nilm/bin/prep stdin
-p /home/nilm/UEC/prep-msufp-text.so > Panel_fullprep${i/.gz/.txt}
      cat UEC2A_fullprep${i/.gz/.txt} | chansift2_12bit.pl 2 >
UEC2A${i/.gz/.txt}
      cat UEC2B_fullprep${i/.gz/.txt} | chansift2_12bit.pl 2 >
UEC2B${i/.gz/.txt}
      cat SCU_fullprep${i/.gz/.txt} | chansift2_12bit.pl 2 >
SCU${i/.gz/.txt}
      cat Panel_fullprep${i/.gz/.txt} | chansift2_12bit.pl 2 >
Panel_${i/.gz/.txt}
      rm -f tempfile1a;
      rm -f tempfile2a;
      rm -f tempfile3a;
      rm -f tempfile;
      rm -f $i
      rm -f ${i/.1.gz/.2.gz}
      rm -f ${i/.1.gz/.3.gz}
fi
done
umount /cdrom
eject
```

```
Unix Script used to process NILM pre-processed data.

Robert W. Cox
July 2006

#!/bin/bash

mount /cdrom
cp /cdrom/* .

for i in *.gz
do
      echo $i;
      gunzip -c $i > tempfile;
      grep -v ^# tempfile | chansift2_12bit.pl 1 2 > LO${i/.gz/.txt}
      rm -f $i
done

rm -f tempfile

umount /cdrom
eject
```

```
MATLAB Script used to convert Processed NILM data to RMS current in
Amperes.

Robert W. Cox
October 2006

Function input definition:
g = gain code value
Rm = measuring resistor value
K = CT conversion factor from data sheet
x = NILM data

function y=prep_to_current(g, Rm, K, x)
y=((x/64)*(g/4096)*(1/(Rm*(1/K))))*(1/sqrt(2));
```

Appendix E LBES NILM Installation Test Plan

A. OBJECTIVE:

Evaluate the use of the Non-Intrusive Load Monitor (NILM) in detecting Shaft Control Unit (SCU) control signals. The NILM will be left in place to allow for the collection of long term normal operating data.

B. BACKGROUND:

Following experiments on board the USCG *Seneca* and at the DDG-51 LBES, the NILM has been shown to be able to diagnose state changes in various mechanical systems. The power feed to the Shaft Control Unit (SCU) may contain information relevant to the diagnosis of specific control signals sent from the SCU to equipment in the propulsion plant, and thus be able to determine state changes in the throughout the entire plant.

C. PREREQUISTES:

1. Ensure NILM sensing box (NEMA-style enclosure) is constructed to monitor 115VAC / 3-phase power.

D. PRELIMINARY:

1. Read through the procedure in its entirety prior to beginning the test.

E. PROCEDURE:

1. Open breaker for 115 VAC / 3-phase power supplying the Shaft Control Unit at power panel 1-282-1. Danger Tag Open.
2. Remove cover plate at power panel 1-282-1.
3. Lift the lead for phase A of Shaft Control Unit power. Thread the power cable through current transformer (type LM-55), and replace the lead.
4. Attach NILM voltage leads to remaining two phases (B & C) of Shaft Control Unit power. This voltage sensing cable is rated for 600V.
5. Route the current transformer cable (step 3) and the voltage sensing cables (step 4) through existing cutouts in the top of power panel 1-282-1 and into the NILM NEMA sensing box.
6. Connect current transformer and voltage cables in the NILM sensing box.
7. Close NILM sensing box.
8. Re-install cover plate for power panel 1-282-1.

9. Remove Danger Tags from breakers for 115 VAC / 3-phase power for Shaft Control Unit at power panel 1-282-1.

10. Shut breakers for 115 VAC / 3-phase power for Shaft Control Unit at power panel 1-282-1.

11. Plug in associated NILM PC and NILM sensing box to standard 120 VAC power outlet and start NILM acquisition software.

12. The NILM system is now ready to record data.